Molybdenum and Tungsten Alkylidyne Complexes Containing Mono-, Bi- and Tridentate *N*-Heterocyclic Carbenes

Iris Elser[±,¤], Jonas Groos[±,¤], Philipp M. Hauser[±,¤], Maximilian Koy[±,?,¤], Melita van der Ende[±,¤], Dongren Wang[±], Wolfgang Frey[≠], Klaus Wurst[ε], Jan Meisner[¥,ʃ], Felix Ziegler[±], Johannes Kästner[¥] and Michael R. Buchmeiser[±,*]

[±]Institute of Polymer Chemistry, [≠]Institute of Organic Chemistry and [¥]Institute for Theoretical Chemistry, University of Stuttgart, Pfaffenwaldring 55, 70569 Stuttgart (Germany); [ε]Institute of General, Inorganic and Theoretical Chemistry, University of Innsbruck, A-6020 Innsbruck (Austria). [¤]Equal contribution.

Contents

1. Literature-known procedures

1.1. Imidazolium salts and carbenes

1,3-Di-*tert*butylimidazolium tetrafluoroborate **2**·**HBF$_4$**,[1] 1,3-dicyclohexylimidazolium tetrafluoroborate **1**·**HBF$_4$**,[2] 1,3-dimesitylimidazolium tetrafluoroborate,[2] 3,4,5-trimethylthiazolium iodide **3**·**HI**,[3] 1,3-dimesitylimidazolinium chloride **4**·**HCl**,[2] 1,3-diisopropylimidazolium chloride **5**·**HCl**,[4] 1-(2,6-dimethylphenyl)-3-(2-hydroxyphenyl)-4,5-dihydroimidazolium chloride **HO1**·**HCl,**[5] 1-(mesityl)-3-(2-hydroxyphenyl)-4,5-dihydroimidazolium chloride **HO2**·**HCl**,[6] 1-(2,6-dimethylphenyl)-3-(2-hydroxyphenyl)-4,5-dihydroimidazolium tetrafluoroborate **HO1**·**HBF$_4$,**[5] 1-(mesityl)-3-(2-hydroxyphenyl)-4,5-dihydroimidazolium tetrafluoroborate **HO2**·**HBF$_4$**,[5] **HO$_2$1**[7] were synthesized according to literature procedures. 1,3-Diisopropylimidazolium chloride was additionally washed with boiling acetone, dried by azeotropic distillation with toluene and dried under vacuum overnight before it was transferred to the glove box. Carbenes **2**, **4** and **5** were applied in their isolated form and were synthesized by deprotonation of the corresponding imidazolium salts with either KHMDS, KO*t*Bu, KH or a mixture of KO*t*Bu/KH in THF or toluene: 1,3-di-*tert*-butylimidazol-2-ylidene **2**,[8] 1,3-dimesitylimidazol-2-ylidene **4**,[9] 1,3-dimesitylimidazolin-2-ylidene,[10] 1,3-diisopropylimidazol-2-ylidene **5**[4].

1.2. Metal precursors

Mo(≡C-(p-OMe-C6H4)(Br)3(dme) ,[11] **Mo-1**,[12] **W-P1**[13] and **W-1**[14] were synthesized according to the literature.

2. General procedures

Alkyne homometathesis: A stock solution of the respective catalyst in toluene (7 mg·mL^{-1}) was prepared. 1-Phenyl-1-propyne (30 mg, 0.3 mmol, 1000 equiv.), *tert*-butylbenzene (approx. 2 drops, internal standard) and molecular sieves 5 Å (300 mg) were dissolved/suspended in toluene (2 mL) and a sample for GC-MS analysis was withdrawn. Then, the appropriate amount of stock solution (1 equiv. catalyst with respect to substrate, 7 mg·mL^{-1} in toluene) was added and the resulting reaction mixtures were stirred at 35 °C. After three and 15 hours samples for GC-MS were withdrawn.

Mechanistic investigations: A solution of the catalyst (approx. 10 mg, 1 equiv.) and CH_2Cl_2 (5 µL, internal standard) in C_6D_6 was prepared and the ^{1}H and ^{19}F NMR spectra were recorded.

The NMR sample was transferred back into the glove box and 1,1,1,3,3,3-hexafluoro-2-methyl-2-propanol (1 equiv.) was added and ^{1}H and ^{19}F NMR spectra were recorded again. The NMR sample was transferred into the glove box and 1-phenyl-1-propyne (5 equiv.) was added to the mixture. Subsequently ^{1}H and ^{19}F NMR spectra were recorded after indicated time spans. Finally, an aliquot of the reaction mixture was subjected to GC-MS analysis to confirm product formation.

3. Novel procedures

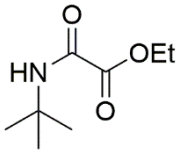

***N*-(*tert*-Butyl)-oxanilic acid ethyl ester (O3a):** Triethylamine (2.08 g, 20.50 mmol, 2.84 mL) was added dropwise over a period of 2 min to a solution of *tert*-butylamine (6.00 g, 82.03 mmol) in dry THF (150 mL) using standard Schlenk technique. The solution was cooled to 0 °C and stirred for 10 min. Ethylchlorooxoacetate (2.80 g, 20.50 mmol, 2.30 mL) was added slowly via a syringe, causing the precipitation of a colorless solid. The solution was stirred for 10 min at 0 °C, allowed to warm to room temperature and stirred for 2 h. The solid was filtered off, the organic layer was washed with 2 M HCl (2x100 mL) and the aqueous layer was then washed with ethyl acetate (100 mL). The combined organic layers were washed with brine (150 mL), dried over $MgSO_4$ and all volatiles were removed *in vacuo*. The product was isolated in form of a colorless liquid (2.52 g, 14.56 mmol, 71%): **^{1}H NMR** (400 MHz, $CDCl_3$): δ = 6.93 (s, 1H), 4.23 (q, 2H; $^{3}J_{HH}$ = 7.1 Hz; ROCH_2CH$_3$), 1.33 (s, 9H; *t*Bu), 1.30 (t, 3H, $^{3}J_{HH}$ = 7.2 Hz; ROCH$_2$CH_3) ppm; **^{13}C NMR** (100 MHz, $CDCl_3$): δ = 161.1, 155.4, 62.7, 51.5, 27.9, 13.7 ppm; **HRMS (ESI)** *m/z* calcd. for $C_8H_{15}NO_3Na^+$ $[M+Na]^+$ 196.0944, found 196.0944. **Anal. calcd.** for $C_8H_{15}NO_3$: C, 55.47; H, 8.73; N, 8.09. Found: C, 55.16; H,8.771; N, 8.00.

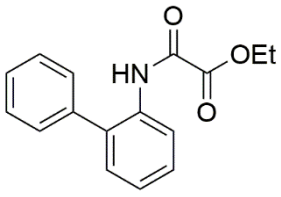

***N*-(2-[1,1'-Biphenyl])-oxanilic acid ethyl ester (O4a):** Triethylamine (3.64 g, 36.0 mmol, 4.99 mL) was added dropwise over a period of 2 min to a solution of 2-aminobiphenyl (7.00 g,

41.4 mmol) in dry THF (150 mL) using standard Schlenk technique. The solution was cooled to 0 °C and stirred for 10 min. Ethylchlorooxoacetate (4.91 g, 36.0 mmol, 4.03 mL) was added slowly via a syringe, causing the precipitation of a colorless solid. The solution was stirred for 10 min at 0 °C, allowed to warm to room temperature and stirred for 2 h. The solid was filtered off, the organic layer was washed with 2 M HCl (2x100 mL) and the aqueous layer was then washed with ethyl acetate (100 mL). The combined organic layers were washed with brine (150 mL), dried over $MgSO_4$ and all volatiles were removed *in vacuo*. The product was isolated in form of a colorless solid (9.16 g, 34.0 mmol, 82%): **^{1}H NMR** (400 MHz, $CDCl_3$): δ = 9.10 (s, 1H, N-*H*), 8.48 (dd, $J_{H\text{-}H}$ = 8.3, 1.1 Hz, 1H), 7.55 – 7.50 (m, 2H), 7.48 – 7.37 (m, 4H), 7.33 – 7.30 (m, 1H), 7.28 – 7.23 (m, 1H), 4.32 (q, $^3J_{H\text{-}H}$ = 7.2 Hz, 2H, Et), 1.35 (t, $^3J_{H\text{-}H}$ = 7.2 Hz, 3H, Et) ppm; **^{13}C NMR** (100 MHz, $CDCl_3$): δ = 160.8 (*C*=O), 153.8 (*C*=O), 137.4, 133.6, 132.7, 130.3, 129.4, 129.4, 128.8, 128.5, 125.5, 120.5, 63.7, 14.1 ppm. **Anal. calcd.** for $C_{16}H_{15}NO_3$: C, 71.36; H, 5.61; N, 5.20. Found: C, 71.49; H, 5.68; N, 5.31.

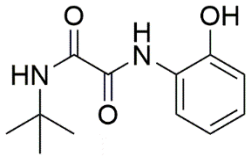

***N*-(*tert*-Butyl)-*N*'-(2-hydroxyphenyl)-oxalamide (O3b):** **O3a** (2.5 g, 14.51 mmol) and 2-aminophenol (1.89 g, 17.34 mmol) were dissolved in toluene (70 mL). Triethylamine (2.93 g, 28.90 mmol, 4.01 mL) was added and the suspension was heated to reflux overnight; then the solution was allowed to cool to room temperature. The precipitated product was re-dissolved through addition of ethyl acetate (250 mL). The solution was washed with 2 M HCl (2x100 mL) and the aqueous layer was then washed with ethyl acetate (100 mL). The combined organic layers were washed with brine (150 mL), dried over $MgSO_4$ and all volatiles were removed *in vacuo*. The product was isolated in form of a colorless solid (3.07 g, 13.01 mmol, 90%): **^{1}H NMR** (400 MHz, $CDCl_3$): δ = 9.67 (s, 1H), 8.47 (s, 1H), 7.60 (dd, 1H, $J_{H\text{-}H}$ = 8.0, 1.5 Hz), 7.52 (s, 1H), 7.11 (ddd, 1H, $J_{H\text{-}H}$ = 8.1, 7.4, 1.6 Hz), 6.97 (dd, 1H, $J_{H\text{-}H}$ = 8.1, 1.4 Hz), 6.91 (ddd, 1H, $J_{H\text{-}H}$ = 8.1, 7.4, 1.6 Hz), 1.46 (s, 9H) ppm; **^{13}C NMR** (100 MHz, CD_3CN): δ = 159.9, 159.3, 147.8, 126.6, 126.2, 116.6, 121.4, 121.3, 52.3, 28.4 ppm. **Anal. calcd.** for $C_{12}H_{16}N_2O_3$: C, 61.00; H, 6.83; N, 11.86. Found: C, 60.90; H, 6.85; N, 11.66.

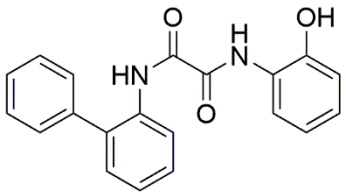

***N*-([1,1'-Biphenyl-2-yl])-*N*'-(2-hydroxyphenyl)-oxalamide (O4b): O4a** (7.00 g, 26.0 mmol) and 2-aminobiphenol (3.40 g, 31.2 mmol) were dissolved in toluene (70 mL). Triethylamine (5.26 g, 52.0 mmol, 7.21 mL) was added and the suspension was heated to reflux overnight. The solution was allowed to cool to room temperature. The precipitated product was redissolved through addition of ethyl acetate (250 mL). The solution was washed with 2 M HCl (2x100 mL) and the aqueous layer was then washed with ethyl acetate (100 mL). The combined organic layers were washed with brine (150 mL), dried over $MgSO_4$ and all volatiles were removed *in vacuo*. The product was isolated in form of a colorless solid (7.83 g, 23.6 mmol, 91%): **^{1}H NMR** (400 MHz, $CDCl_3$): δ = 9.61 (s, 1H, N-*H*), 9.47 (s, 1H N-*H*), 8.44 (d, $^3J_{H\text{-}H}$ = 8.2 Hz, 1H), 7.62 – 7.52 (m, 3H), 7.52 – 7.40 (m, 5H), 7.40 – 7.34 (m, 1H), 7.30 (t, $^3J_{H\text{-}H}$ = 7.4 Hz, 1H), 7.20 – 7.11 (m, 1H), 7.01 – 6.89 (m, 2H) ppm; **^{13}C NMR** (100 MHz, $CDCl_3$): δ = 158.7 (*C*=O), 157.0 (*C*=O), 148.4 (O-C_{Ar}), 137.8 (N-C_{Ar}), 133.7 (N-C_{Ar}), 131.0, 129.8, 129.8, 129.0, 128.9, 128.0, 126.1, 124.6, 122.6, 121.5, 121.0, 119.1 ppm. **Anal. calcd.** for $C_{20}H_{16}N_2O_3$: C, 72.28; H, 4.89; N, 8.47. Found: C, 72.01; H, 4.93; N, 8.50.

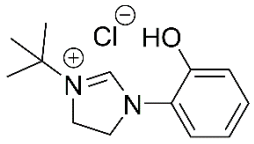

1-(*tert*-Butyl)-3-(2-hydroxyphenyl)-4,5-dihydroimidazolium chloride (HO3·HCl): BH_3-THF (1M in THF, 100 mL) was added slowly via a syringe to **O3b** (3.00 g, 12.71 mmol) using standard Schlenk technique, causing the colorless solution to turn orange. The solution was heated to reflux overnight. The now colorless solution was allowed to cool to room temperature. Methanol (100 mL) was added slowly, followed by the addition of conc. HCl (4.5 mL). All volatiles were removed *in vacuo*. The residue was dissolved in methanol (200 mL) and the solvent was removed under reduced pressure. The procedure was repeated three times to remove the remaining boron as $B(OMe)_3$. Triethyl orthoformate (40 mL) was added and the suspension was heated to 100 °C for 5 min, causing the product to precipitate. The solid was filtered off and washed with diethyl ether and methylene chloride. The product was isolated in form of a colorless solid (2.07 g, 9.53 mmol, 75%): **^{1}H NMR** (400 MHz, DMSO-d_6): δ = 11.12 (s, 1H), 8.92 (s, 1H), 7.35 (dd, $^3J_{H\text{-}H}$ = 8.0 Hz, $^4J_{H\text{-}H}$ = 1.6 Hz, 1H), 7.25 (dd, $^3J_{H\text{-}H}$ = 8.2, $^4J_{H\text{-}H}$ = 1.5 Hz, 1H), 7.22 – 7.13 (m, 1H), 6.93 – 6.83 (m, 1H), 4.44 – 4.31 (m, 2H), 4.18 – 4.08 (m, 2H), 1.42 (s, 9H) ppm; **^{13}C NMR** (100 MHz, DMSO-d_6): δ = 155.1, 150.6, 128.4, 124.1, 123.6, 119.3, 117.0, 56.7, 49.9, 44.9, 27.4 ppm; **HRMS (ESI)** *m/z* calcd. for $C_{13}H_{19}N_2O^+$ $[M]^+$ 219.1492, found 219.1492.

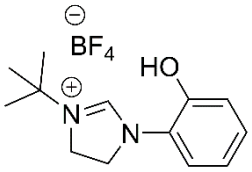

1-(*tert*-Butyl)-3-(2-hydroxyphenyl)-4,5-dihydroimidazolium tetrafluoroborate (HO3·HBF$_4$): **HO3·HCl** (2.31 g, 7.6 mmol, 1 eq) was dissolved in acetonitrile and a solution of $NaBF_4$ (0.92 g, 8.4 mmol, 1.1 eq) in water was added and the solution was stirred overnight. All volatiles were removed and the residue was taken up in CH_2Cl_2 and washed with water (2 x 100 mL). The organic phase was dried over $MgSO_4$ and all the volatiles were removed under reduced pressure. The resulting solid was crystallized from CH_2Cl_2 (1.75 g, 5.7 mmol, yield: 75%). **^{1}H NMR** (400 MHz, DMSO-d_6) δ = 10.67 (s, 1H) 8.90 (s, 1H), 7.36 (dd, $^3J_{H\text{-}H}$ = 8.0 Hz, $^4J_{H\text{-}H}$ = 1.6 Hz, 1H), 7.20 (ddd, $^3J_{H\text{-}H}$ = 8.2 Hz, 7.4 Hz,$^4J_{H\text{-}H}$ = 1.6 Hz, 1H), 7.04 (dd, $^3J_{H\text{-}H}$ = 8.2 Hz, $^4J_{H\text{-}H}$ = 1.3 Hz, 1H), 6.91 – 6.96 (m, 1H), 4.36 (dd, $^2J_{H\text{-}H}$ = 12.4 Hz, $^3J_{H\text{-}H}$ = 9.0 Hz, 2H), 4.13 (dd, $^2J_{H\text{-}H}$ = 12.3 Hz, $^3J_{H\text{-}H}$ = 9.1 Hz, 2H), 1.43 (s, 9H) ppm; **^{13}C NMR** (101 MHz, CD_3CN) δ = 155.5, 150.5, 129.7, 125.0, 123.9, 121.7, 117.9, 58.3, 51.1, 46.0, 27.9 ppm; **^{19}F NMR** (376 MHz, CD_3CN) δ =-151.78, -151.73, ppm; . **Anal. calcd.** for $C_{13}H_{19}N_2OBF_4$: C, 51.01; H, 6.26: N, 9.15. Found: C, 51.01; H, 6.42; N, 9.27.

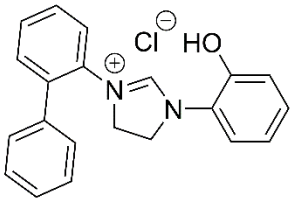

1-([1,1'-Biphenyl-2-yl])-3-(2-hydroxyphenyl)-4,5-dihydroimidazolium chloride (HO4·HCl): BH_3-THF (1M in THF, 150 mL) was added slowly via a syringe to **O4b** (6.00 g, 18.1 mmol) using standard Schlenk technique, causing the colorless solution to turn orange. The solution was heated to reflux overnight. The now colorless solution was allowed to cool to room temperature. Methanol (100 mL) was added slowly, followed by the addition of conc. HCl (4.5 mL). All volatiles were removed *in vacuo*. The residue was dissolved in methanol (200 mL) and the solvent was removed under reduced pressure. The procedure was repeated three times to remove the remaining boron as $B(OMe)_3$. Triethyl orthoformate (50 mL) was added and the suspension was heated to 100 °C for 5 min, causing the product to precipitate. The solid was filtered off and washed with diethyl ether and methylene chloride. The product was isolated in form of a colorless solid (5.30 g, 15.1 mmol, 84%): **^{1}H NMR** (400 MHz, DMSO-d_6): δ = 11.11 (s, 1H, N-C*H*-N), 9.11 (s, 1H, O-*H*), 7.78 – 7.72 (m, 1H), 7.63 – 7.57 (m, 2H), 7.57 – 7.51 (m, 5H),

7.51 – 7.44 (m, 1H), 7.22 – 7.18 (m, 2H), 7.16 (d, $^{3}J_{H\text{-}H}$ = 7.9 Hz, 1H), 6.91 – 6.84 (m, 1H), 4.40 (m, 2H, CH_2), 4.14 (m, 2H, CH_2) ppm; **^{13}C NMR** (100 MHz, DMSO-d_6): δ = 157.6 (N*C*N), 150.6 (O-C_{Ar}), 137.1 (N-C_{Ar}), 137.0 (N-C_{Ar}), 134.0, 131.4, 129.7, 129.2, 129.2, 129.1, 128.8, 128.4, 126.1, 123.4, 123.2, 119.4, 117.1, 50.8, 50.6 ppm; **HRMS (ESI)** *m/z* calcd. for $C_{21}H_{19}N_2O^+$ $[M]^+$ 315.1492, found 315.1492.

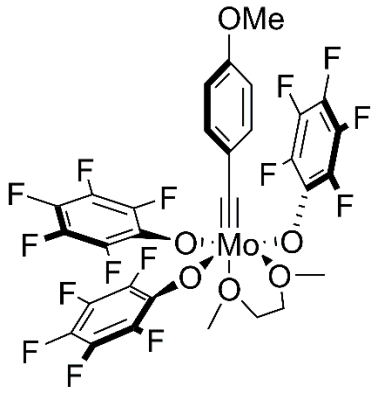

Synthesis of *p*-OMe-C_6H_4≡Mo$(OC_6F_5)_3$(DME) (Mo-2): Mo(≡C-(p-OMe-C6H4)$(Br)_3$(dme) (813 mg, 1.5 mmol) was dissolved in diethyl ether and cooled to -40 °C. A suspension of potassium pentafluorophenoxide (995 mg, 4.5 mmol) in diethyl ether was added and the mixture was stirred overnight. Subsequently solvent was removed and the resulting residue was dissolved in CH_2Cl_2 and filtered over celite. Again, all volatiles were removed and the resulting residue was crystallized from a mixture of diethyl ether and *n*-pentane to afford **Mo-2** in 60% isolated yield. **^{1}H NMR** (400 MHz, CD_2Cl_2): δ = 6.63 (d, $^{3}J_{H\text{-}H}$ = 8.8 Hz, 2H, H_{Ar}), 6.20 (d, $^{3}J_{H\text{-}H}$ = 8.7 Hz, 2H, H_{Ar}), 3.64 (s, 3H, Me), 3.42 (s, 4H), 3.23 (s, 6H) ppm. **^{19}F NMR** (375 MHz, CD_2Cl_2): δ = -161.51 (d, $^{3}J_{F\text{-}F}$ = 24.4 Hz, 2F), -166.90 (t, $^{3}J_{F\text{-}F}$ = 22.3 Hz, 2F), -171.52 (s, 1F) ppm. **^{13}C NMR** (100 MHz, CD_2Cl_2): δ = 302.2 (Mo≡*C*), 161.5 (N-*C*-N), 145.4 (t, $^{2}J_{CF}$ = 13.0 Hz), 139.8 (dd, $^{1}J_{C\text{-}F}$ = 243.3 Hz, $^{2}J_{C\text{-}F}$ = 11.2 Hz, C_6F_5), 138.6 (dt, $^{1}J_{C\text{-}F}$ = 247.3 Hz, $^{2}J_{C\text{-}F}$ = 13.6 Hz, C_6F_5), 136.2, 135.2 (dt, $^{1}J_{C\text{-}F}$ = 243.5 Hz, $^{2}J_{C\text{-}F}$ = 13.9 Hz, C_6F_5), 132.0 (C_{Ar}), 113.6 (C_{Ar}), 55.9 (Me) ppm. **Anal. calcd.** for $C_{30}H_{17}O_6F_{15}Mo$: C 42.17, H 2.01. Found: C 42.34, H 2.195.

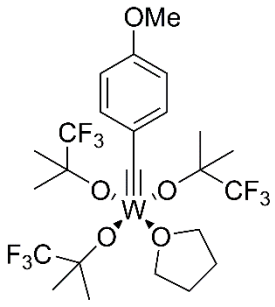

***p*-OMe-C_6H_4C≡W$(OC(CF_3)(CH_3)_2)_3$·THF (W-2)**: $LiOC(CF_3)(CH_3)_2$ (0.22 g, 1.62 mmol, 3.1 equiv.) was dissolved in THF and **W-P1** (0.33 g, 0.52 mmol, 1 equiv.) was added at room temperature in

portions as a solid. The clear solution was stirred overnight at room temperature and the solvent was removed under reduced pressure. After extraction with *n*-pentane, the yellowish green solution was filtered through celite and the solvent was concentrated *in vacuo*. The product was isolated in the form of yellow crystals by recrystallization from *n*-pentane / Et_2O (0.35g, 0.47 mmol, yield: 90%). **^{1}H NMR** (400 MHz, C_6D_6) δ = 7.04 – 7.08 (m, 2H; Ar*H*), 6.76 – 6.79 (m, 2H; Ar*H*), 3.82 – 3.89 (m, 4H; THF), 3.31 (s, 3H; OCH_3-Ar), 1.62 (s, 18H; -CH_3), 1.40 – 1.46 (m, 4H; THF) ppm; **^{19}F NMR** (375 MHz, C_6D_6) δ = -82.44 ppm; **^{13}C NMR** (100 MHz, C_6D_6) δ = , 263.3 (W≡*C*), 159.3, 140.7, 135.0, 128.2 (q, $^1J_{C\text{-}F}$ = 284.7 Hz, *C*F_3), 113.2, 82.3 (q, $^2J_{C\text{-}F}$ = 28.3 Hz, *C*(CF_3)Me_2)*, 68.8 (THF), 54.9, 25.6 (THF), 25.5 ppm. Despite numerous efforts, inconsistent elemental analysis data were obtained**.**

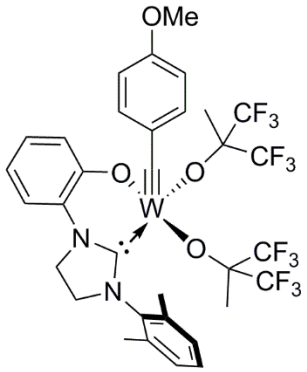

Alternative route for the synthesis of *p*-OMe-C_6H_4C≡W(O1)(OCMe(CF_3)$_2$)$_2$ (W-3): HO1·HBF_4 (0.05 g, 0.14 mmol, 1 equiv.) was suspended in THF and at -40 °C. LiHMDS (0.05 g, 0.30 mmol, 2.1 equiv.) was added as a solid. The yellow reaction mixture was stirred for one hour at room temperature and then cooled again to -40 °C. Separately, **W-1** (0.13 g, 0.14 mmol, 1 equiv.) was dissolved in THF and added dropwise at -40 °C to the NHC solution. The reaction mixture was stirred overnight, filtered through celite and the solvent was removed under reduced pressure. The residue was washed with *n*-pentane and the clean orange product **W-3** was crystallized from diethyl ether (0.05 g, 0.05 mmol, yield: 38%). NMR spectra were identical to those reported in the manuscript: **^{1}H NMR** (400 MHz, C_6D_6) δ = 7.38 (dd, $^3J_{H\text{-}H}$ = 8.1, $^4J_{H\text{-}H}$ = 0.9 Hz; 1H) 7.02 (ddd, $^3J_{H\text{-}H}$ = 8.1, 7.5, $^4J_{H\text{-}H}$ = 1.6 Hz; 1H,), 6.85 – 6.70 (m, 4H), 6.56 – 6.47 (m, 3H), 6.46 – 6.41 (m, 2H), 3.13 (s, 3H), 3.11– 2.93 (m, 2H), 2.80 – 2.71 (m, 1H), 2.59 – 2.47 (m, 1H), 2.17 (s, 3H), 2.10 (s, 3H), 1.99 (s, 3H), 1.72 (s, 3H) ppm; **^{19}F NMR** (375 MHz, C_6D_6) δ = -75.91 (q, $^4J_{F\text{-}F}$ = 8.9 Hz, 3F), -76.46 (q, $^4J_{F\text{-}F}$ = 9.8 Hz, 3F), -76.98 (q, $^4J_{F\text{-}F}$ = 9.1 Hz, 3F), -77.31 (q, $^4J_{F\text{-}F}$ = 9.1 Hz, 3F) ppm; **^{13}C NMR** (100 MHz, C_6D_6) δ = 292.9 (W≡*C*), 215.1 (N*C*N), 160.4, 160.1, 138.8, 138.2, 135.4, 135.2, 134.1, 133.1, 129.7, 129.5, 125.9, 122.0 (m, *C*F_3)*, 119.7, 118.3, 117.9, 112.3, 82.9 (m, *C*(CF_3)$_2$Me)**, 54.6, 53.1, 49.2, 20.7, 19.7, 19.2, 19.1 ppm; **Anal. calcd.** for

$C_{33}H_{30}F_{12}WN_2O_4$: C, 42.60; H, 3.25; N, 3.01. Found: C, 42.75; H, 3.22; N, 3.15. *Quartet signals poorly resolved, overlapping with the C_6D_6 signals. **Septet poorly resolved.

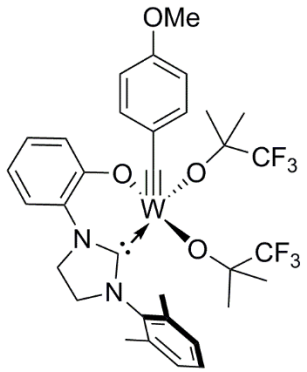

Alternative route for the synthesis of *p*-OMe-C_6H_4C≡W(O1)(OC(CF_3)Me_2)$_2$ (W-6): W-6 was prepared analogously to **W-3** by the reaction of **HO1·HBF_4** with **W-2** in THF and isolated as yellow solid (0.04 g, 0.05 mmol, yield: 30%). NMR Spectra were identical to those reported in the manuscript: **^{1}H NMR** (400 MHz, $CDCl_3$) δ=7.17 – 7.11 (m, 4H), 7.07 (m, 2H), 6.91 – 6.83 (m, 1H), 6.56 (d, $^3J_{H\text{-}H}$ = 9.0 Hz, 2H), 6.12 (d, $^3J_{H\text{-}H}$ = 8.9 Hz, 2H), 4.55 – 4.43 (m, 1H), 4.20 – 4.04 (m, 2H), 3.69 (s, 3H), 3.62 (m, 1H), 2.42 (s, 3H), 2.21 (s, 3H), 1.62 (s, 3H), 1.50 (s, 3H), 1.35 (s, 3H), 0.74 (s, 3H). **^{19}F NMR** (375 MHz, $CDCl_3$) δ = -80.97 (s, 3F), -82.01 (s, 3F). **^{13}C NMR** (100 MHz, $CDCl_3$) δ = 284.9 (W≡*C*), 217.7 (NCN), 161.8, 158.5, 139.5, 139.3, 135.1, 134.6, 134.2, 133.1, 129.9, 129.6, 128.3, 127,9 (q, $^1J_{C\text{-}F}$ = 285.3 Hz, *C*F_3), 126.6 (q, $^1J_{C\text{-}F}$ = 286.9 Hz, *C*F_3)*, 125.2, 118.5, 117.5, 117.0, 112.0, 80.7 (q, $^2J_{C\text{-}F}$ = 28.6 Hz, *C*(CF_3)Me_2), 98.0 (q, $^2J_{C\text{-}F}$ = 28.3 Hz, *C*(CF_3)Me_2) , 55.3, 53.6, 49.5, 26.1, 25.6, 25.3, 23.2, 20.0, 19.1 ppm; **Anal. calcd.** for $C_{33}H_{36}F_6WN_2O_4$: C, 48.19; H, 4.41; N, 3.41. Found: C, 48.18; H, 4.50; N, 3.39. *One signal of quartet overlaps with signal at δ = 125.19 ppm.

4. *Deprotonation of **HO3·HBF$_4$** and **HO3·HCl***

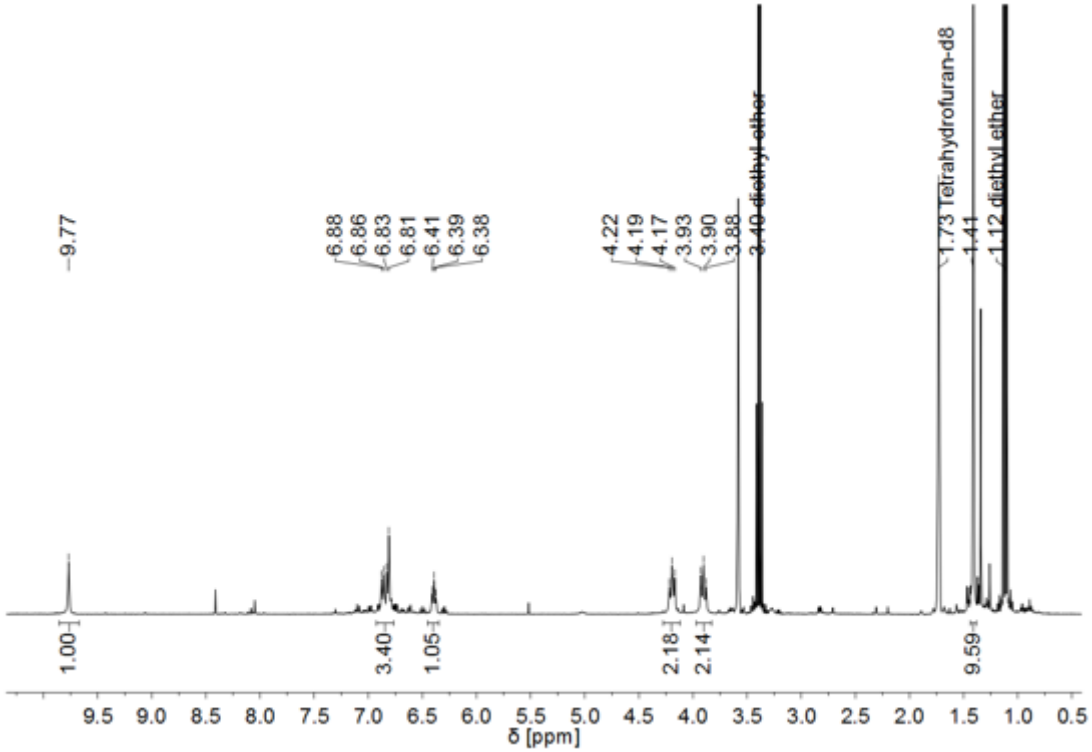

Figure S1: ^{1}H NMR (400 MHz, THF-d$_8$) spectrum of the crude reaction mixture of the deprotonation of **HO3·HBF$_4$** with two equivalents KH in THF-d8. Remaining signal of the imidazolium proton at δ = 9.77 ppm.

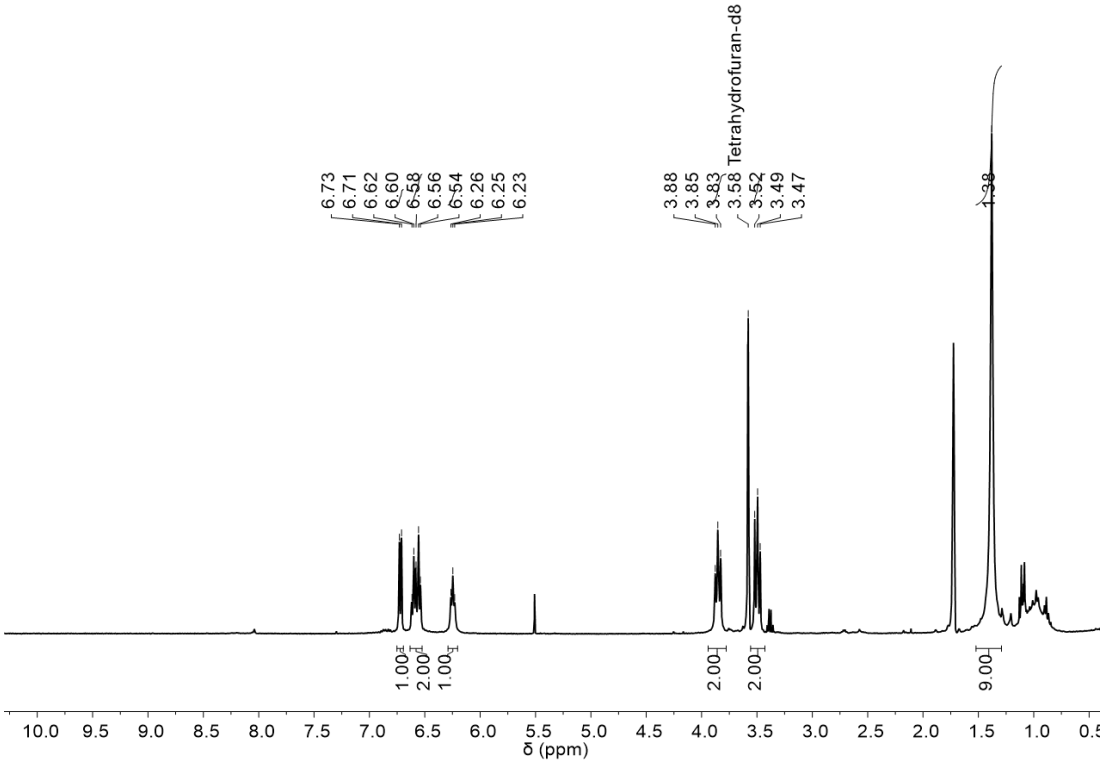

Figure S2: ^{1}H NMR (400 MHz, THF-d$_8$) spectrum of the crude reaction mixture of the deprotonation of **HO3·HCl** with two equivalents LiHMDS in THF-d8. Complete deprotonation was observed.

5. Calculation of Tolman´s electronic parameter

In Gusev's seminal publication on the calculation of Tolman's electronic parameter of 76 NHCs,[15] no values are given for the NHCs used in complexes **Mo-4** and **Mo-5**. Therefore, these parameters haenve be calculated.

We used the M06[16] functional and the def2-TZVPP basis set[17] to determine the symmetric vibration of CO in the corresponding $Ni(NHC)(CO)_3$ complexes. DFT calculations were done using the Turbomole v. 7.0.1 program package.[18] SCF energies were converged up to the point where the energy of two successive iterations did not change by more than 10^{-9} atomic units. The fine *m5* grid was used for the integration of the electron density. We optimized the geometries to the maximum where the component of the nuclear gradient did not change by more than $4.5 \cdot 10^{-04}$ atomic units. Optimized structures were proven to be true minima by the absence of any imaginary frequencies. Geometry optimization was done using the DL-Find optimization library,[19] which was interfaced to Turbomole via the Chemshell interface.[20] To obtain the correct values for the electronic Tolman parameters, the harmonic frequencies were scaled with 0.953 according to Alecu *et al*.[21]

The Cartesian coordinates of the optimized structures are given in the supporting xyz-file.

6. *Spectra of novel compounds*

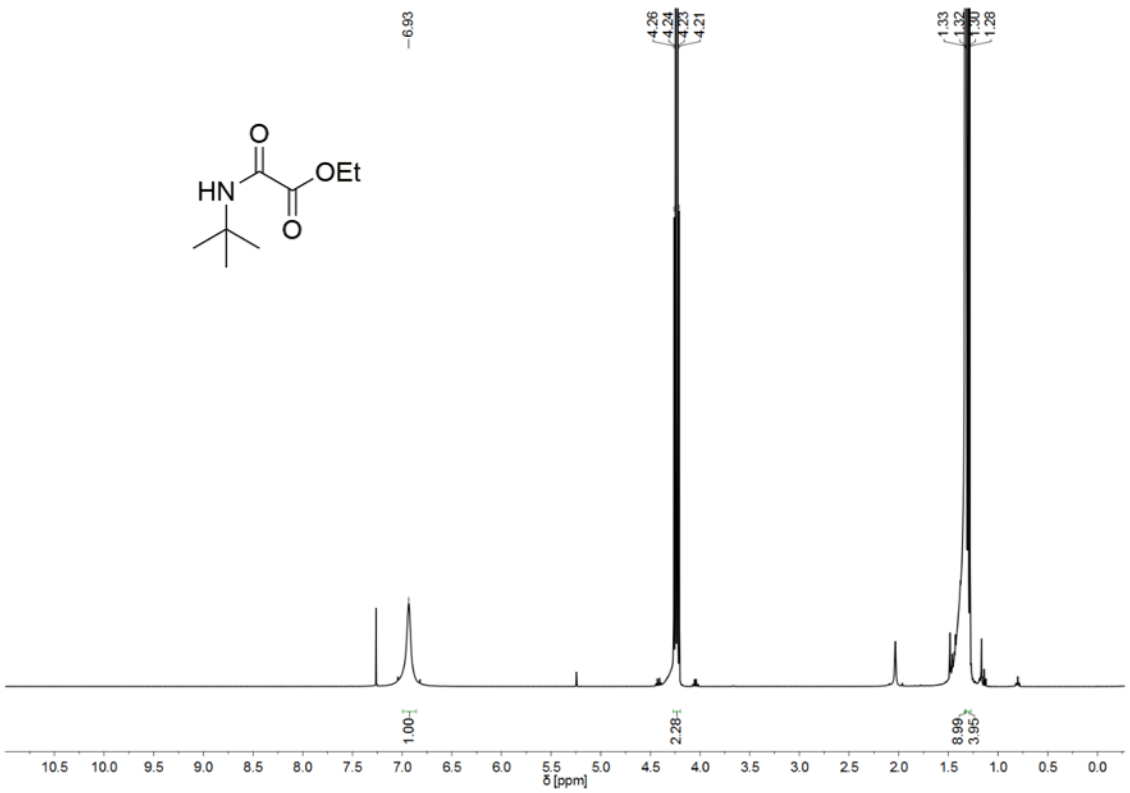

Figure S3: ^{1}H NMR (400 MHz, $CDCl_3$) spectrum of **O3a**.

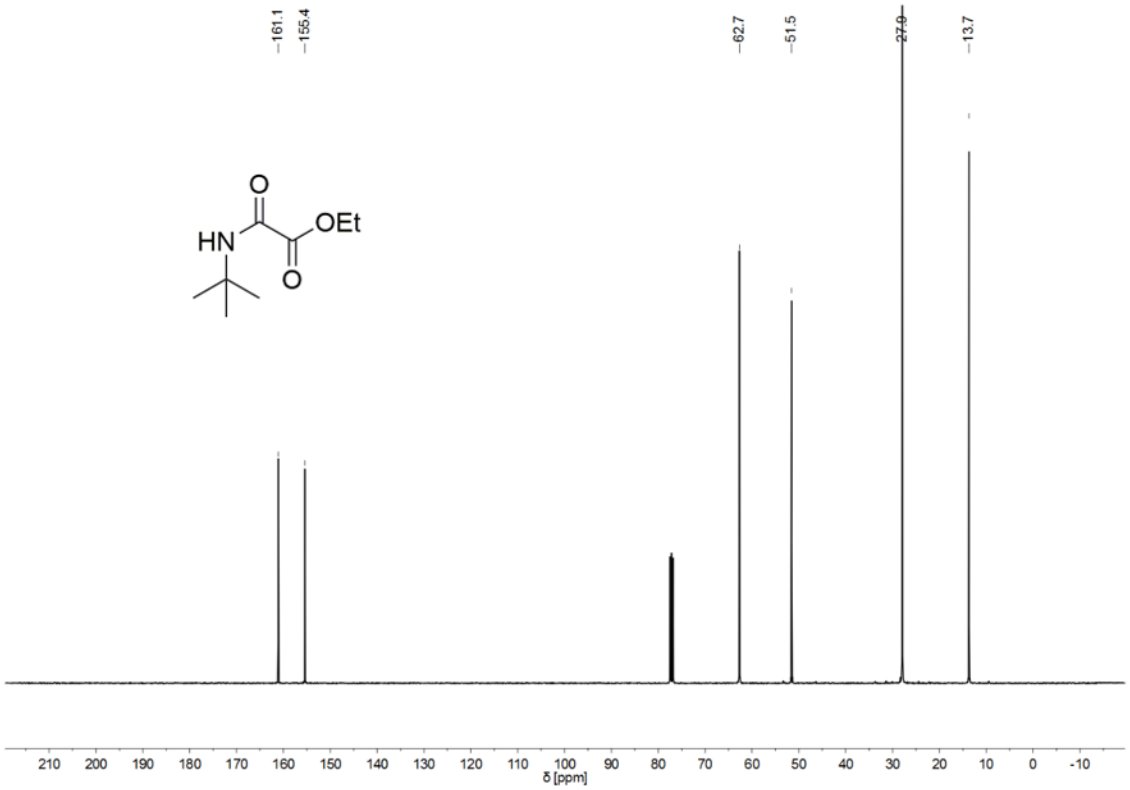

Figure S4: ^{13}C NMR (100 MHz, $CDCl_3$) spectrum of **O3a**.

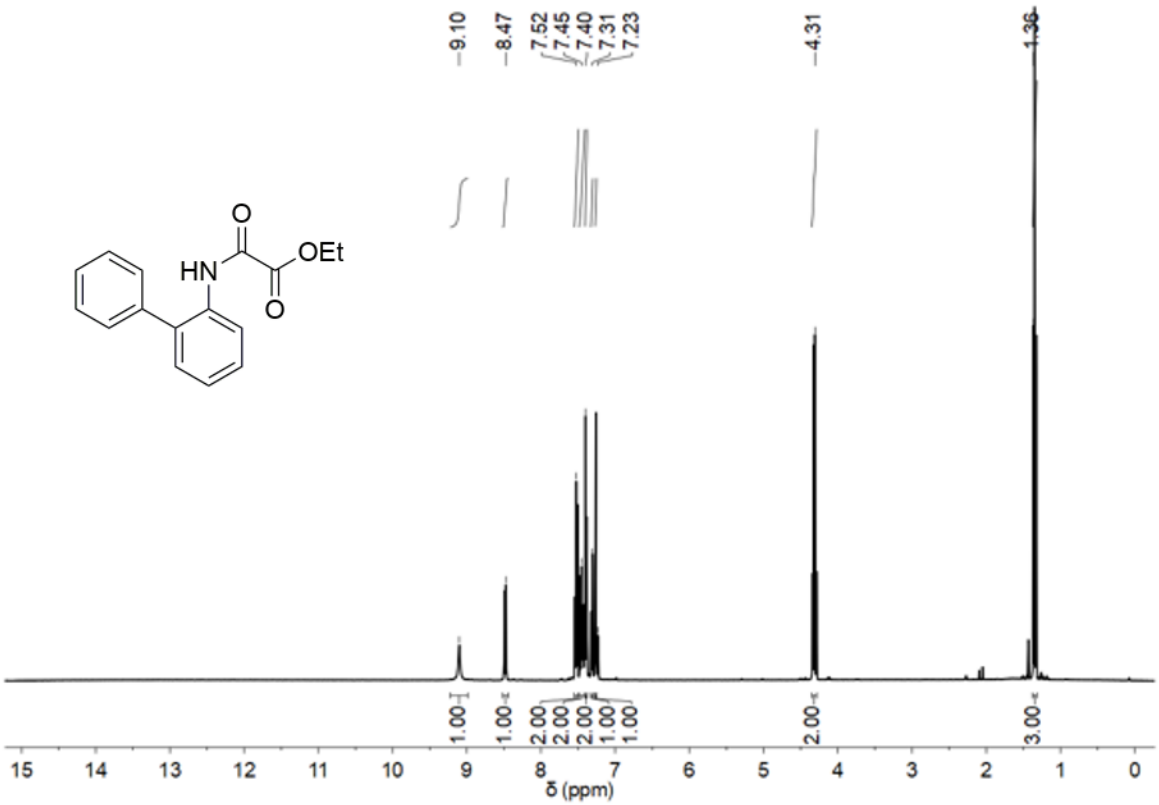

Figure S5: ^{1}H NMR (400 MHz, $CDCl_3$) spectrum of **O4a**.

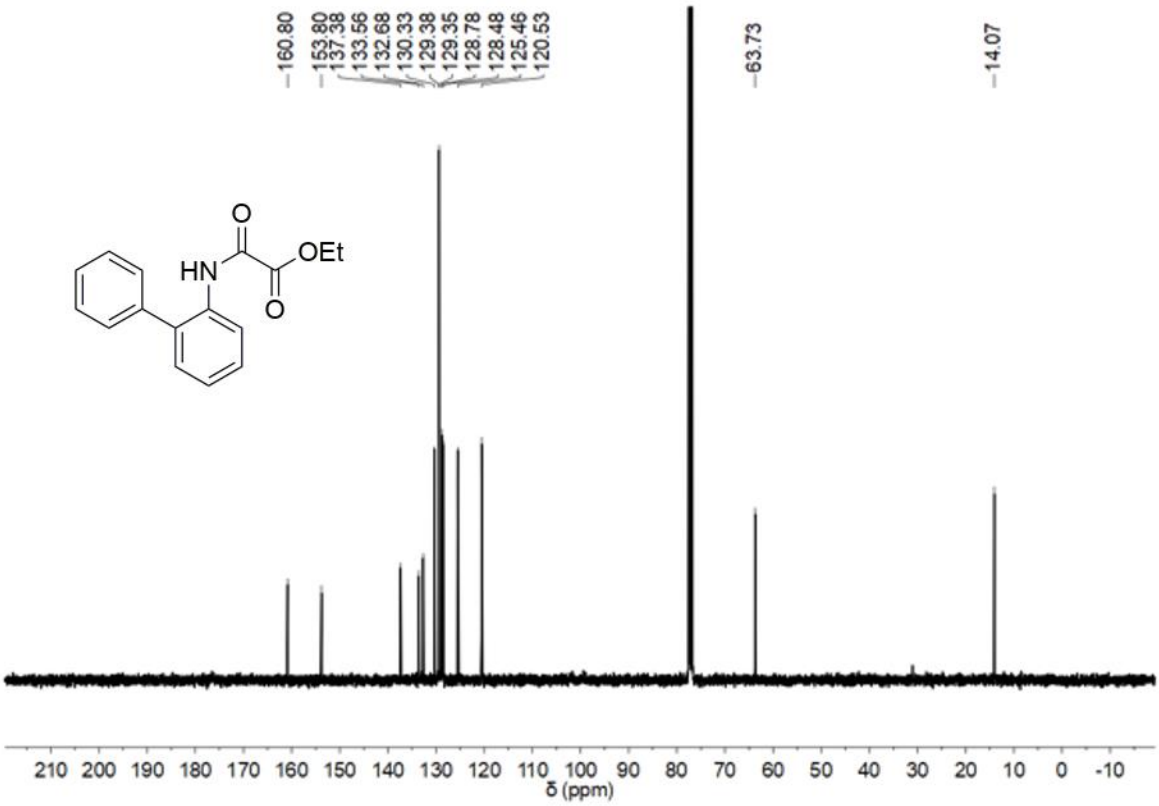

Figure S6: ^{13}C NMR (100 MHz, $CDCl_3$) spectrum of **O4a**.

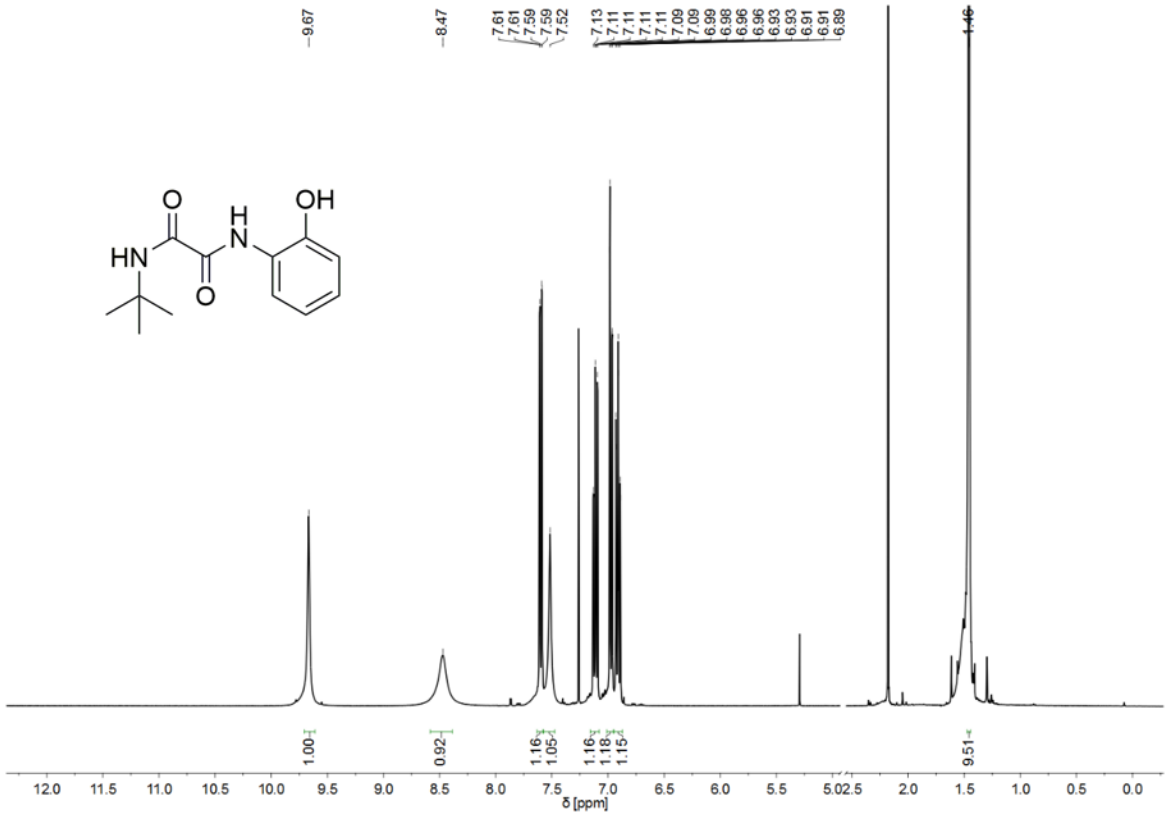

Figure S7: ^{1}H NMR (400 MHz, CD_2Cl_2) spectrum of **O3b**.

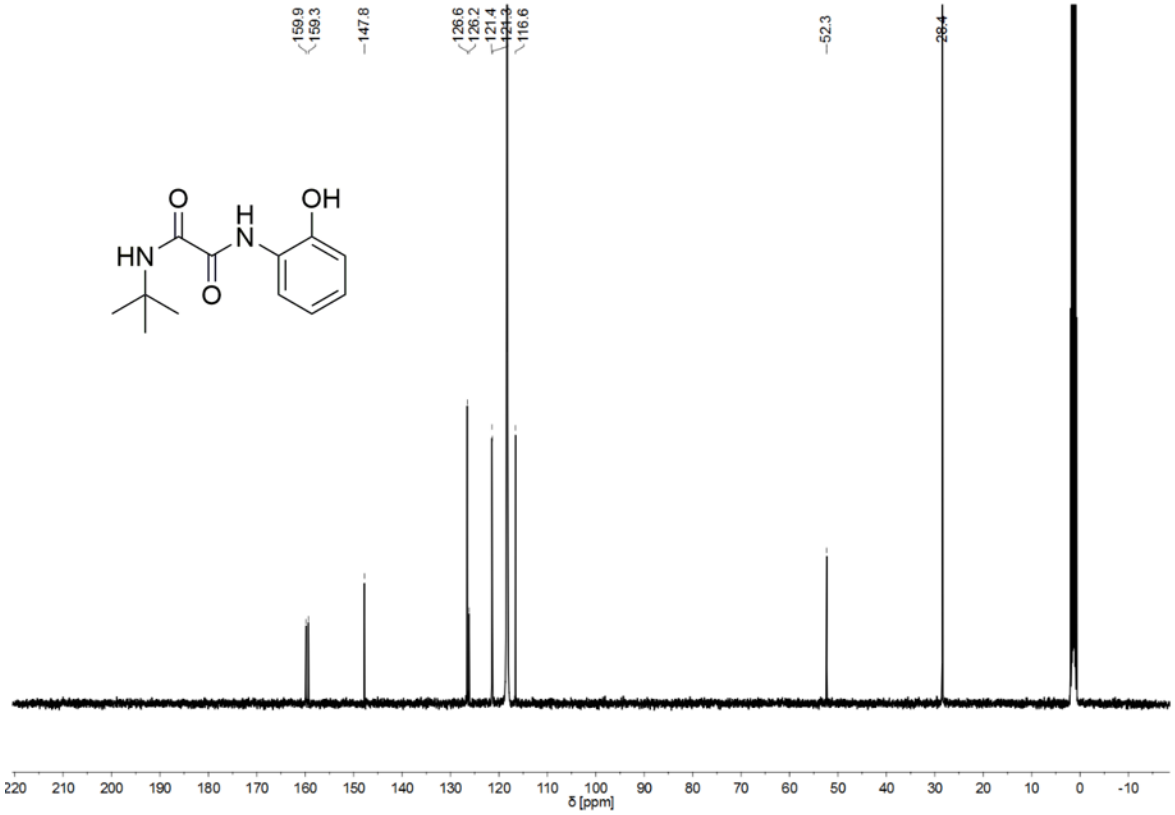

Figure S8: ^{13}C NMR (100 MHz, CD_2Cl_2) spectrum of **O3b**.

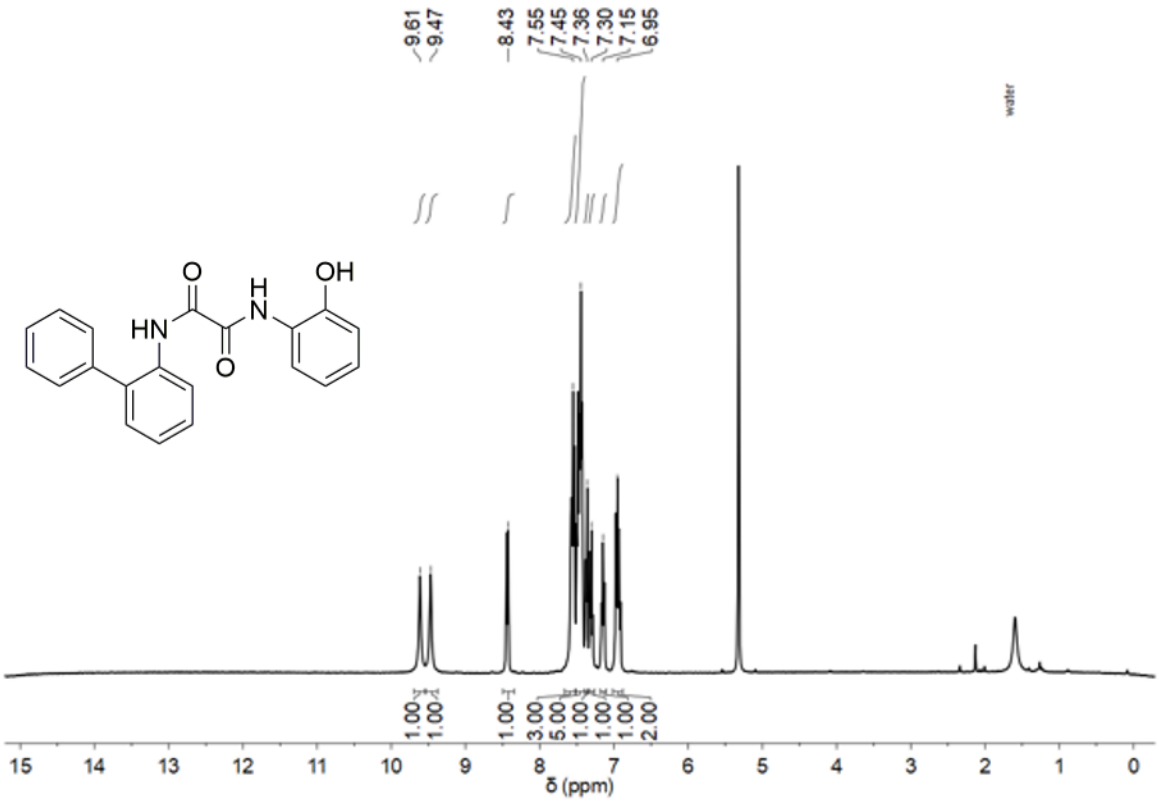

Figure S9: ^{1}H NMR (400 MHz, CD_2Cl_2) spectrum of **O4b**.

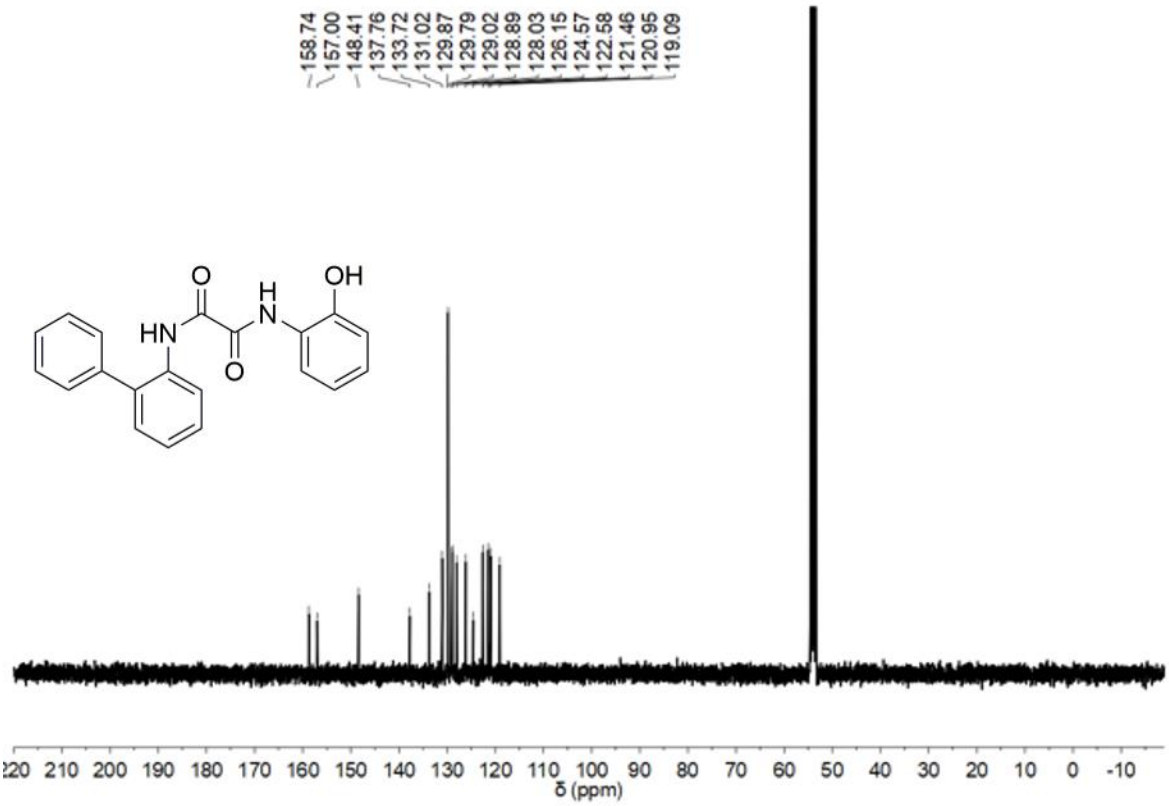

Figure S10: ^{13}C NMR (100 MHz, CD_2Cl_2) spectrum of **O4b**.

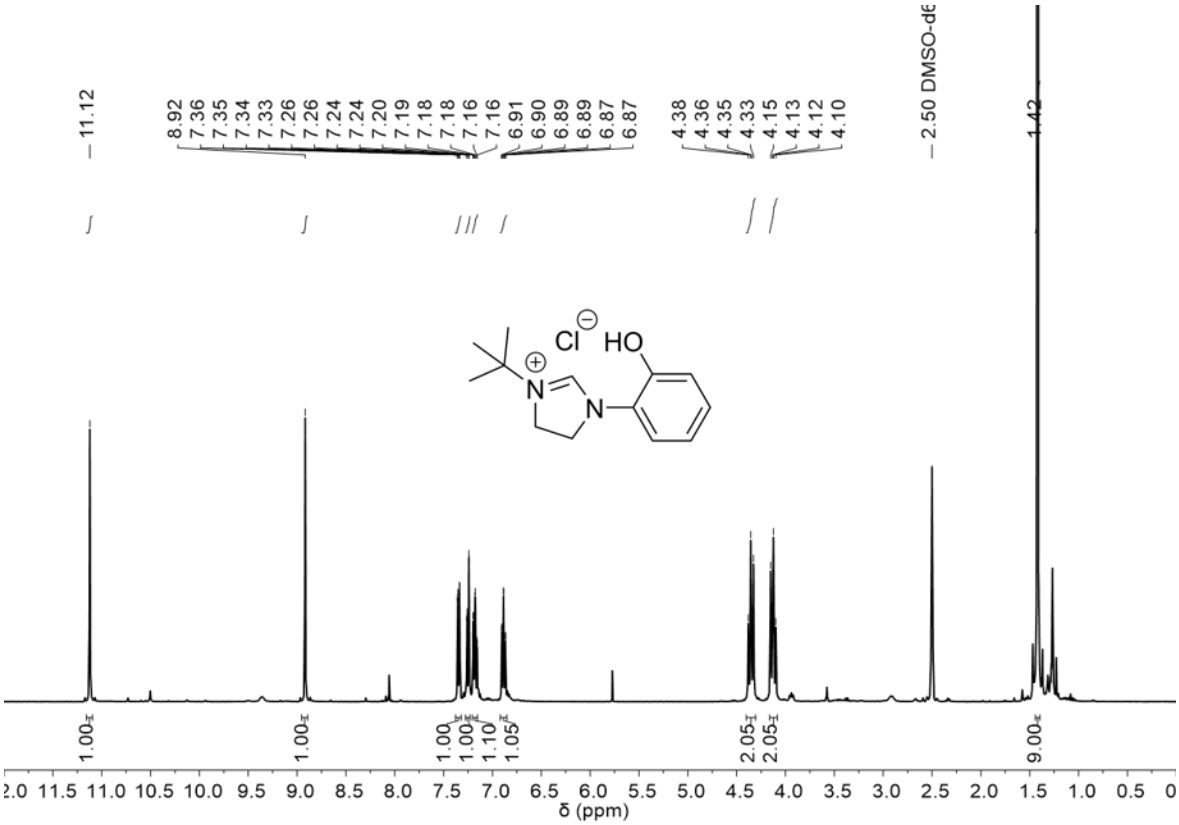

Figure S11: ^{1}H NMR (400 MHz, DMSO-d_6) spectrum of **HO3·HCl**.

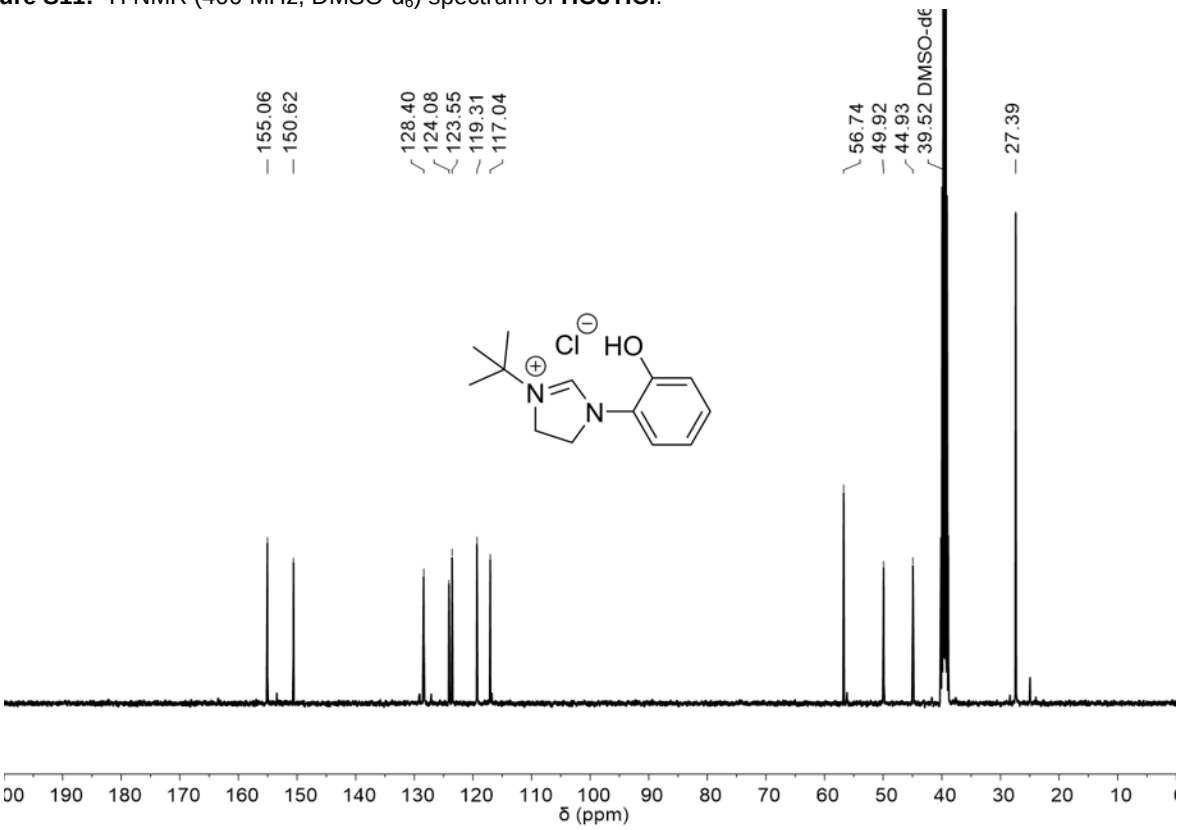

Figure S12: ^{13}C NMR (100 MHz, DMSO-d_6) spectrum of **HO3·HCl**.

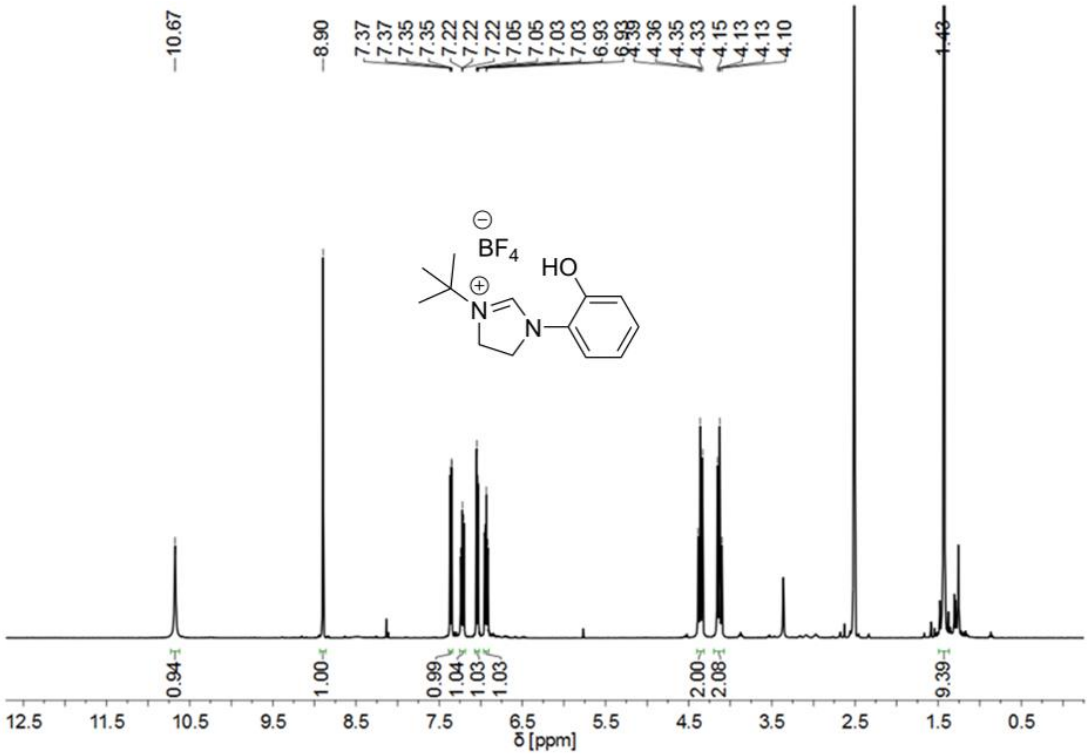

Figure S13: ^{1}H NMR (400 MHz, DMSO-d_6) spectrum of **HO3·HBF$_4$.**

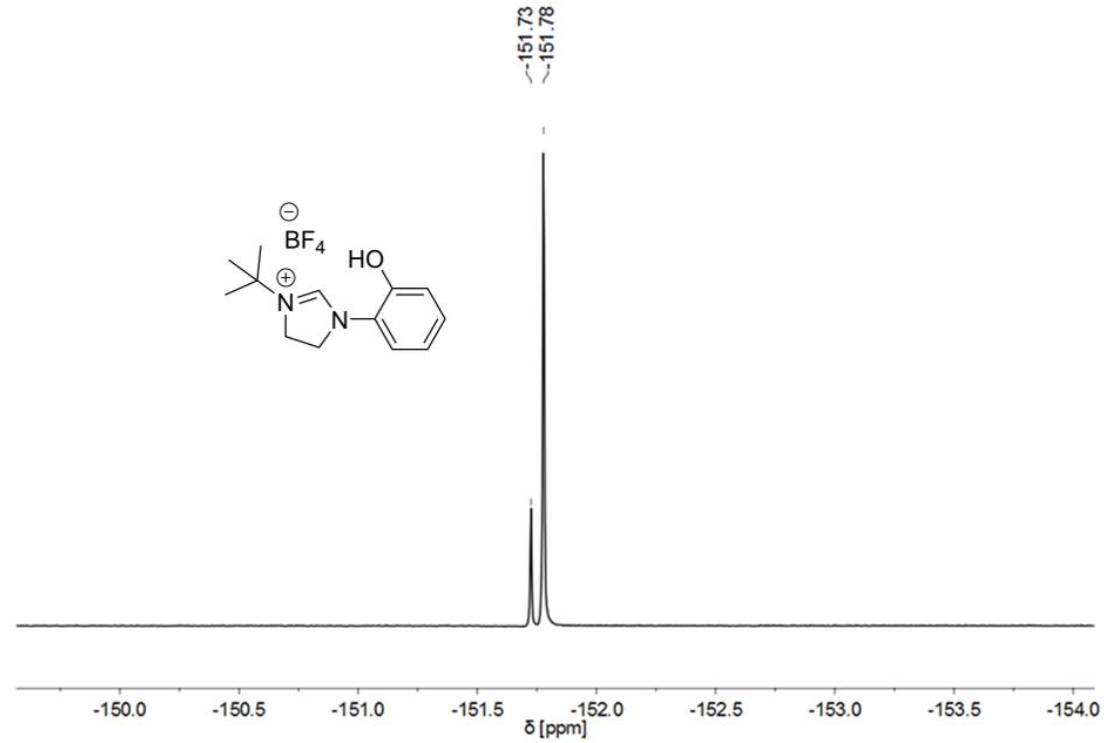

Figure S14: ^{19}F NMR (375 MHz, DMSO-d_6) spectrum of **HO3·HBF$_4$.**

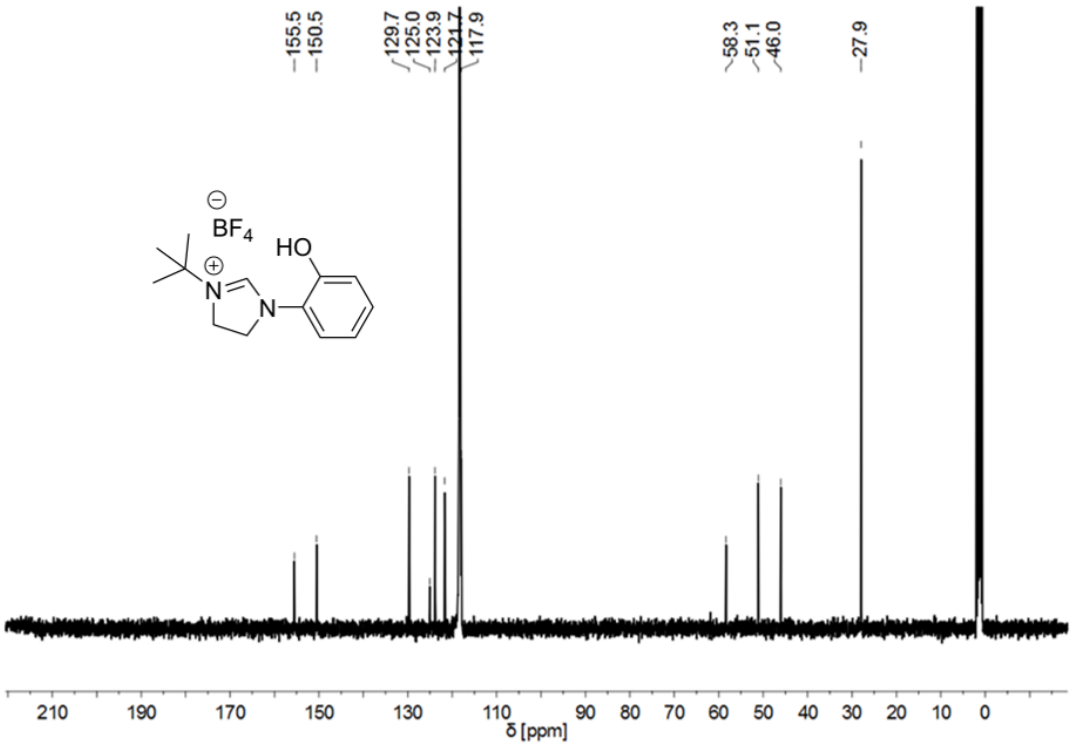

Figure S15: ^{13}C NMR (100 MHz, DMSO-d_6) spectrum of **HO4·HBF$_4$**.

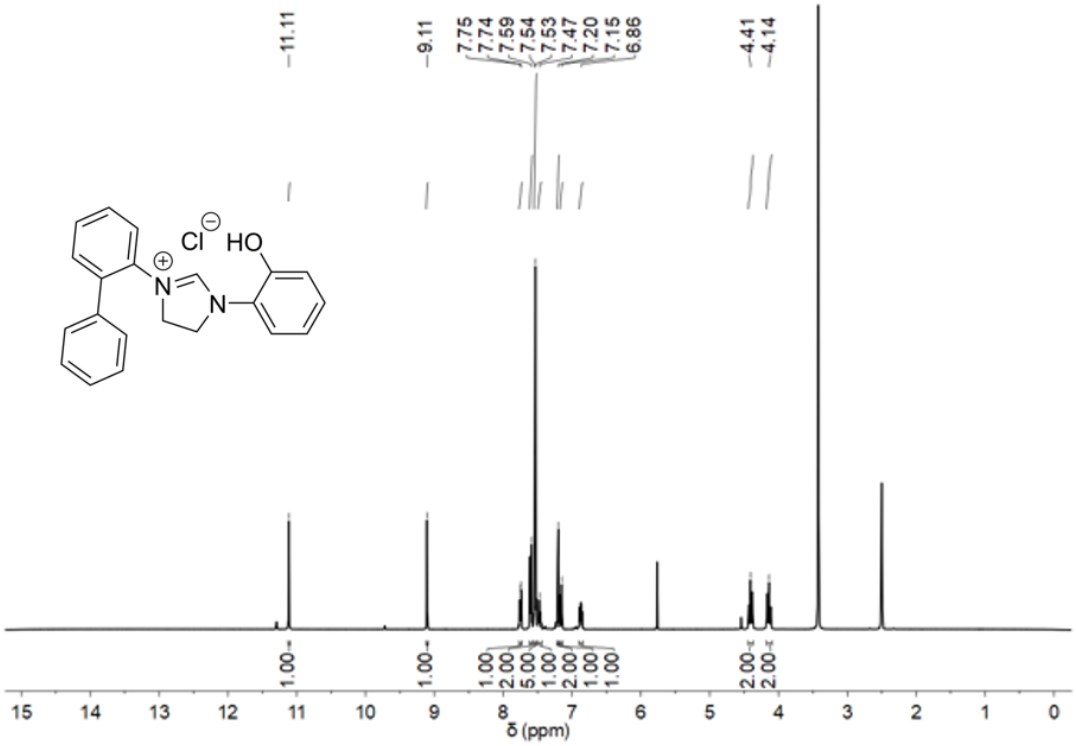

Figure S16: ^{1}H NMR (400 MHz, DMSO-d_6) spectrum of **HO4·HCl**.

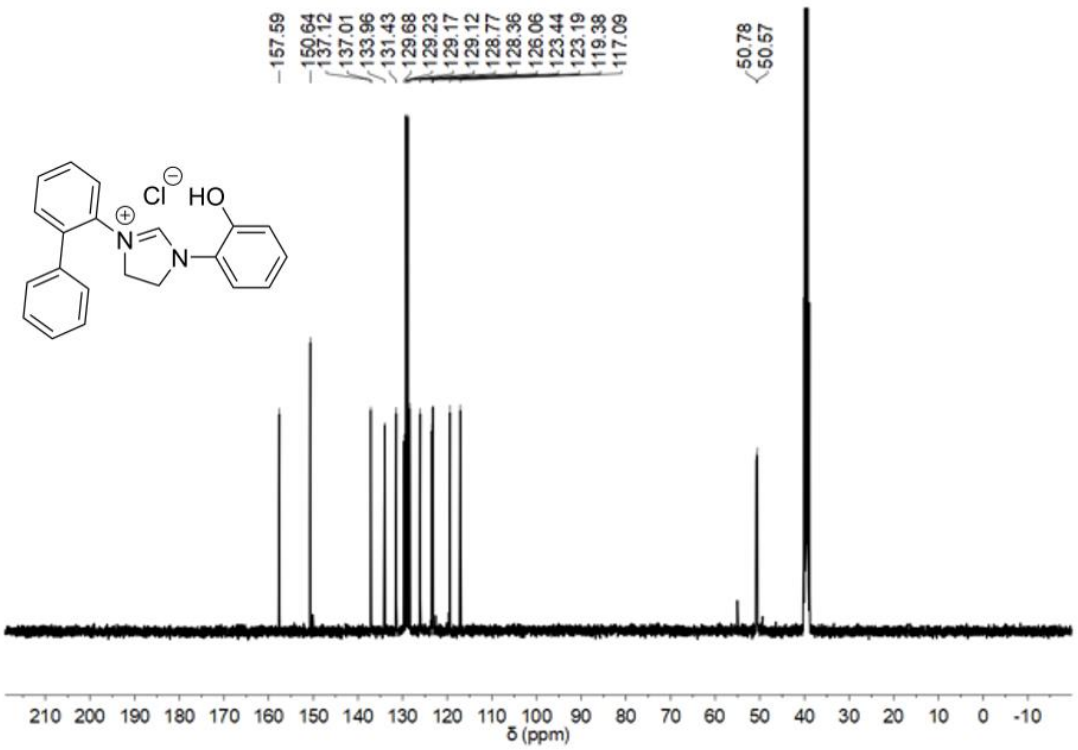

Figure S17: ^{13}C NMR (100 MHz, DMSO-d_6) spectrum of **HO4·HCl**.

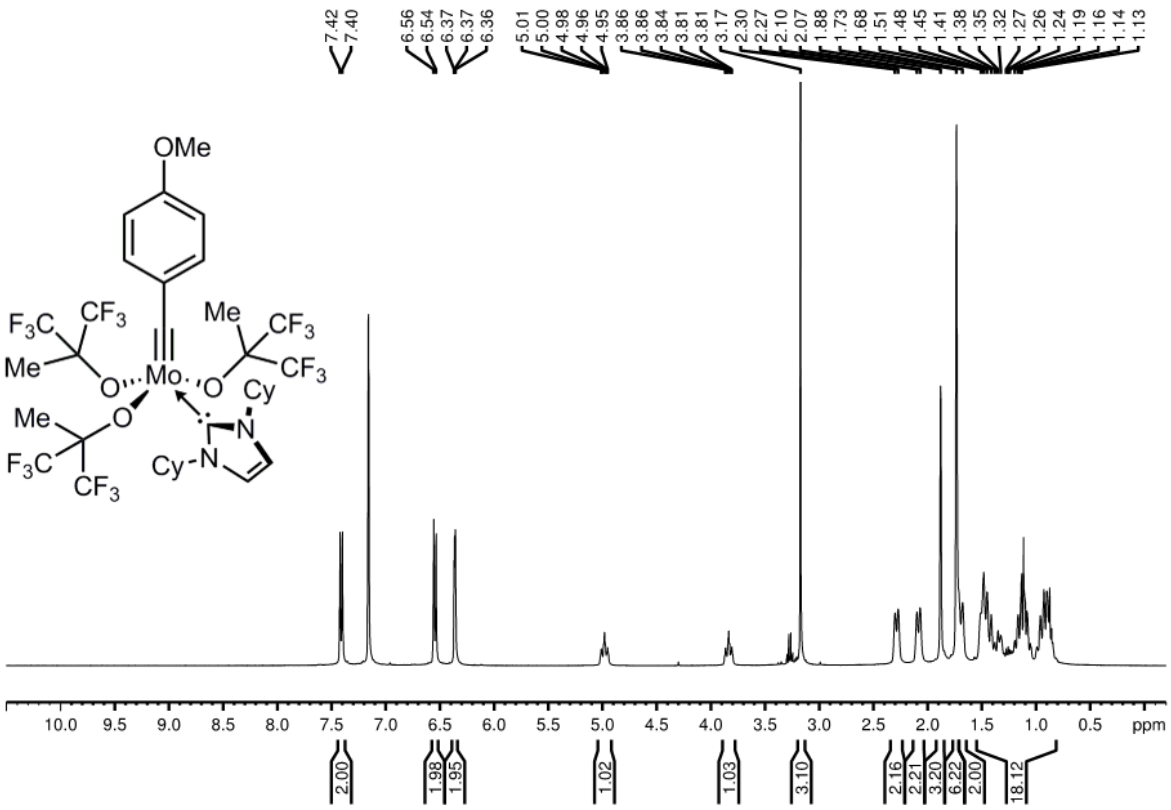

Figure S18: ^{1}H NMR (400 MHz, C_6D_6) of **Mo-3**.

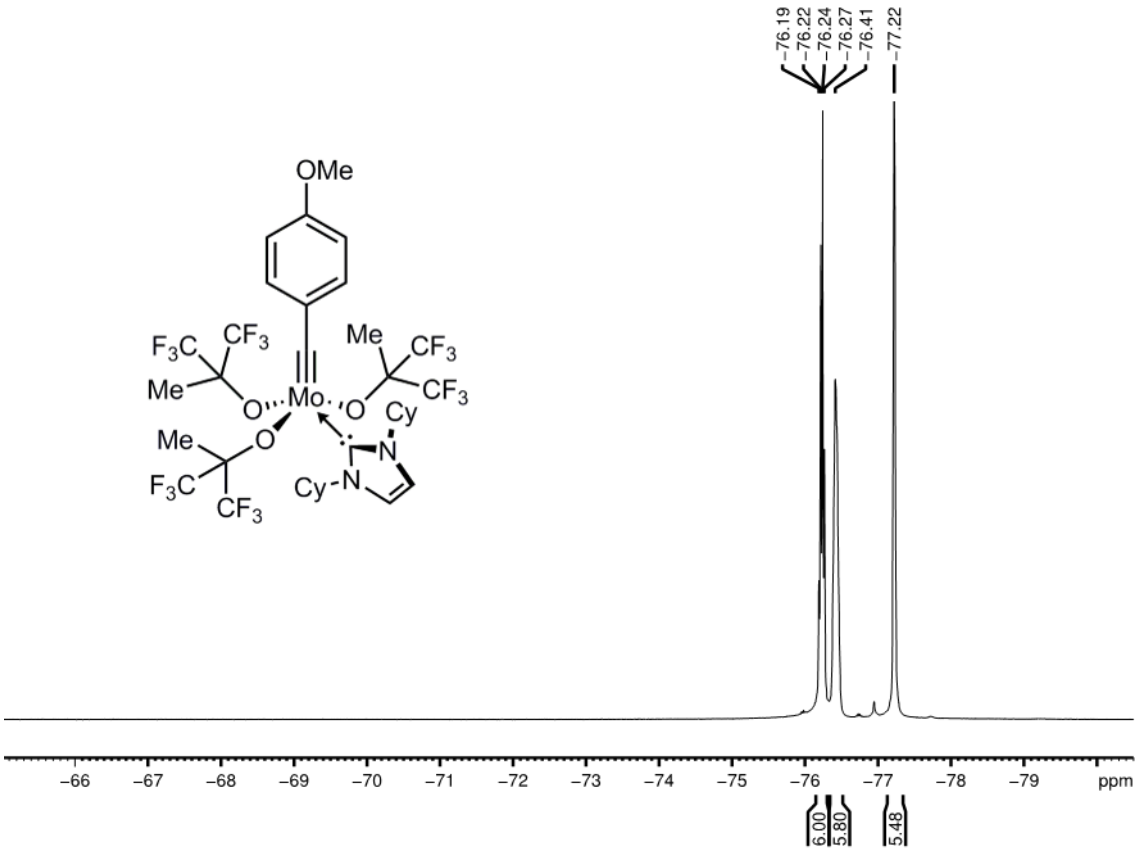

Figure S19: ^{19}F NMR (375 MHz, C_6D_6) of **Mo-3**.

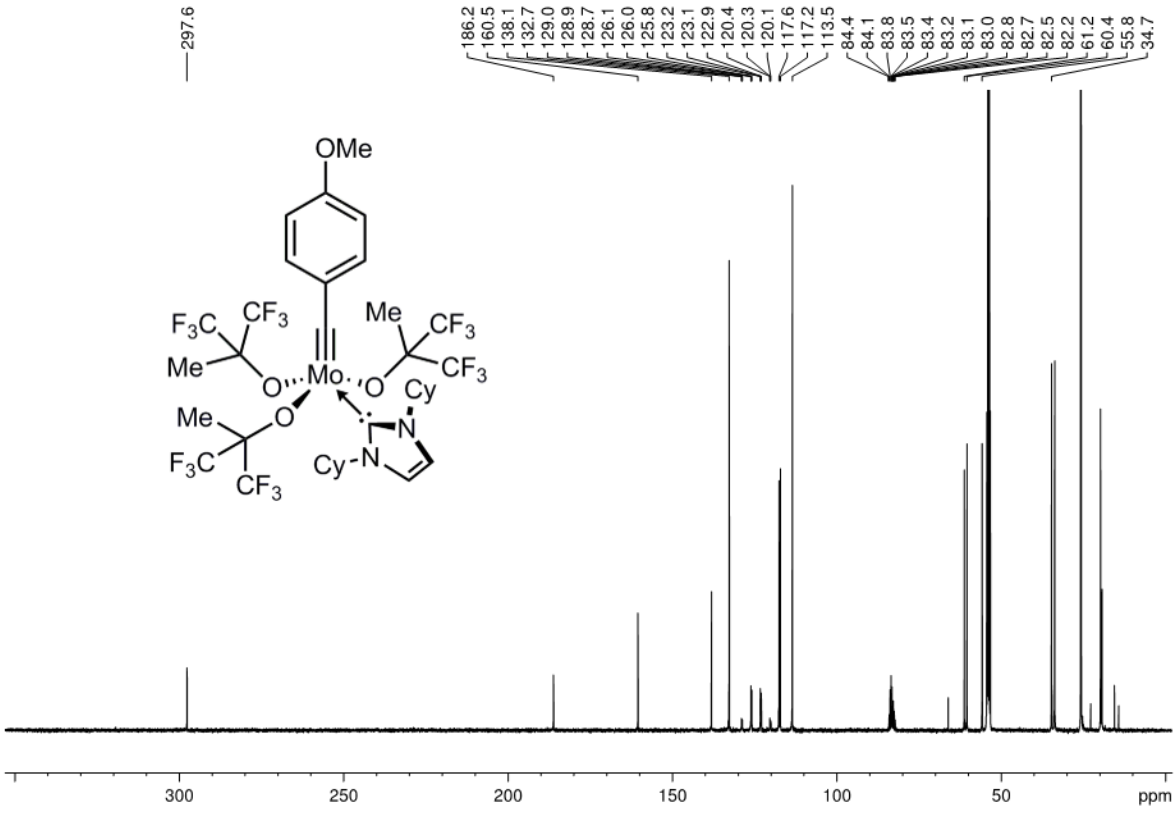

Figure S20: ^{13}C NMR (100 MHz, CD_2Cl_2) of **Mo-3**.

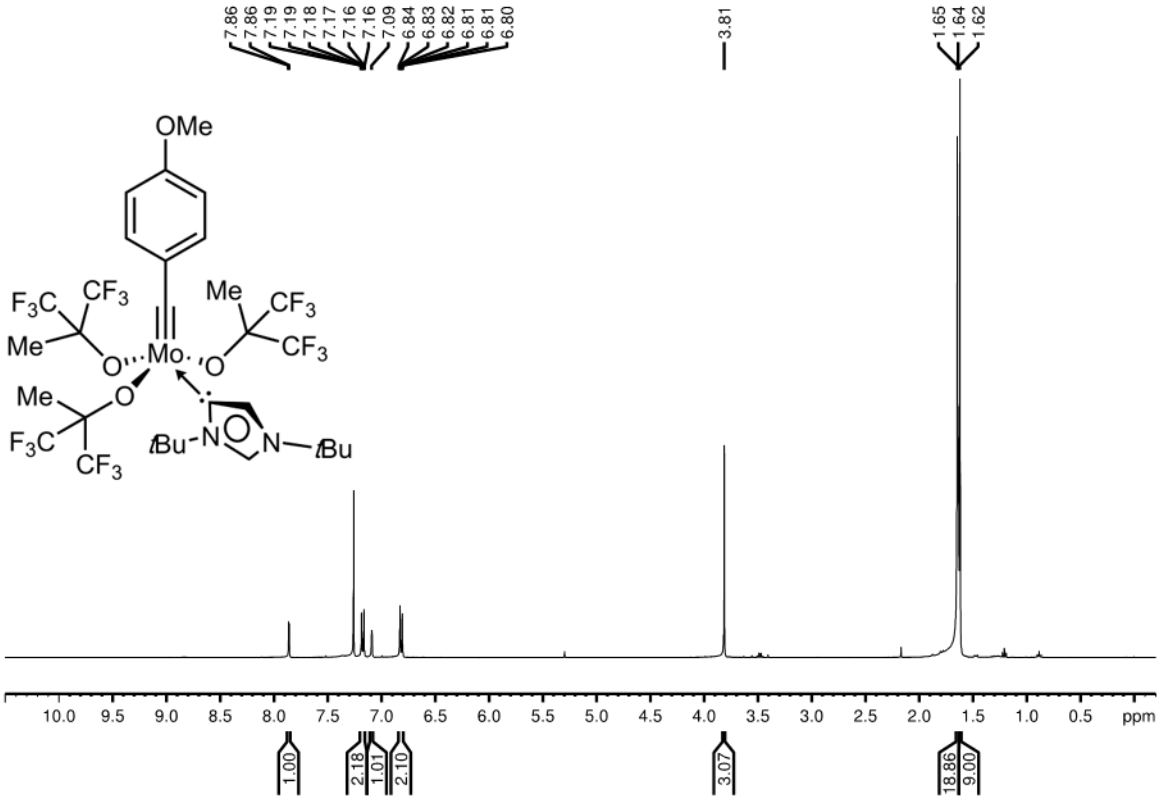

Figure S21: ^{1}H NMR (400 MHz, $CDCl_3$) of **Mo-4**.

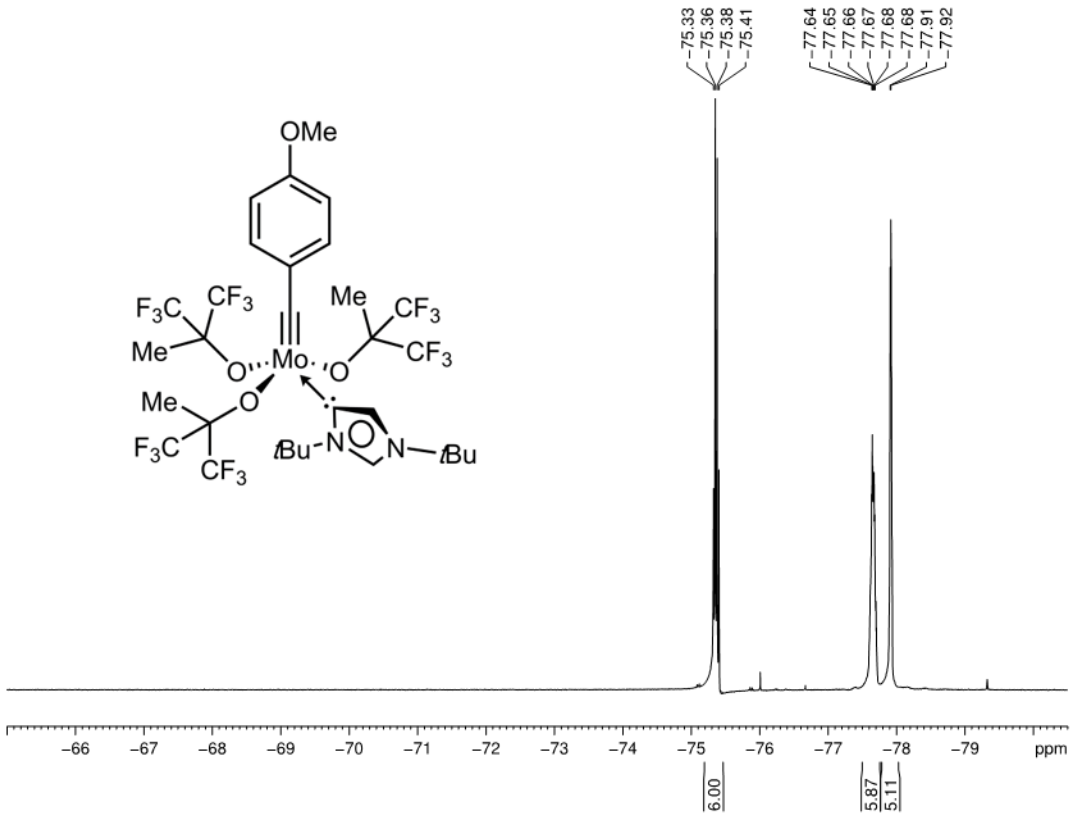

Figure S22: ^{19}F NMR (375 MHz, $CDCl_3$) of **Mo-4**.

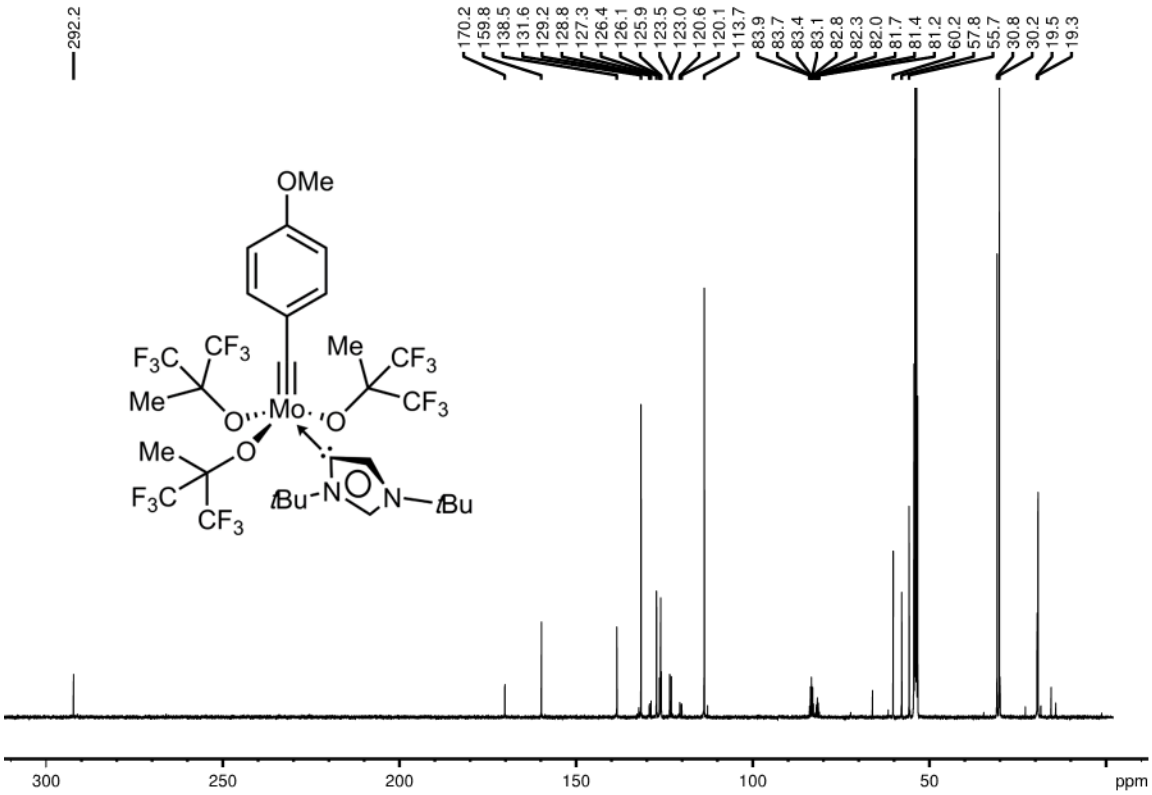

Figure S23: ^{13}C NMR (100 MHz, $CDCl_3$) of **Mo-4**.

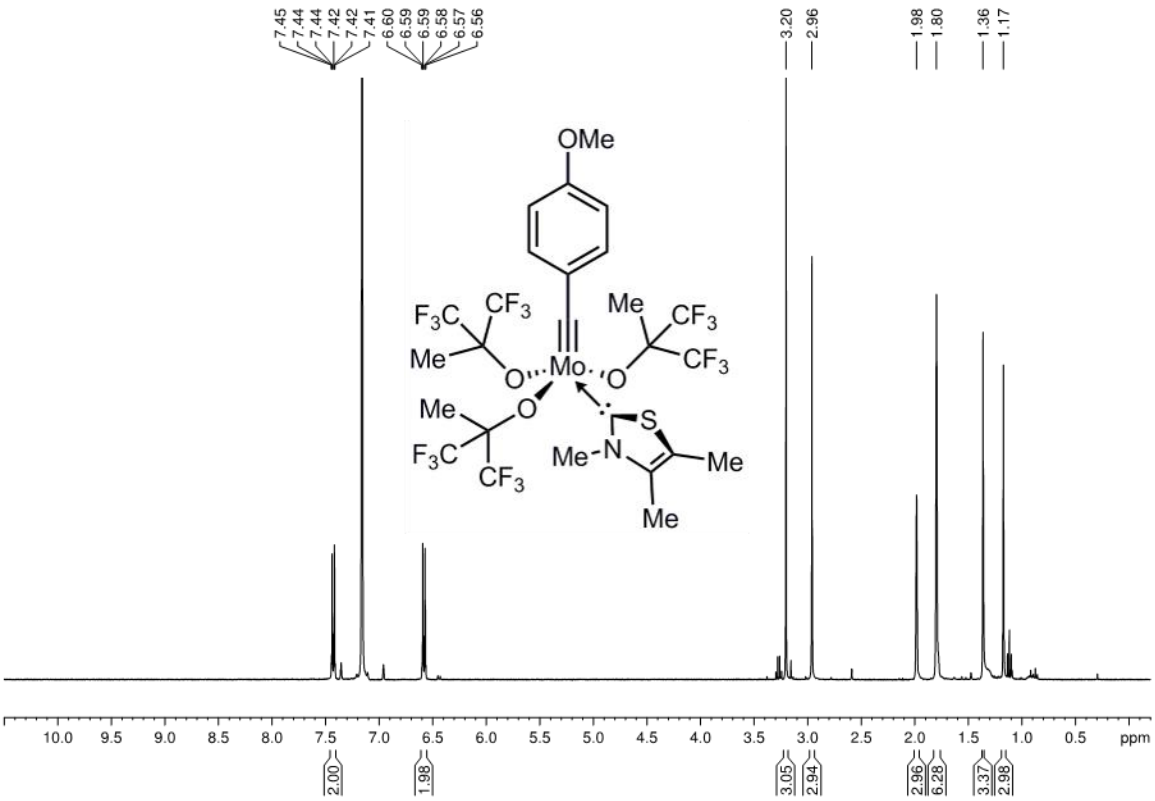

Figure S24: ^{1}H NMR (400 MHz, CD_2Cl_2) spectrum of **Mo-5.**

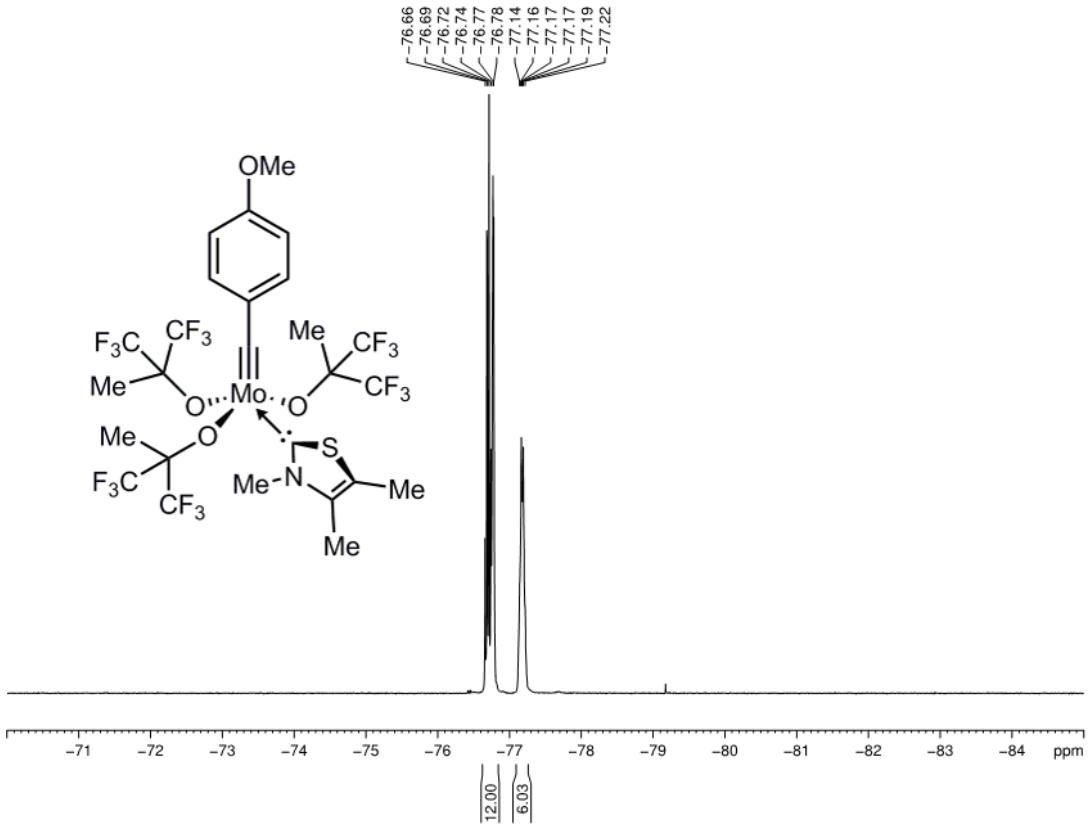

Figure S25: ^{19}F NMR (375 MHz, C_6D_6) of **Mo-5**.

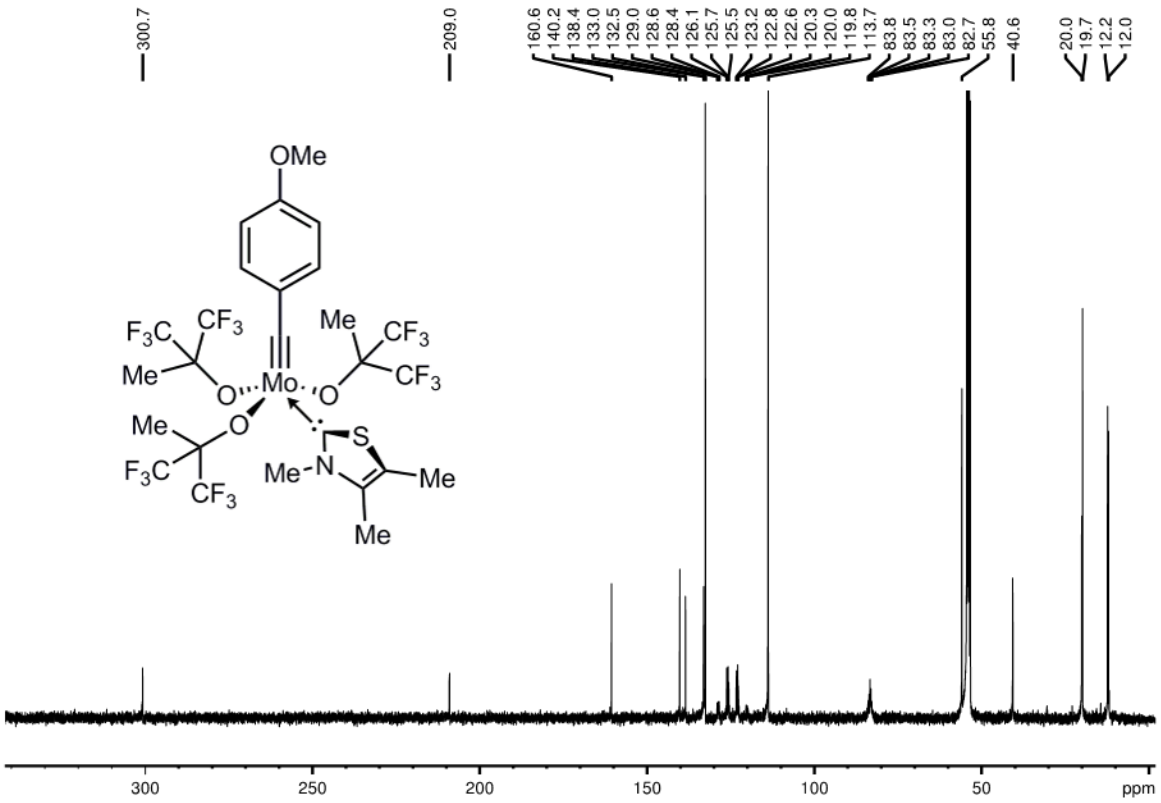

Figure S26: ^{13}C NMR (100 MHz, CD_2Cl_2) spectrum of **Mo-5.**

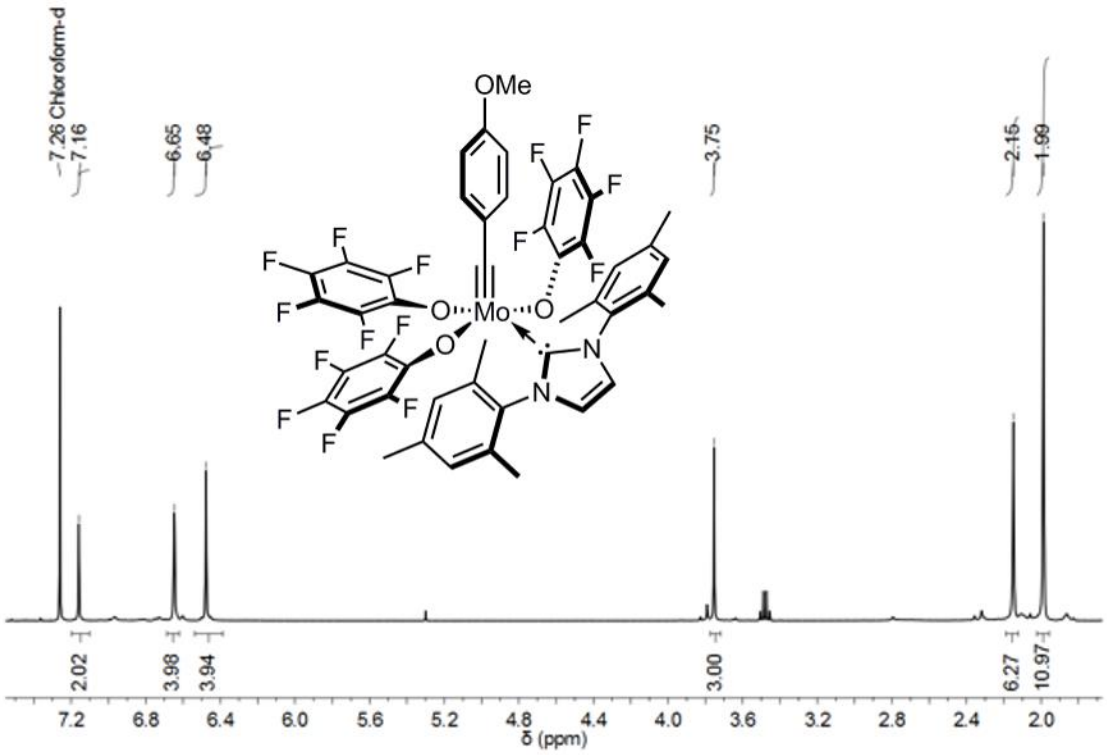

Figure S27: ^{1}H NMR (400 MHz, $CDCl_3$) spectrum of **Mo-6**.

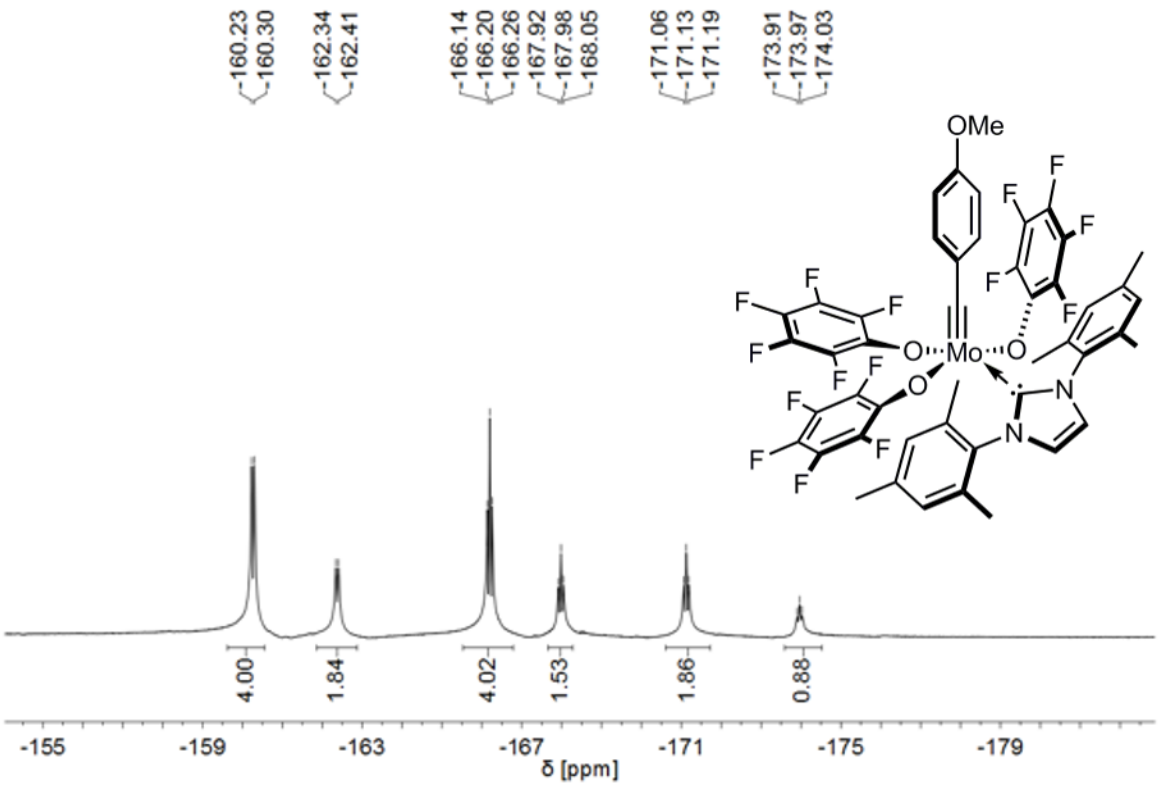

Figure S28: ^{19}F NMR (375 MHz, $CDCl_3$) spectrum of **Mo-6.**

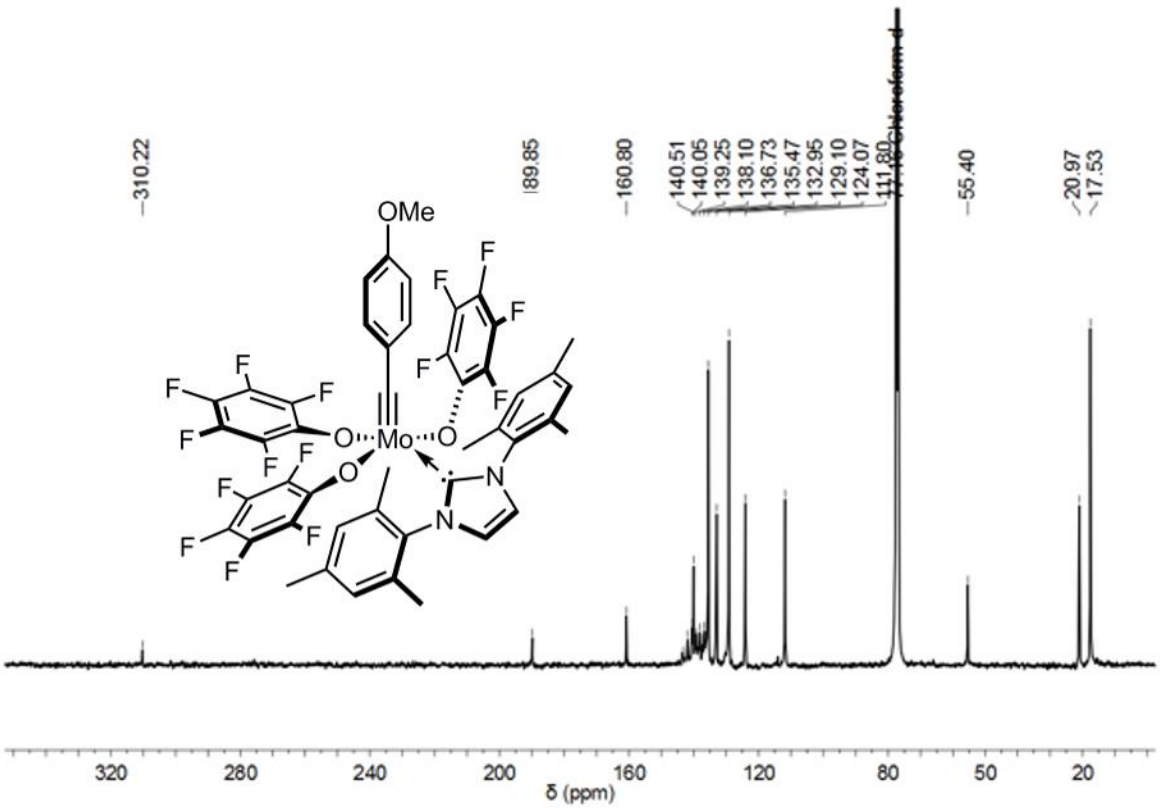

Figure S29: ^{13}C NMR (100 MHz, $CDCl_3$) spectrum of **Mo-6.**

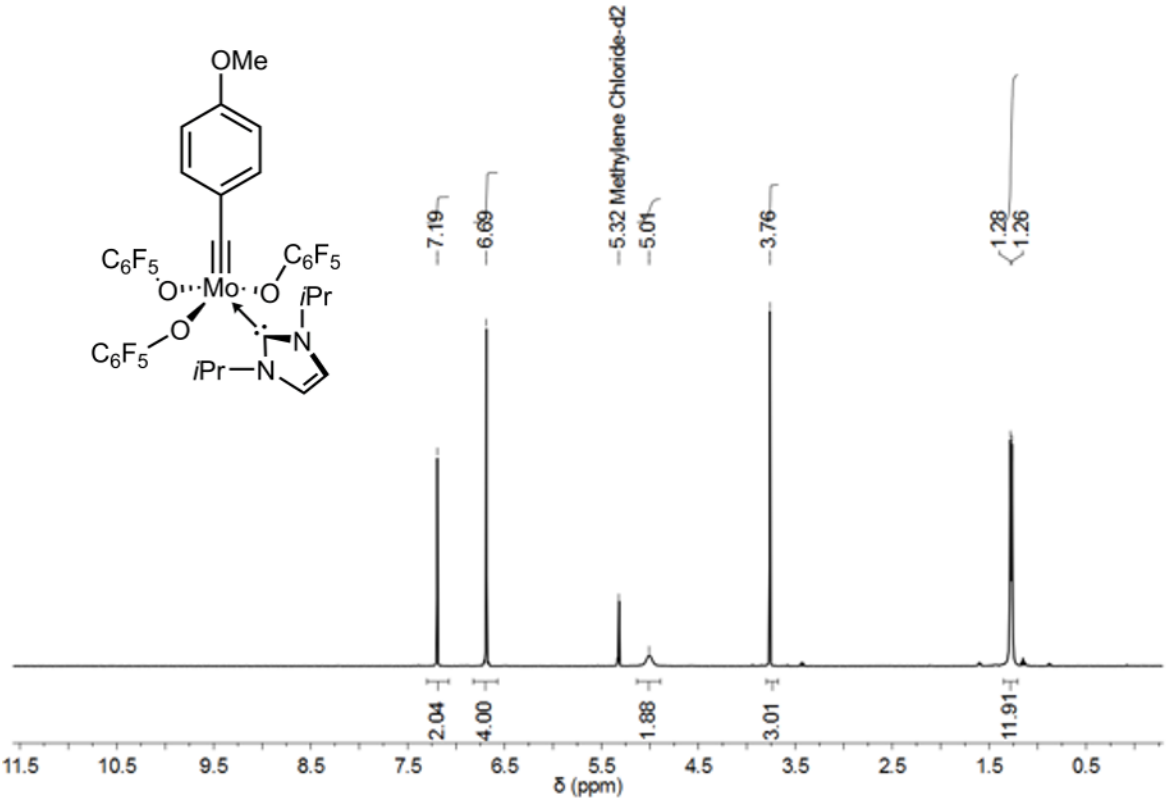

Figure S30: ^{1}H NMR (400 MHz, CD_2Cl_2) spectrum of **Mo-7**.

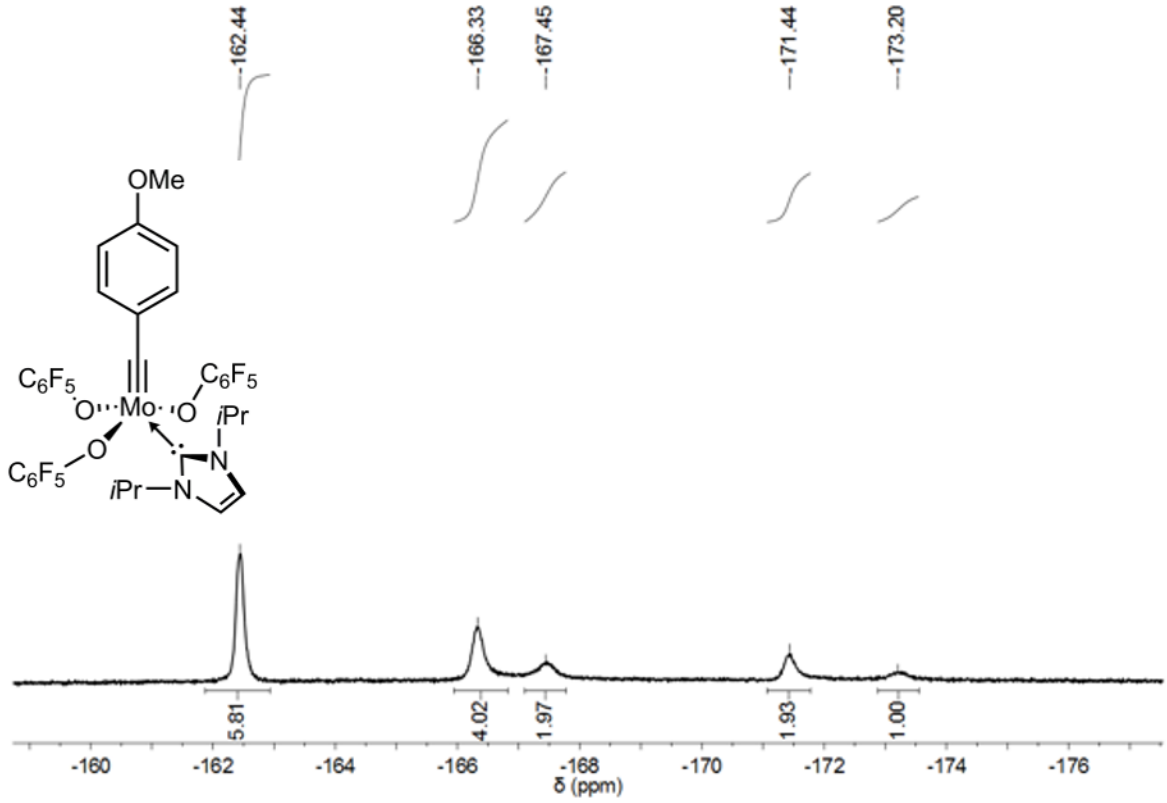

Figure S31: ^{19}F NMR (375 MHz, CD_2Cl_2) spectrum of **Mo-7.**

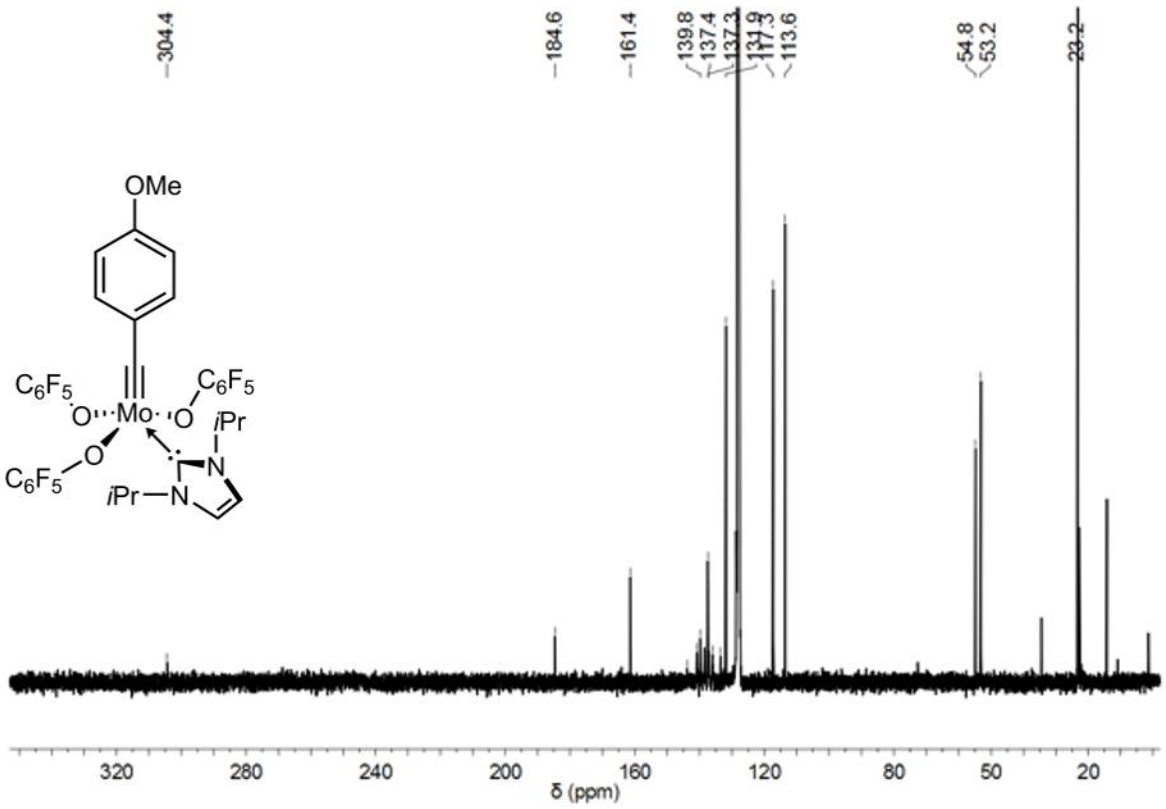

Figure S32: ^{13}C NMR (100 MHz, C_6D_6) spectrum of **Mo-7.**

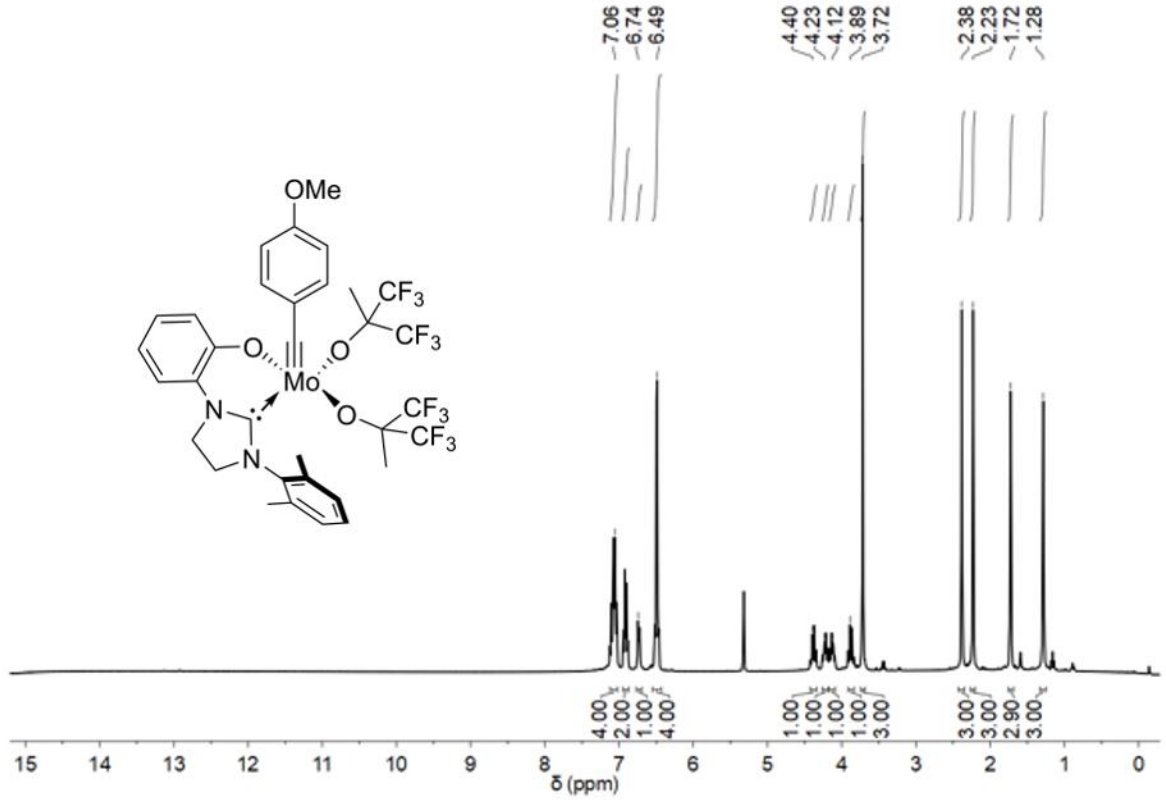

Figure S33: ^{1}H NMR (400 MHz, CD_2Cl_2) spectrum of **Mo-8**.

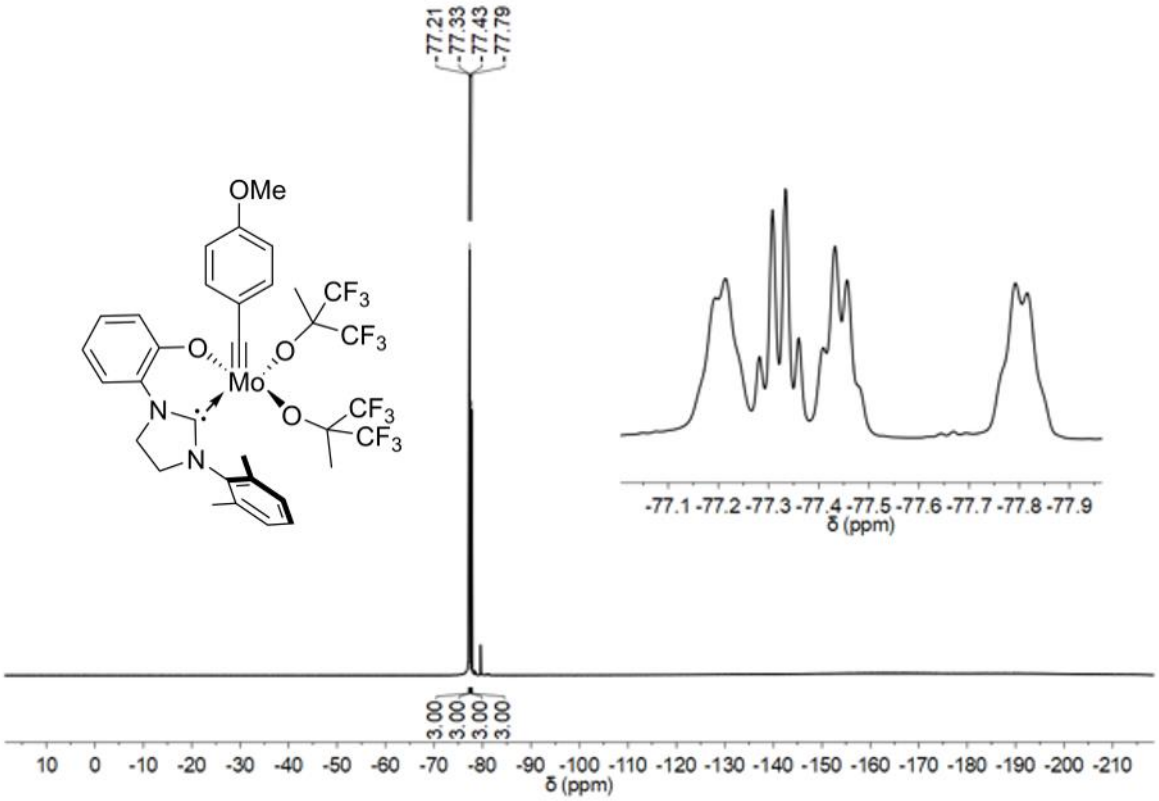

Figure S34: ^{19}F NMR (375 MHz, CD_2Cl_2) spectrum of **Mo-8**.

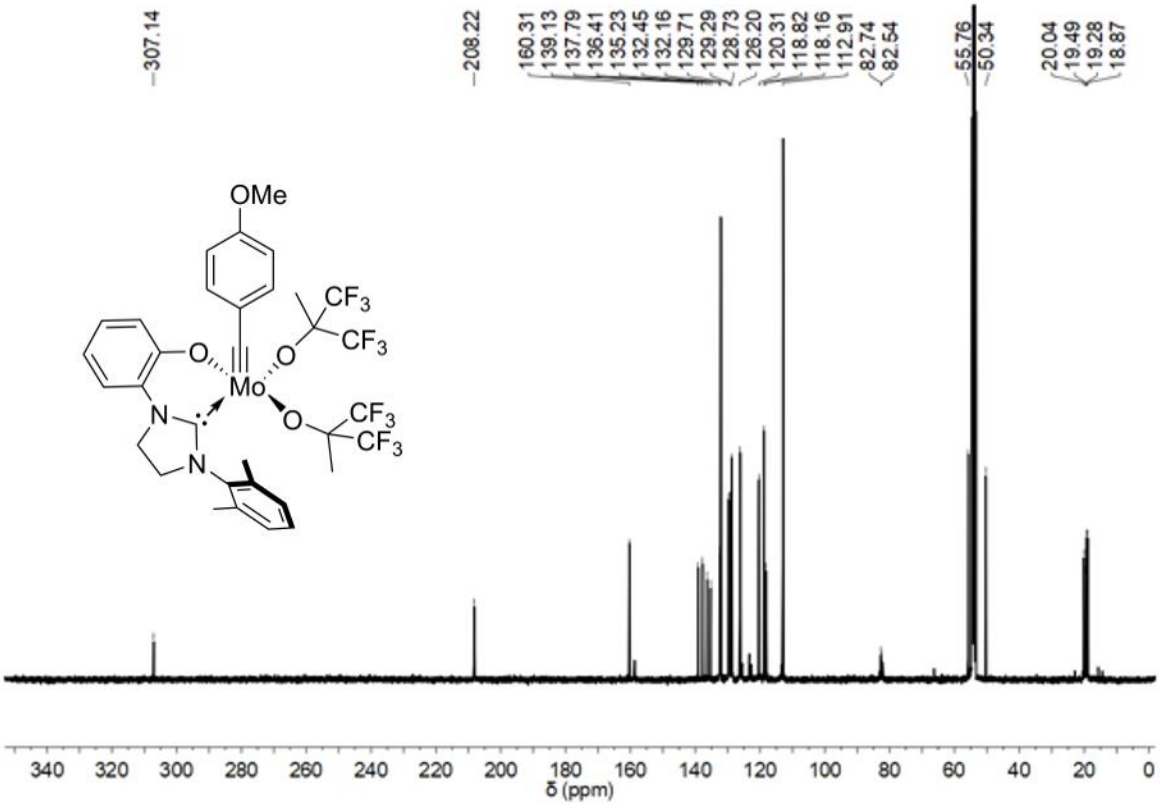

Figure S35: ^{13}C NMR (100 MHz, CD_2Cl_2) spectrum of **Mo-8**.

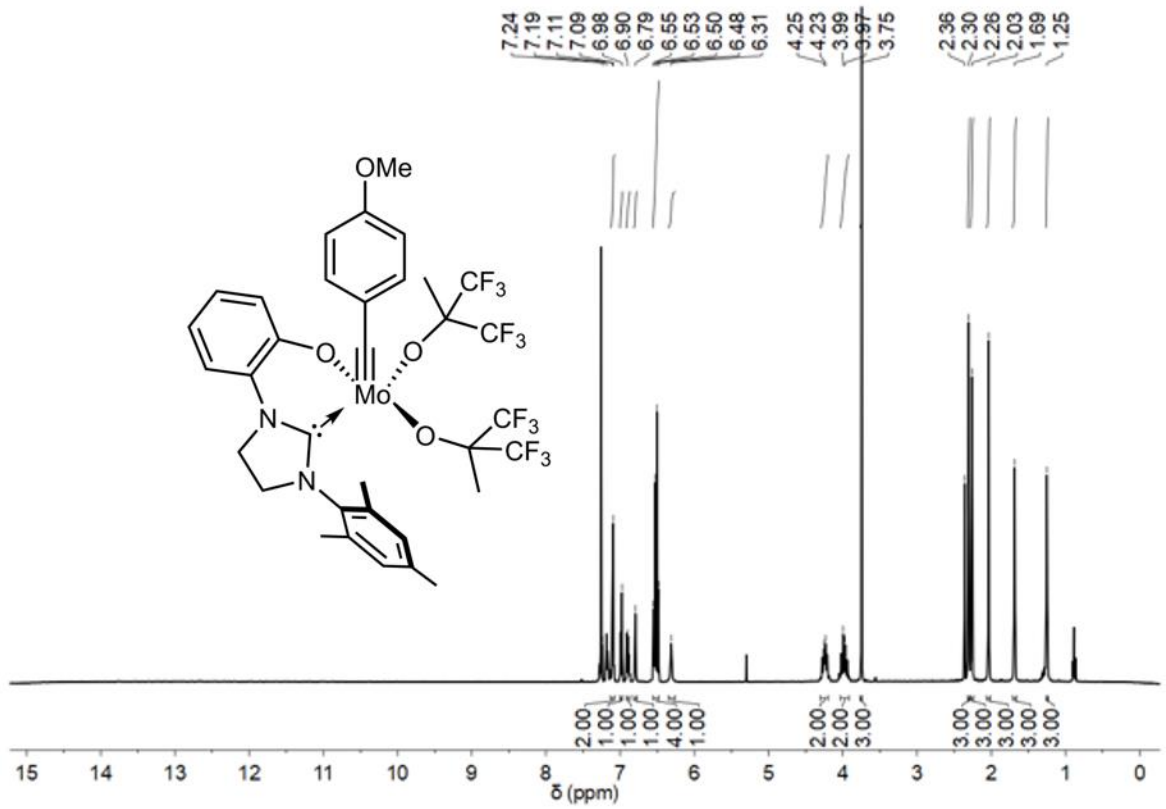

Figure S36: ^{1}H NMR (400 MHz, $CDCl_3$) spectrum of **Mo-9**.

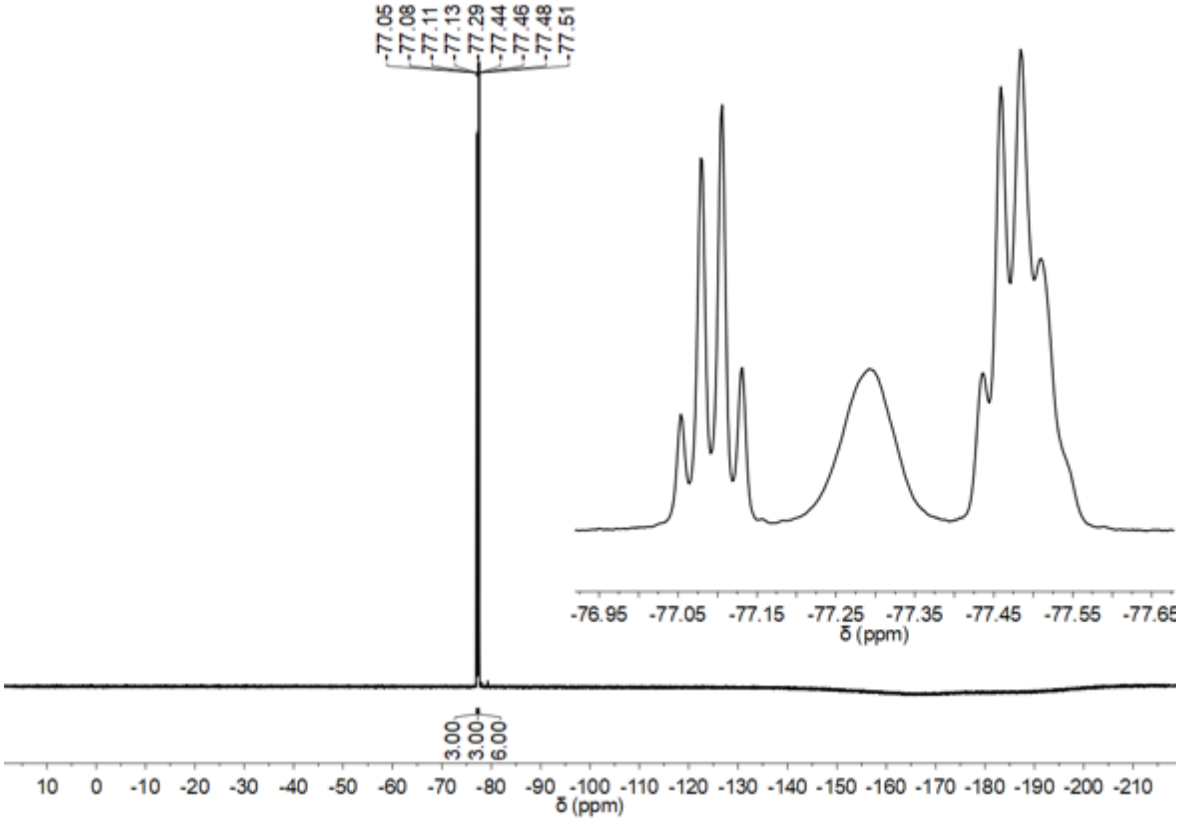

Figure S37: ^{19}F NMR (375 MHz, $CDCl_3$) spectrum of **Mo-9**.

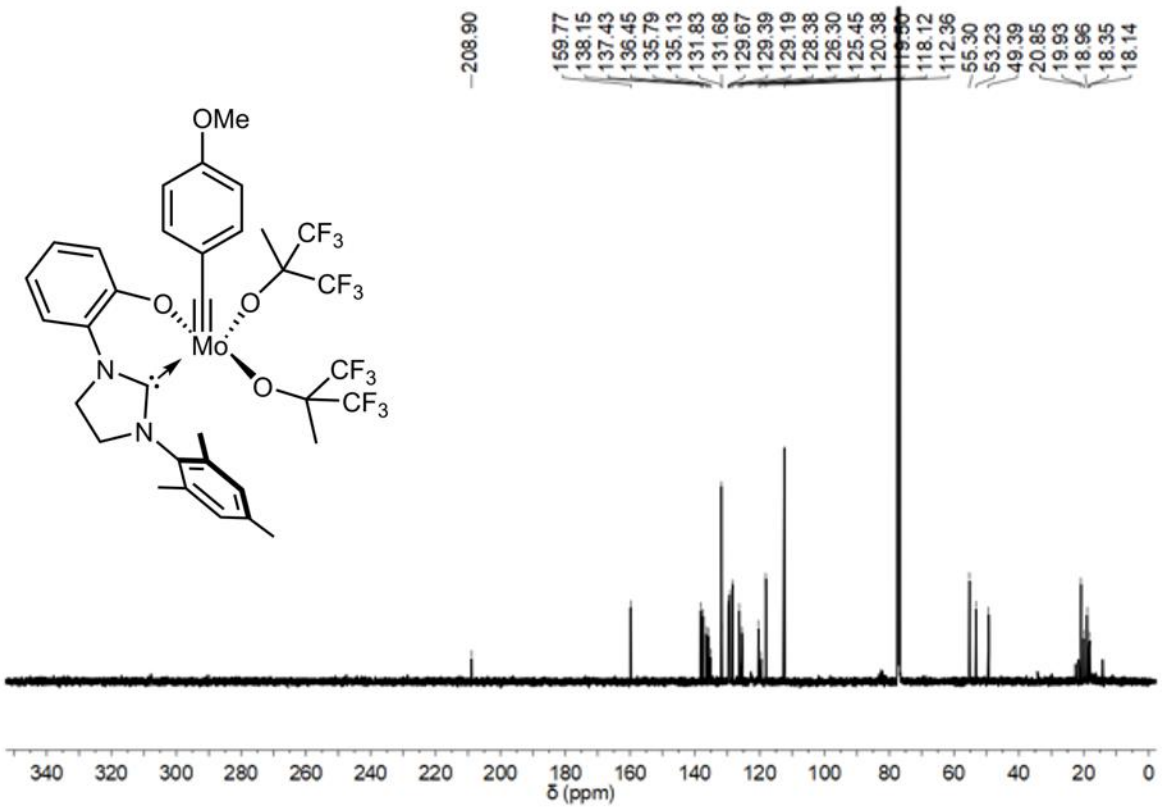

Figure S38: ^{13}C NMR (100 MHz, $CDCl_3$) spectrum of **Mo-9**.

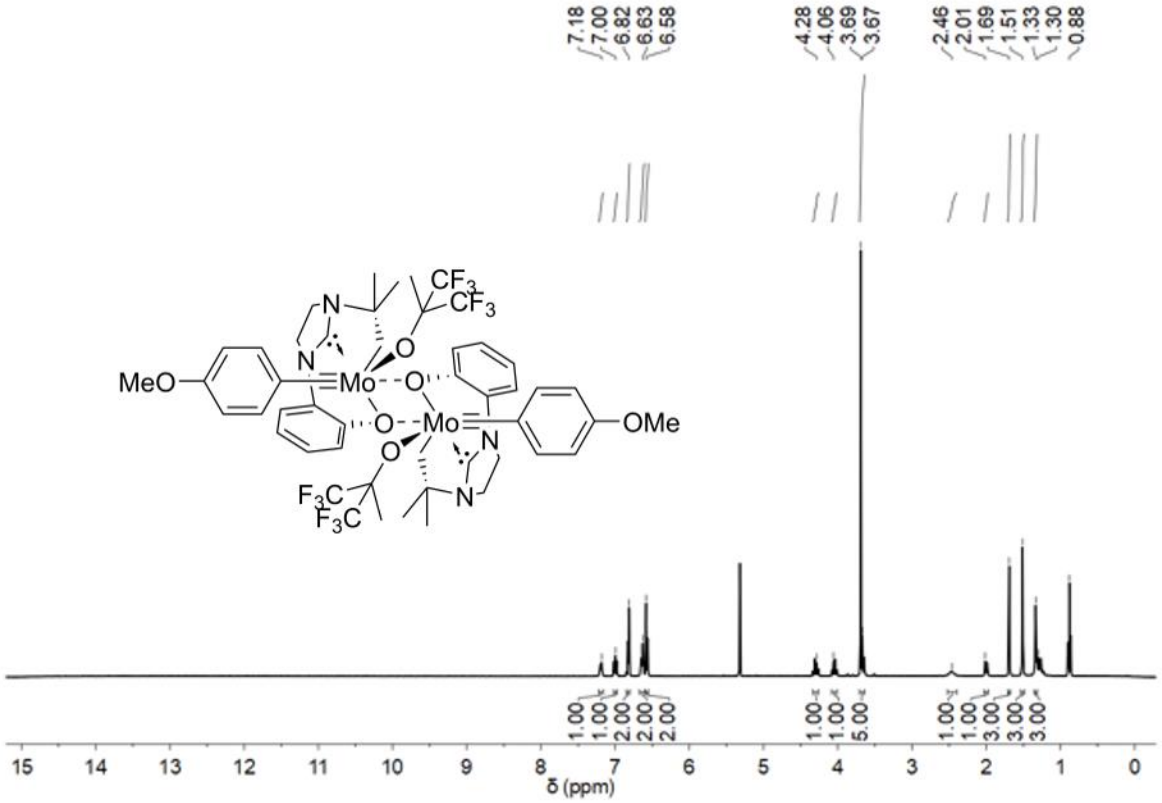

Figure S39: ^{1}H NMR (400 MHz, CD_2Cl_2) spectrum of **Mo-10**.

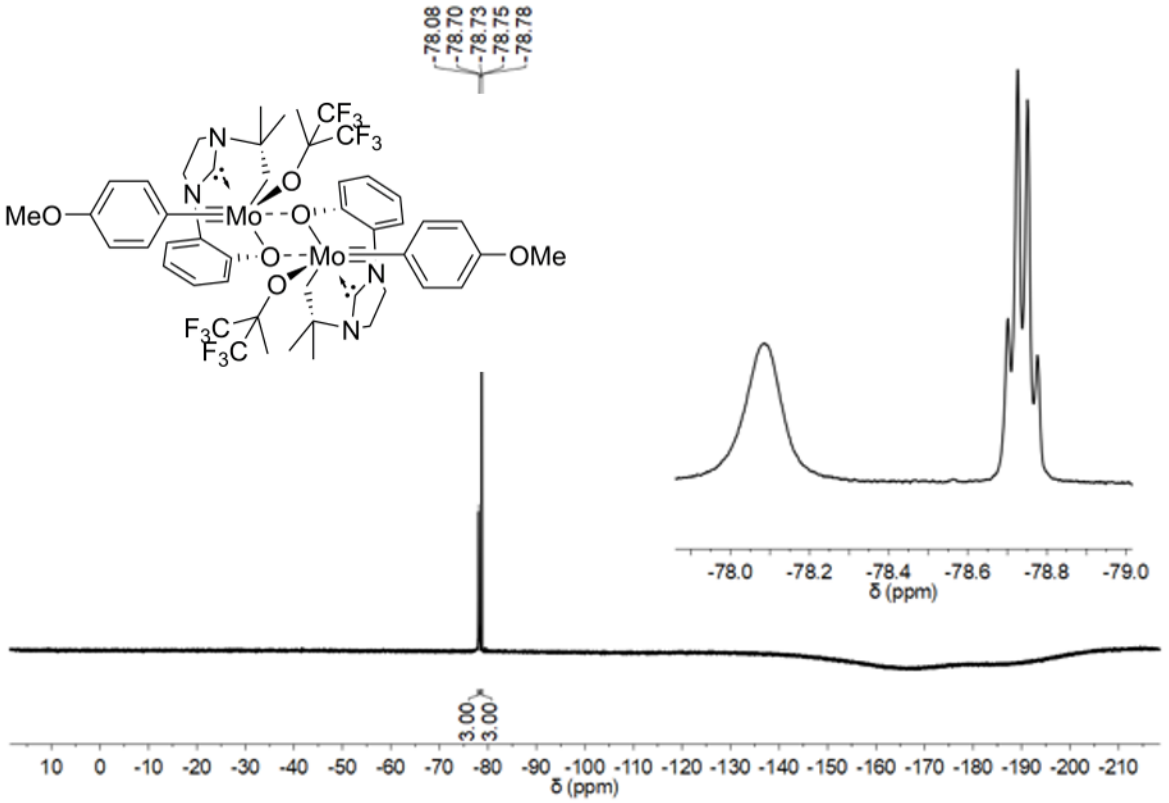

Figure S40: ^{19}F NMR (375 MHz, CD_2Cl_2) spectrum of **Mo-10**.

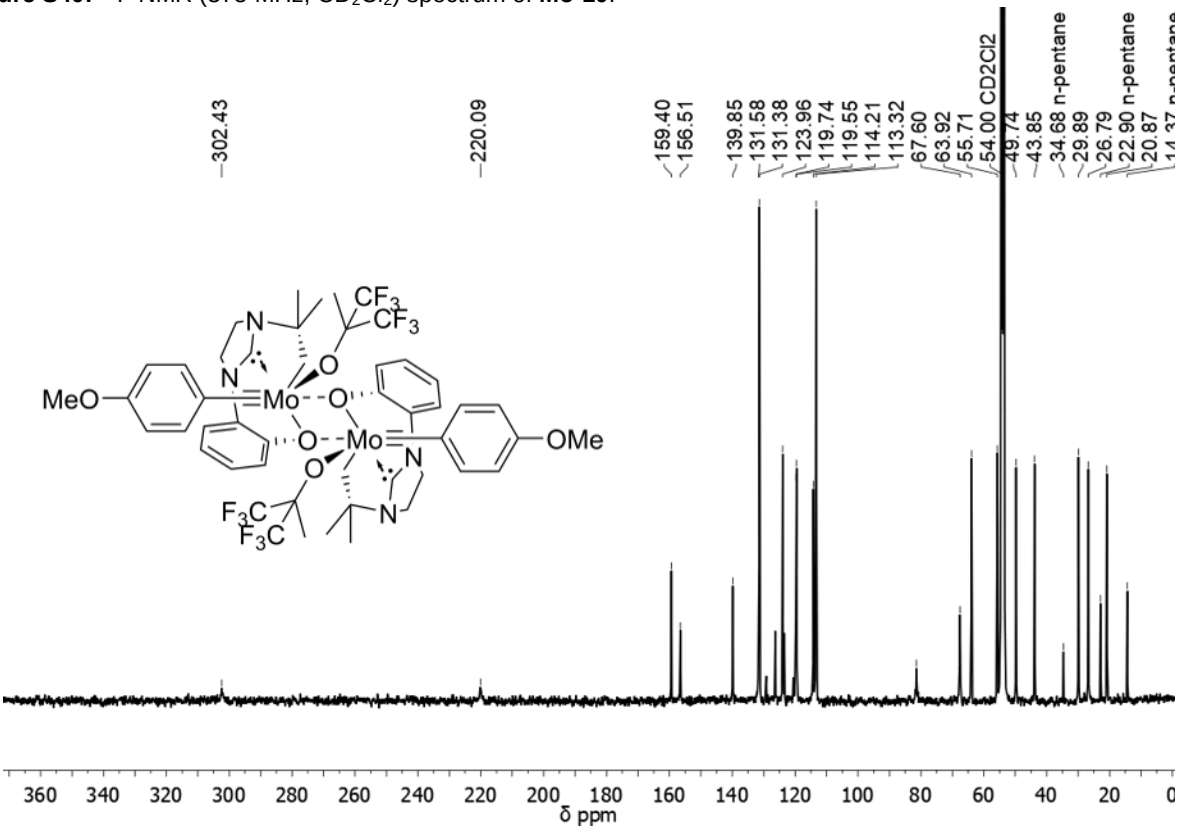

Figure S41: ^{13}C NMR (100 MHz, CD_2Cl_2) spectrum of **Mo-10**.

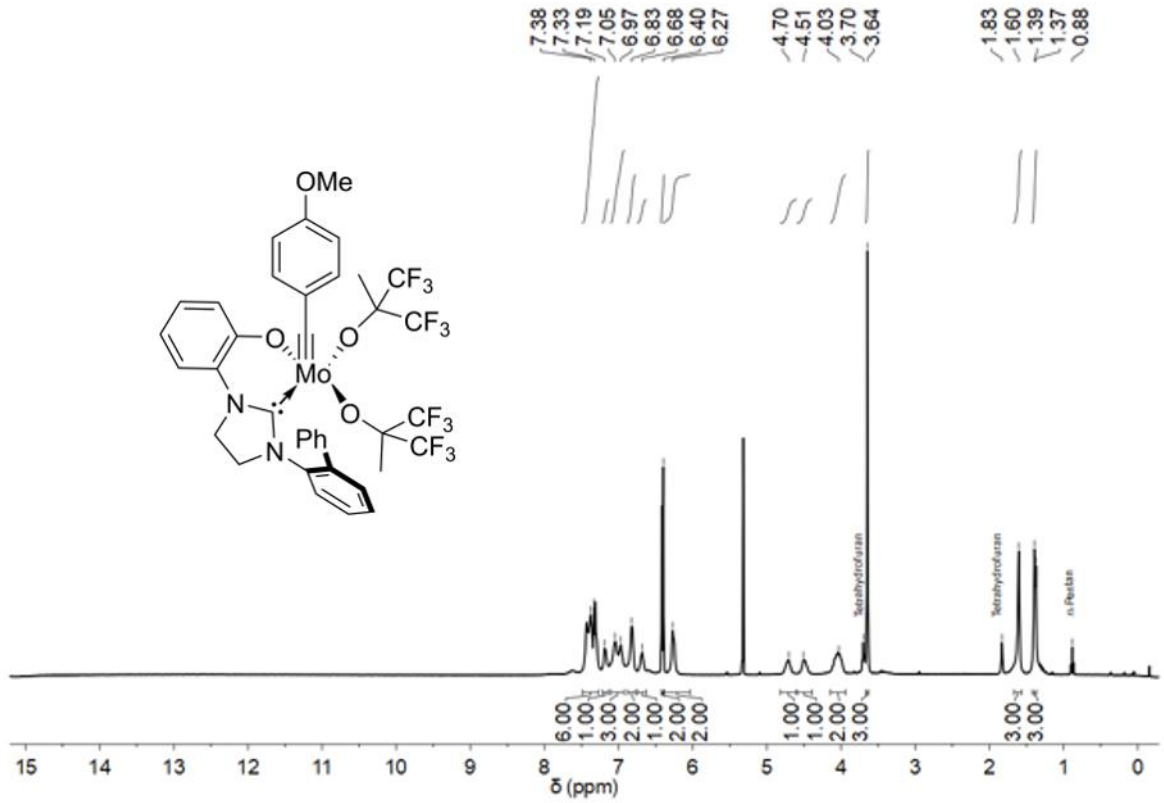

Figure S42: ^{1}H NMR (400 MHz, CD_2Cl_2) spectrum of **Mo-11**.

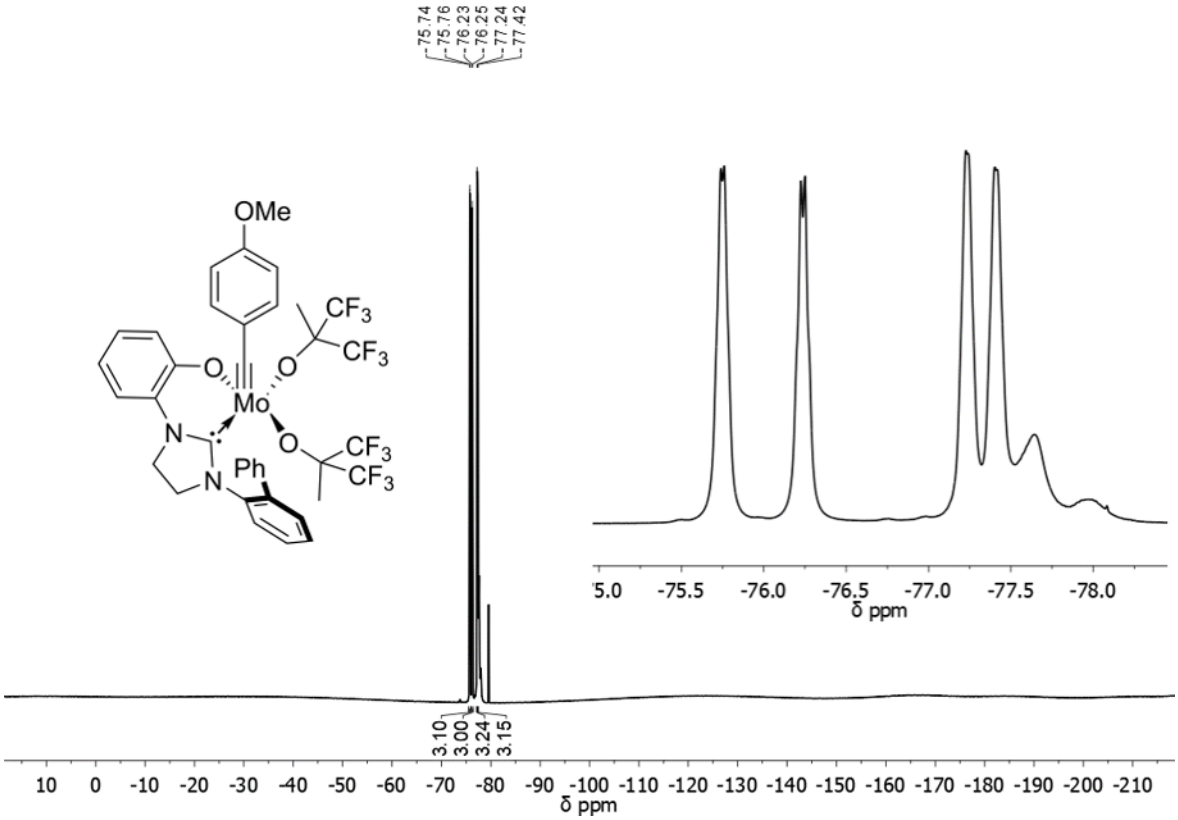

Figure S43: ^{19}F NMR (375 MHz, CD_2Cl_2) spectrum of **Mo-11**.

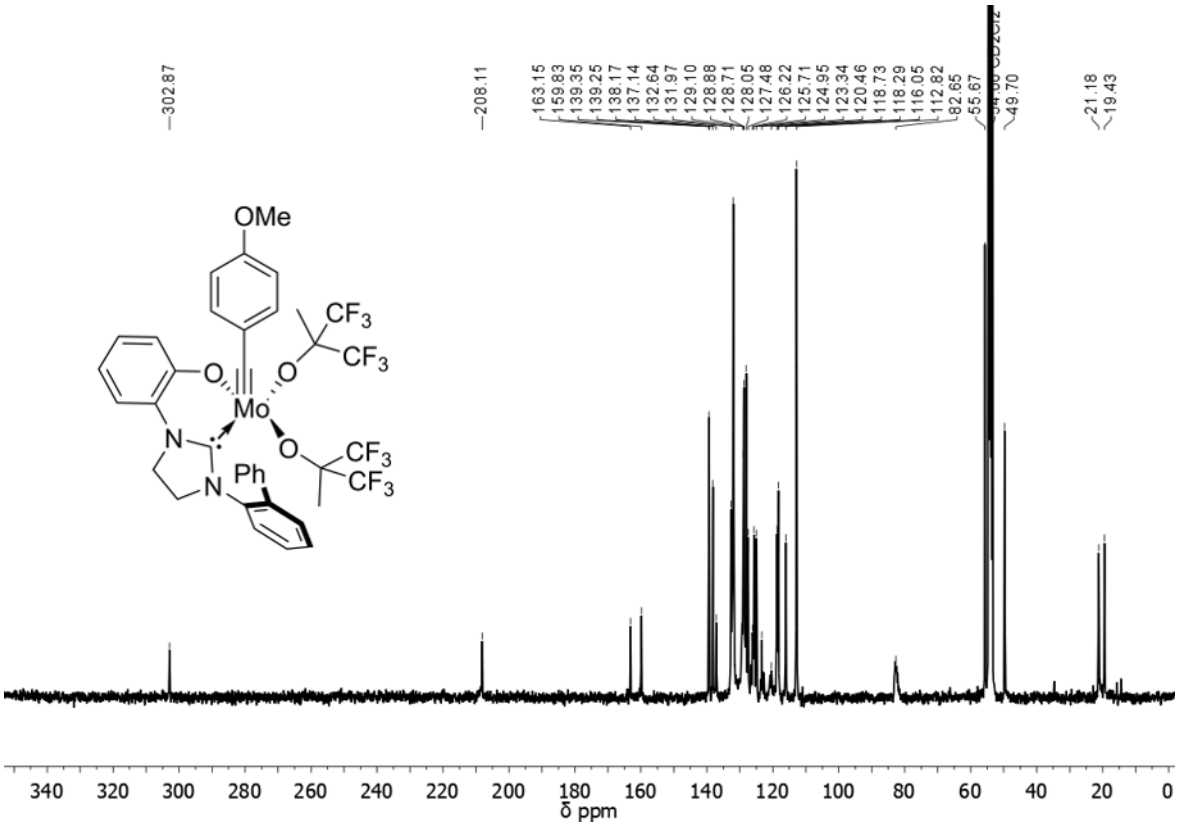

Figure S44: ^{13}C NMR (100 MHz, CD_2Cl_2) spectrum of **Mo-11**.

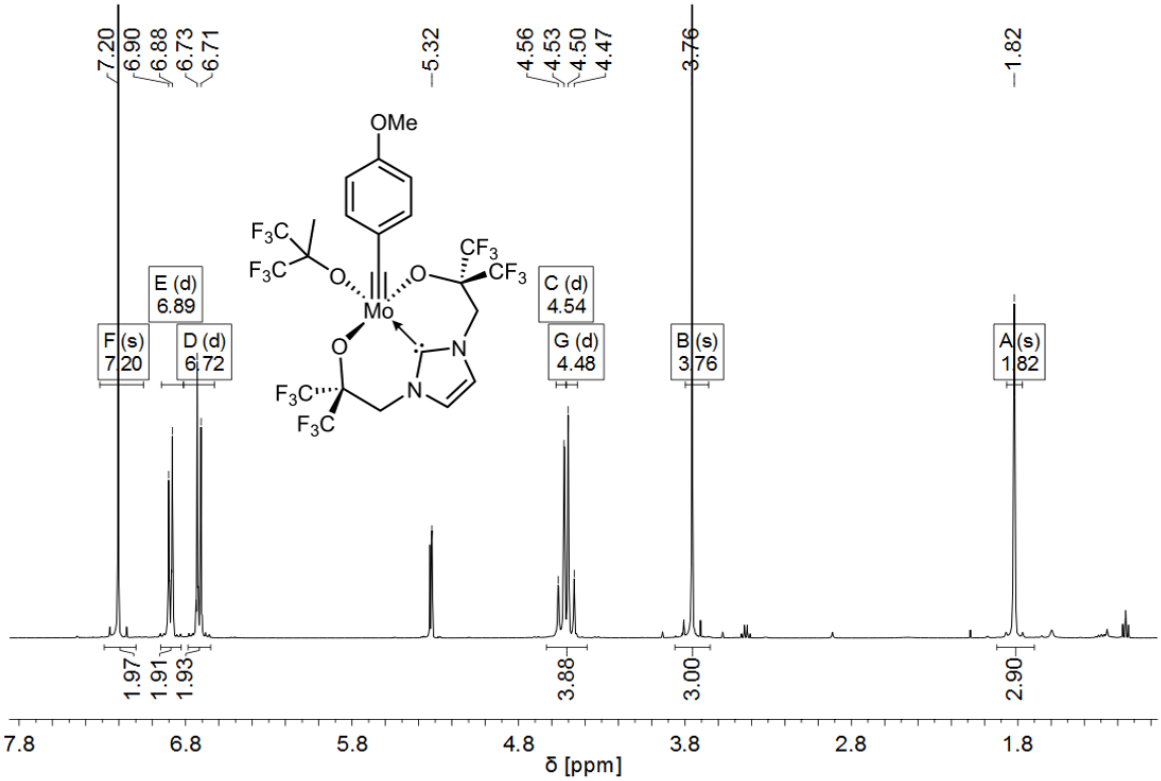

Figure S45: ^{1}H NMR (400 MHz, $CDCl_3$) spectrum of **Mo-13**.

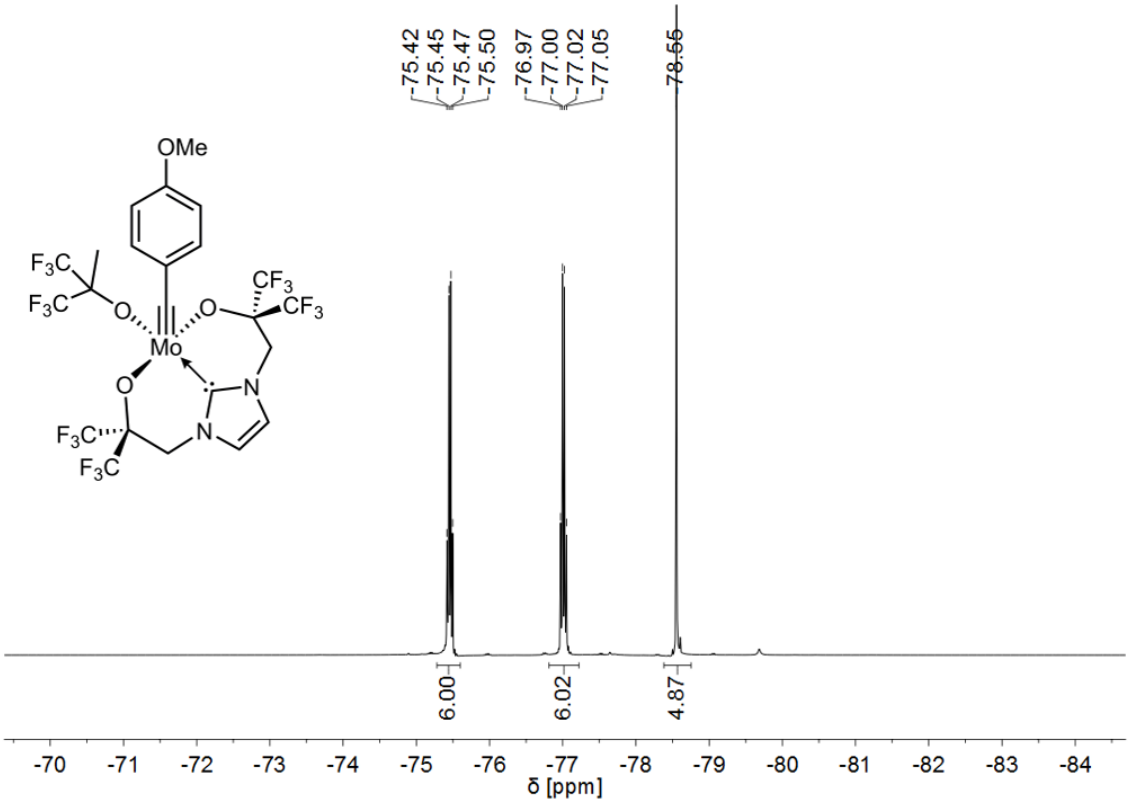

Figure S46: ^{19}F NMR (375 MHz, $CDCl_3$) spectrum of **Mo-13**.

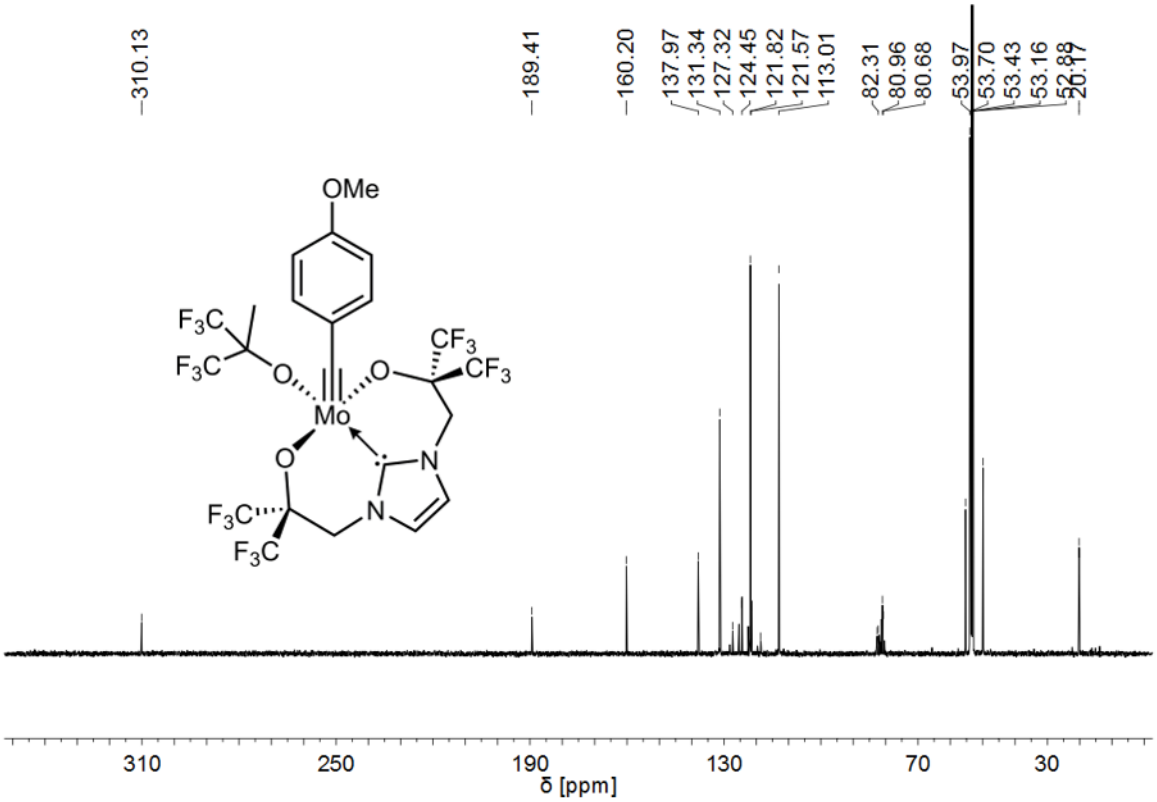

Figure S47: ^{13}C NMR (100 MHz, $CDCl_6$) spectrum of **Mo-13**.

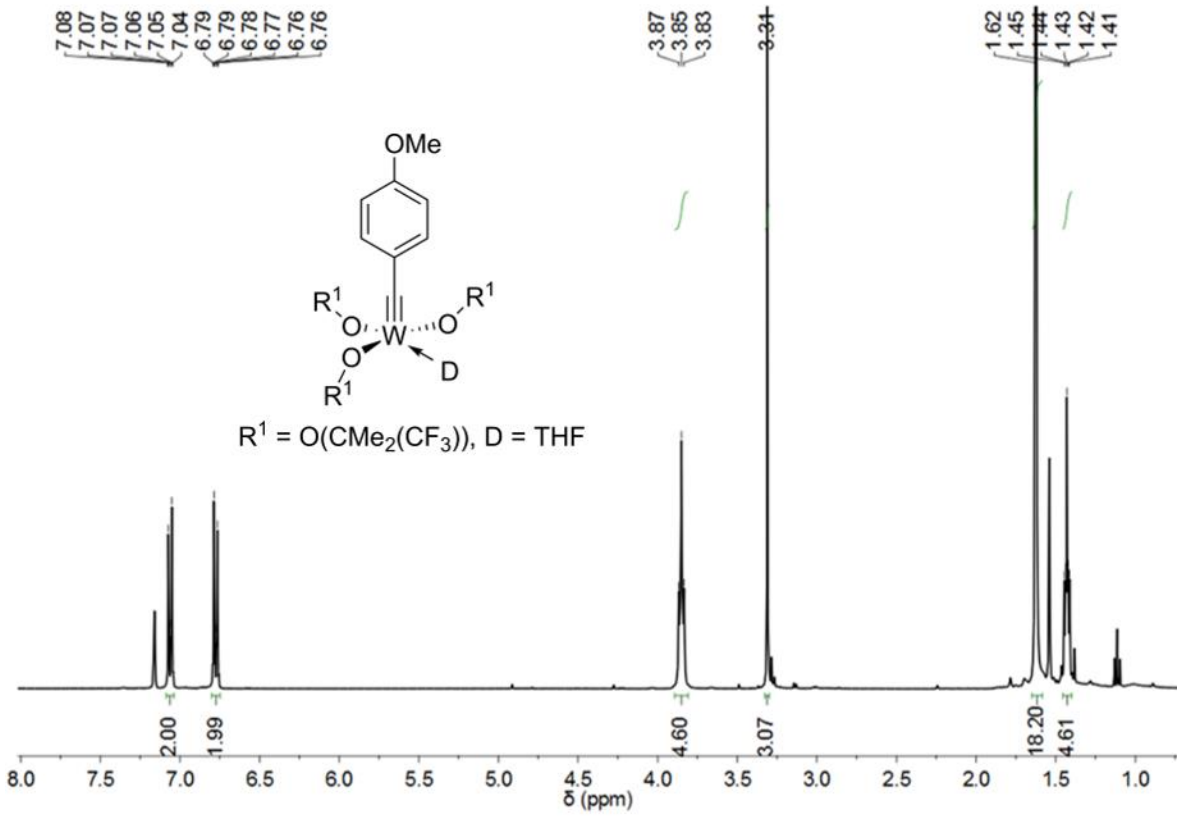

Figure S48: ^{1}H NMR (400 MHz, C_6D_6) spectrum of **W-2**.

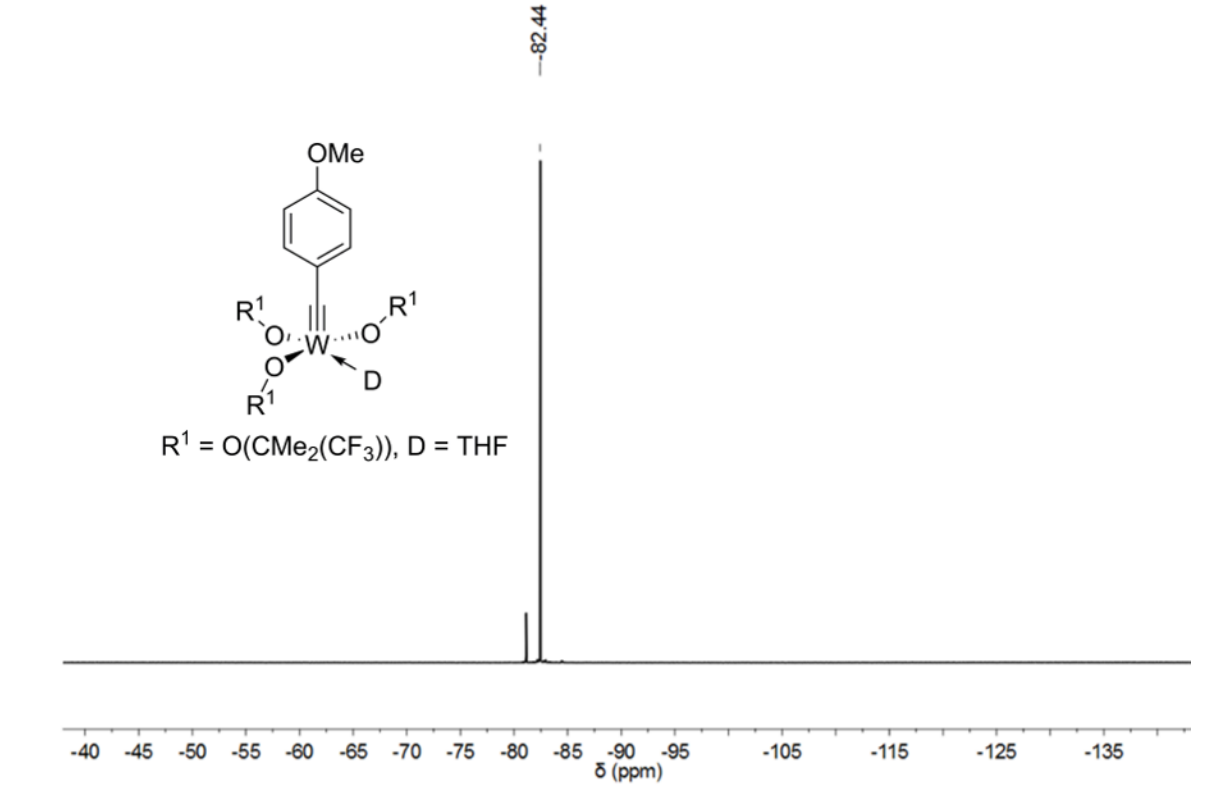

Figure S49: ^{19}F NMR (375 MHz, C_6D_6) spectrum of **W-2**.

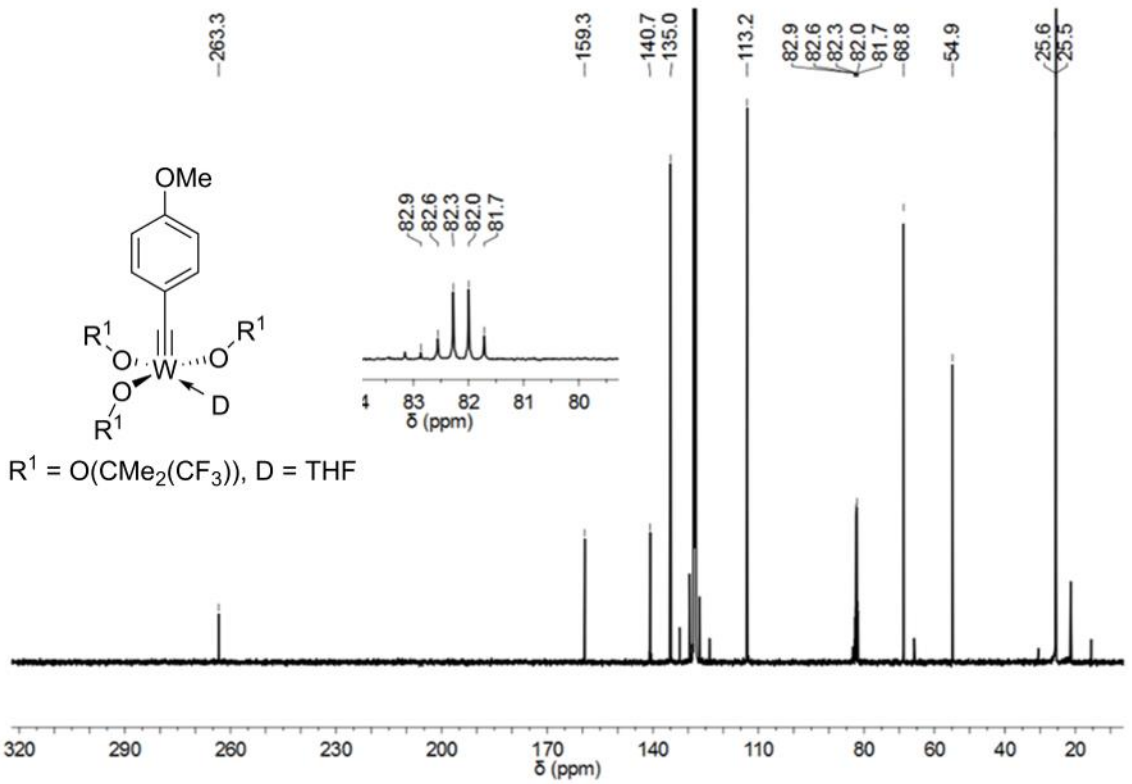

Figure S50: ^{13}C NMR (100 MHz, C_6D_6) spectrum of **W-2**.

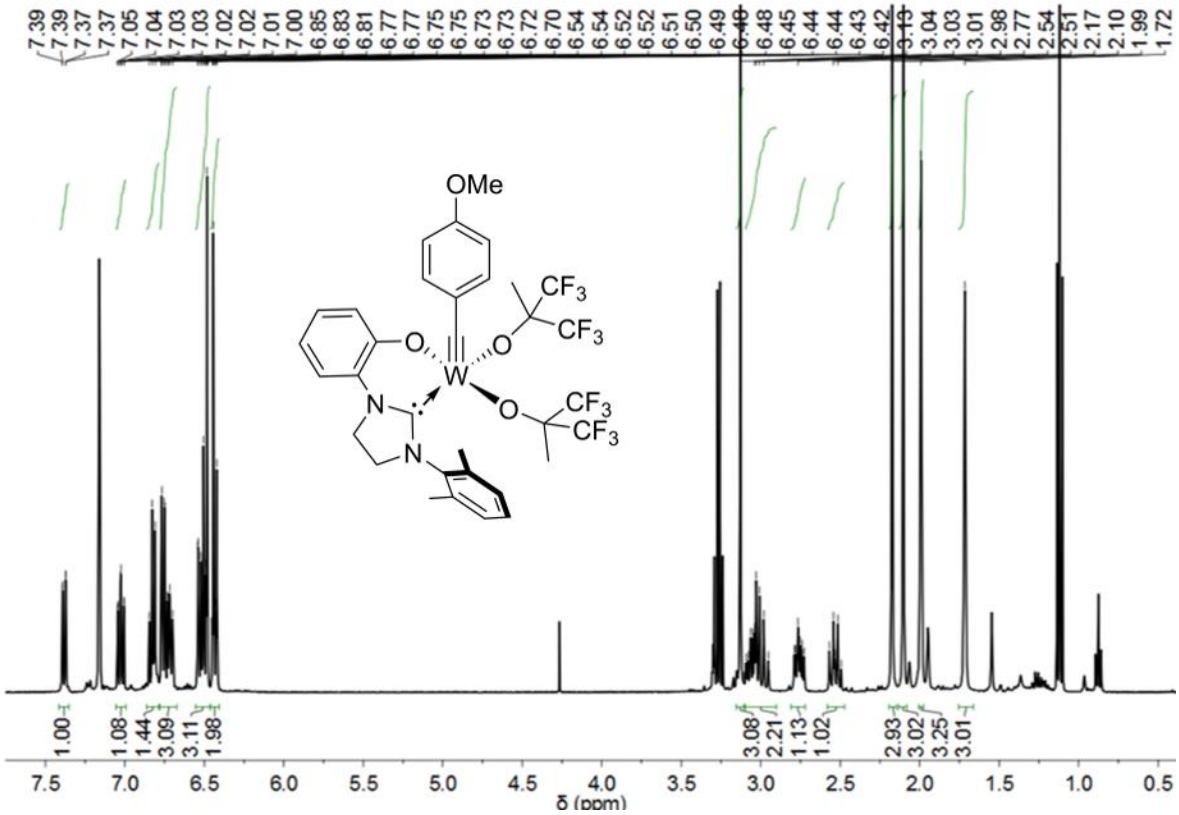

Figure S51: ^{1}H NMR (400 MHz, C_6D_6) spectrum of **W-3**.

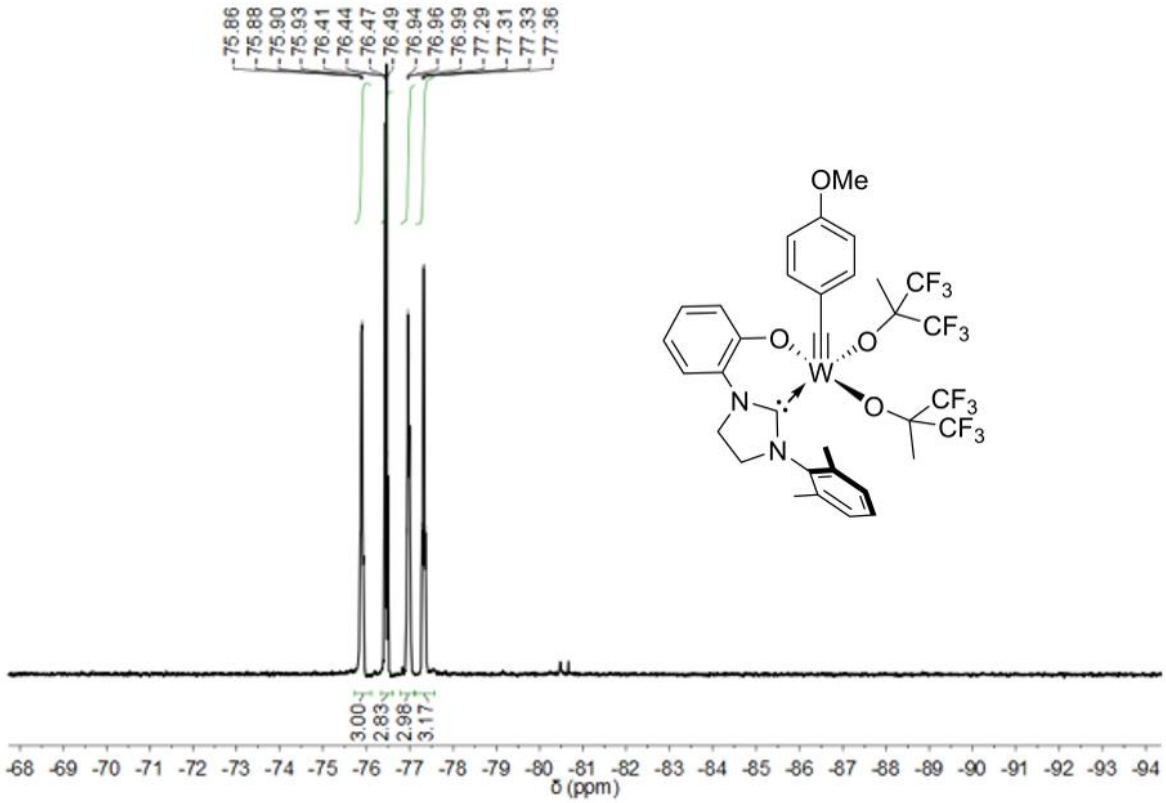

Figure S52: ^{19}F NMR (375 MHz, C_6D_6) spectrum of **W-3**.

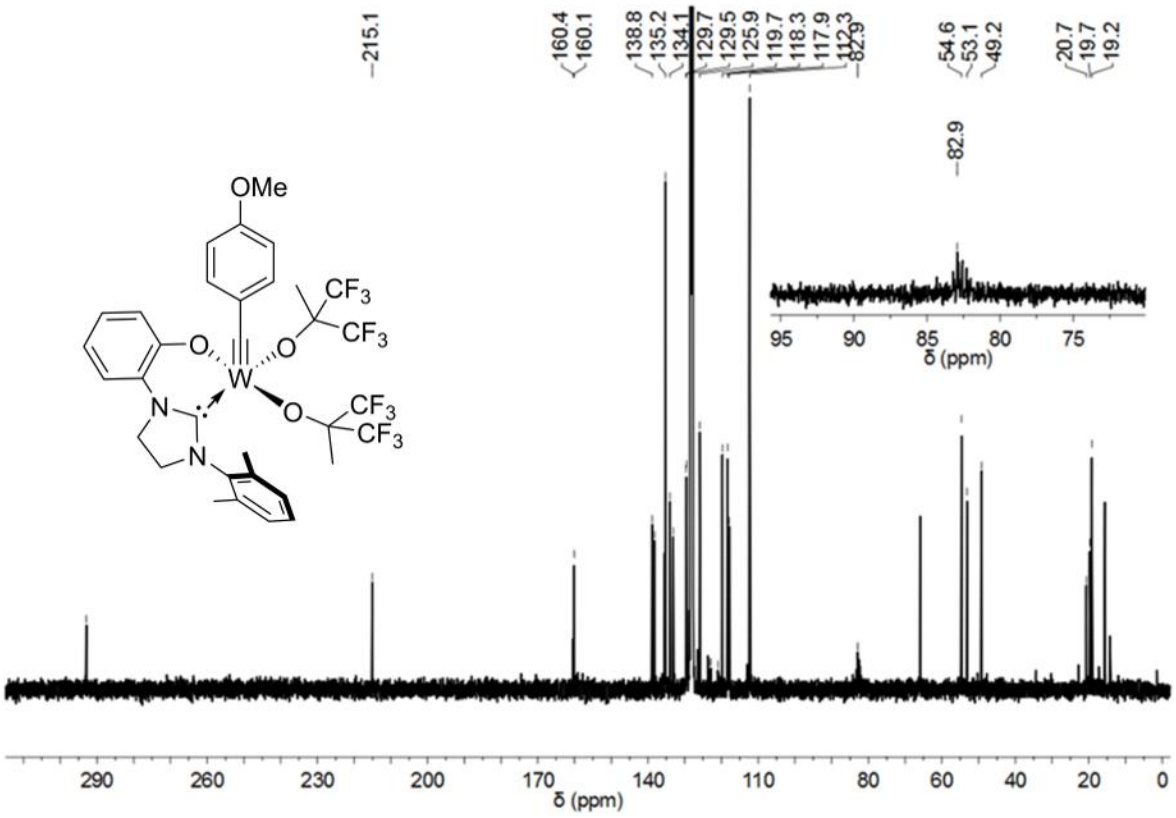

Figure S53: ^{13}C NMR (100 MHz, C_6D_6) spectrum of **W-3**.

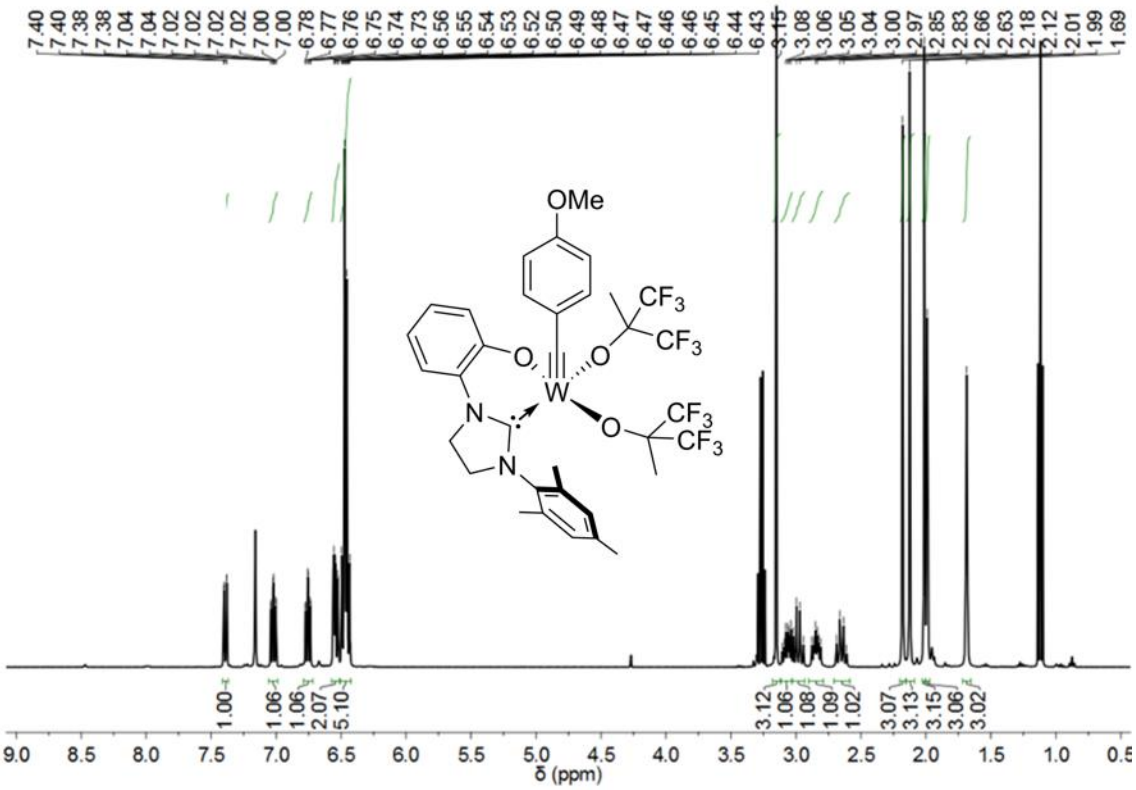

Figure S54: ^{1}H NMR (400 MHz, C_6D_6) spectrum of **W-4**.

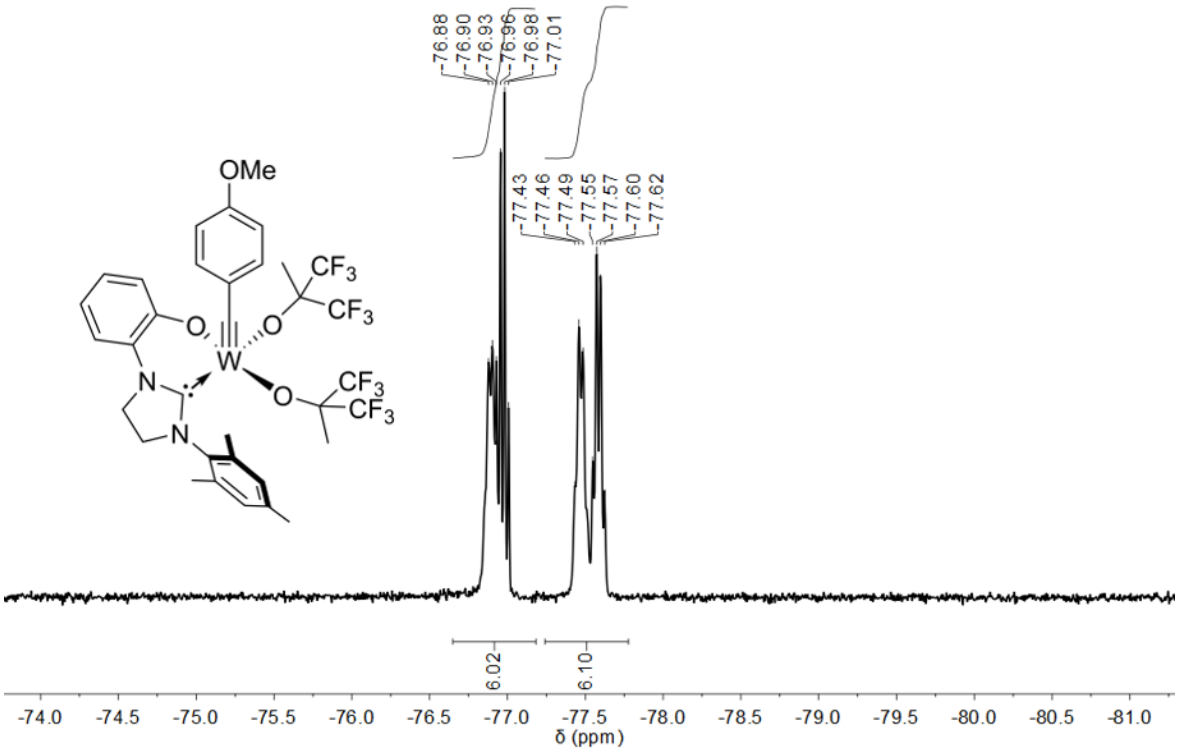

Figure S55: ^{19}F NMR (375 MHz, $CDCl_3$) spectrum of **W-4**.

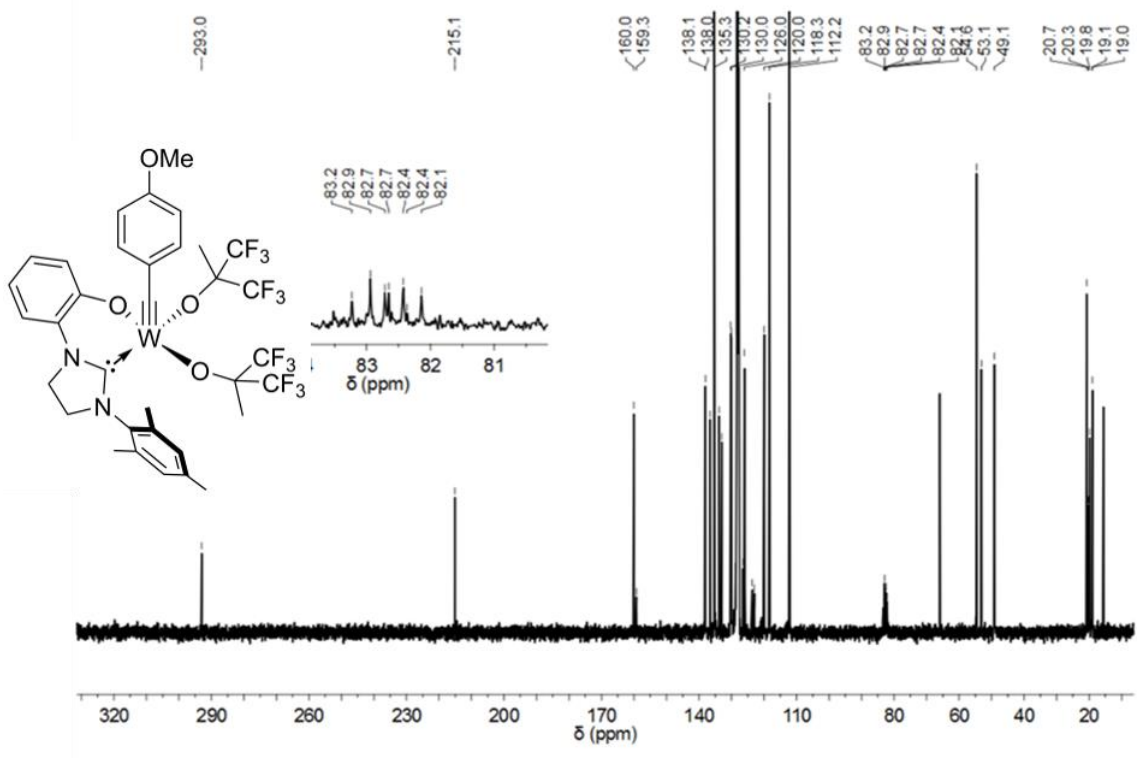

Figure S56: ^{13}C NMR (100 MHz, C_6D_6) spectrum of **W-4**.

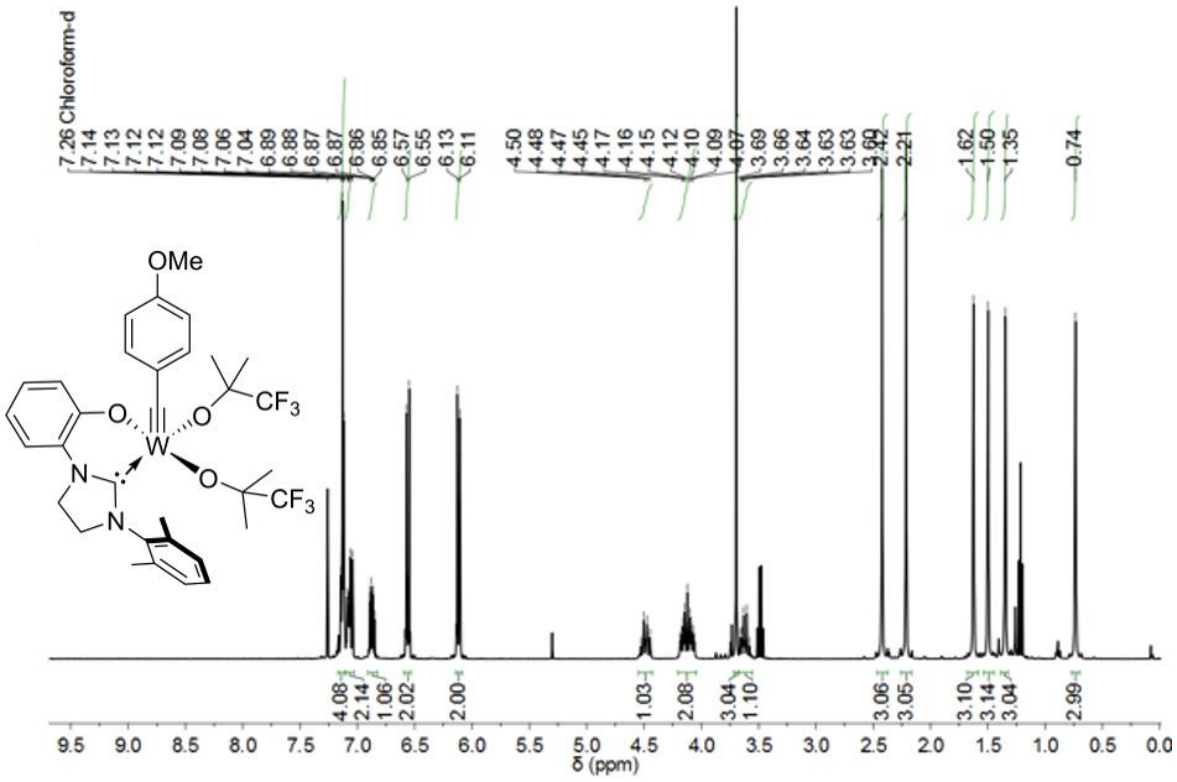

Figure S57: ^{1}H NMR (400 MHz, $CDCl_3$) spectrum of **W-6**.

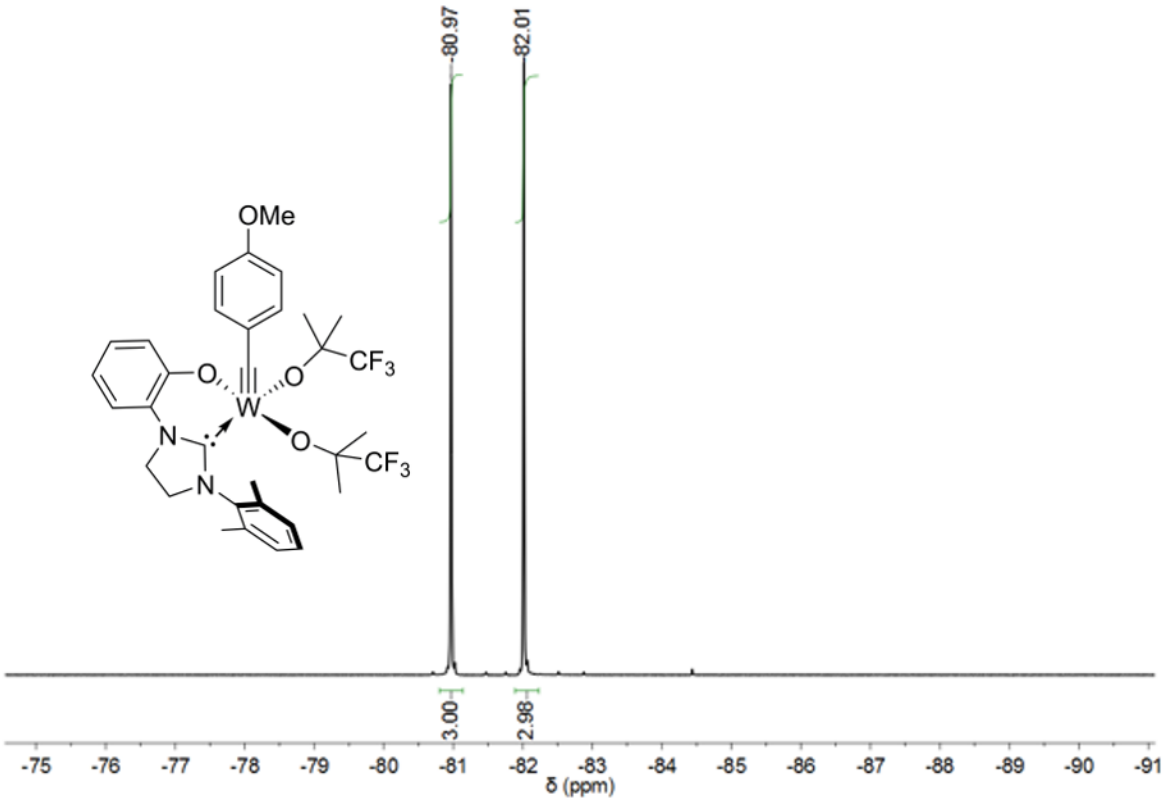

Figure S58: ^{19}F NMR (375 MHz, $CDCl_3$) spectrum of **W-6**.

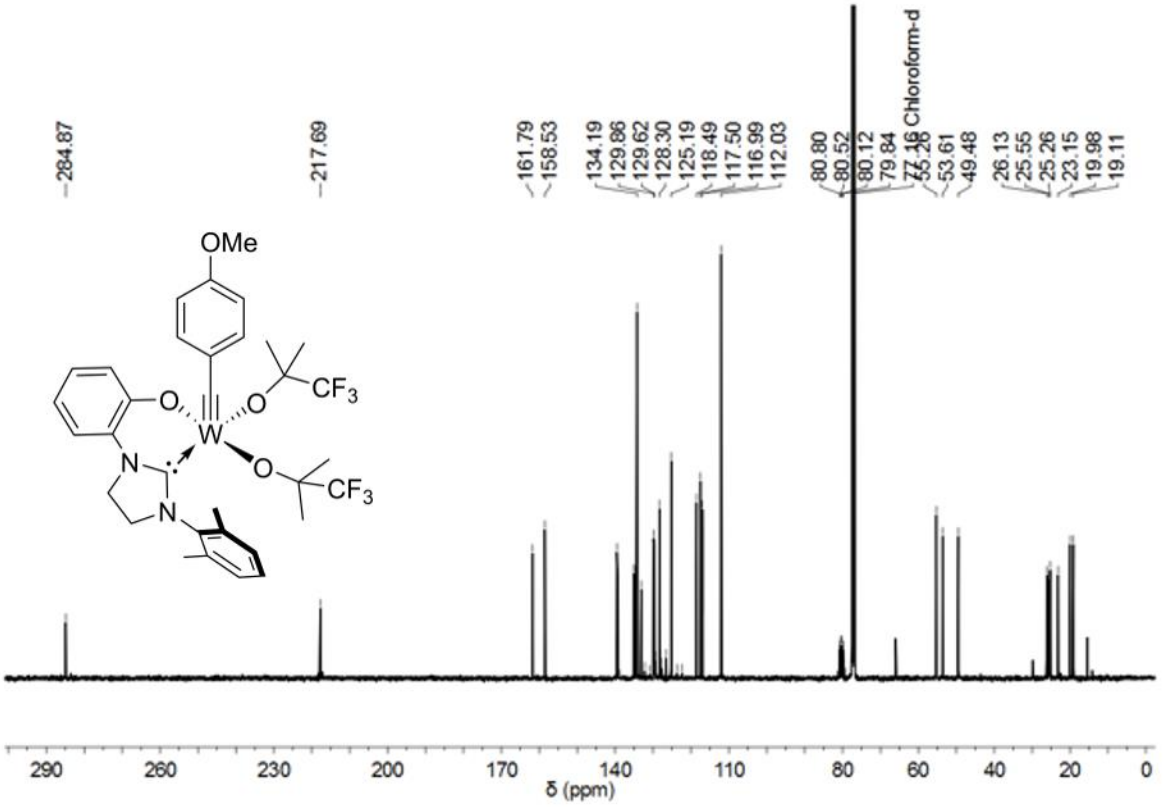

Figure S59: ^{13}C NMR (100 MHz, $CDCl_3$) spectrum of **W-6**.

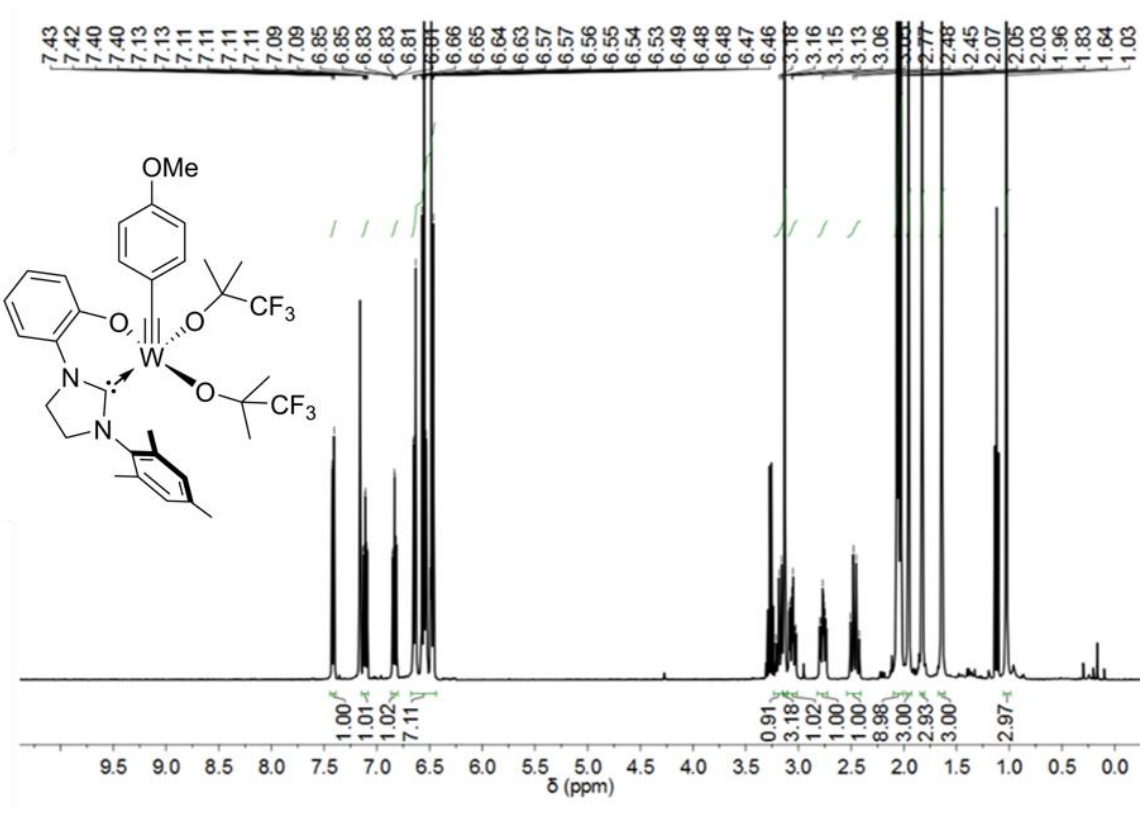

Figure S60: ^{1}H NMR (400 MHz, C_6D_6) spectrum of **W-7**.

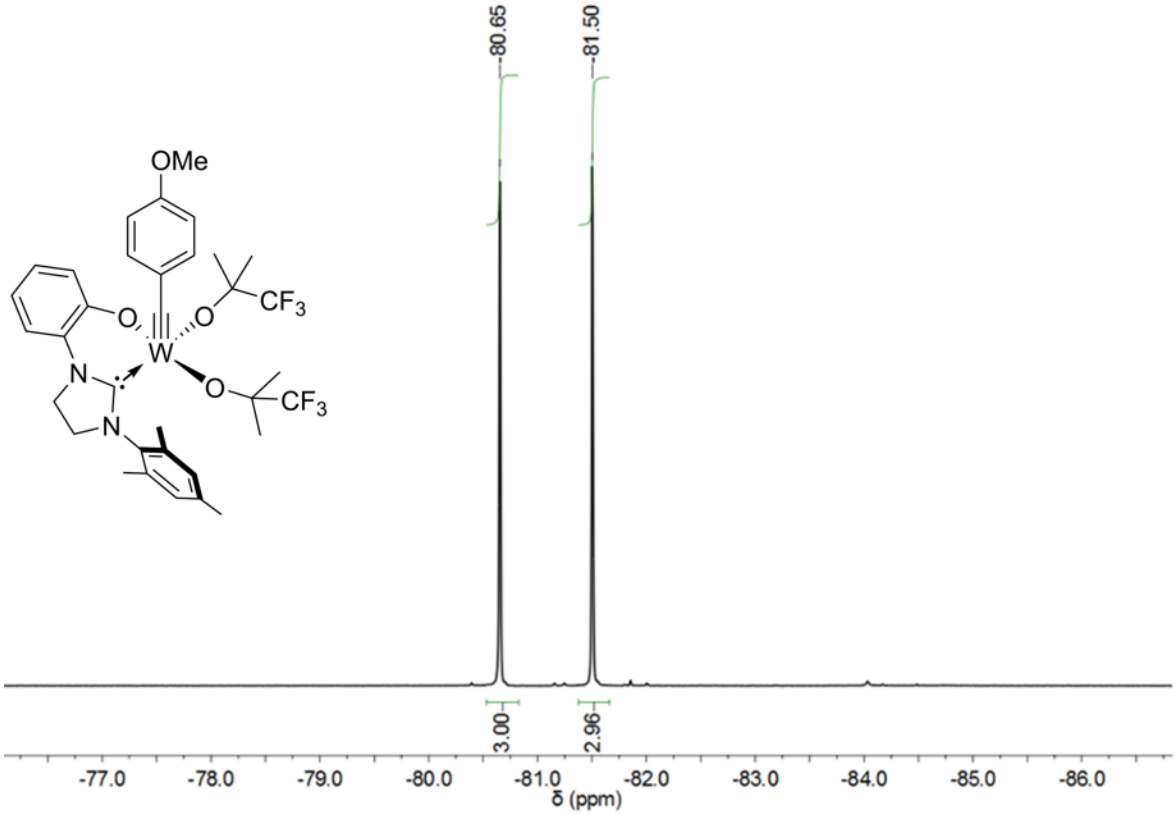

Figure S61: ^{19}F NMR (375 MHz, C_6D_6) spectrum of **W-7**.

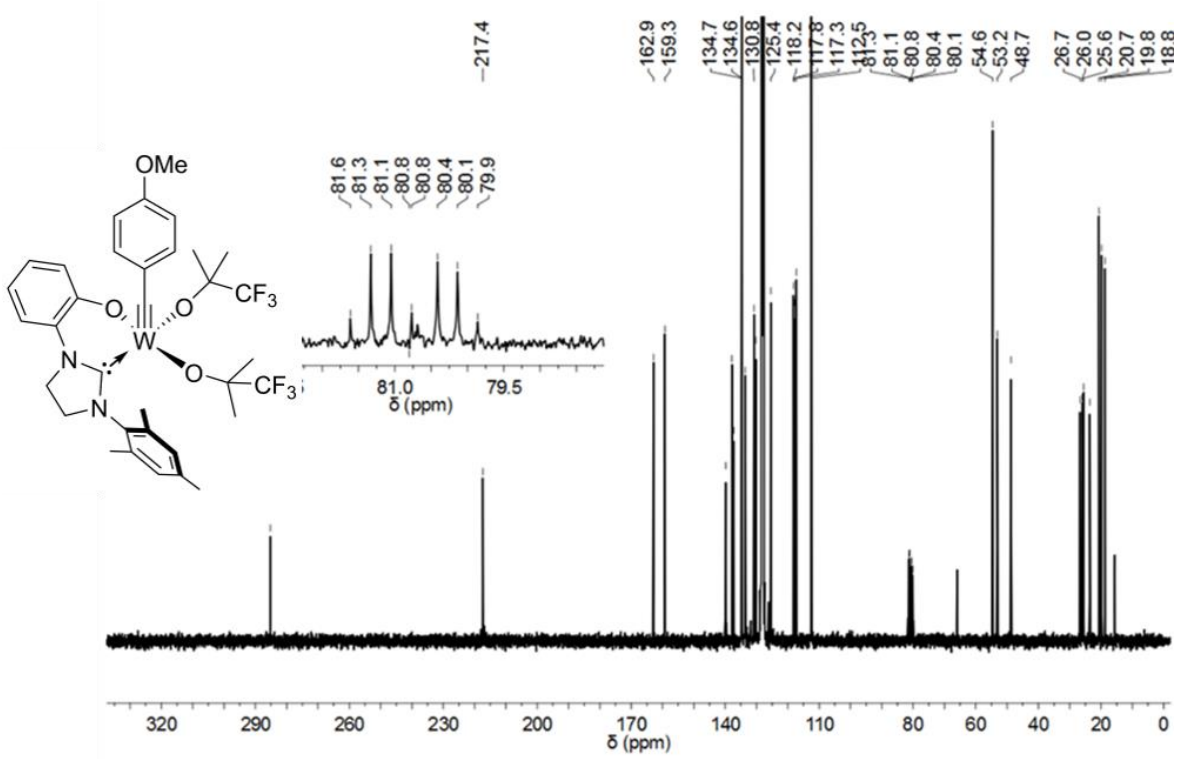

Figure S62: ^{13}C NMR (100 MHz, C_6D_6) spectrum of **W-7**.

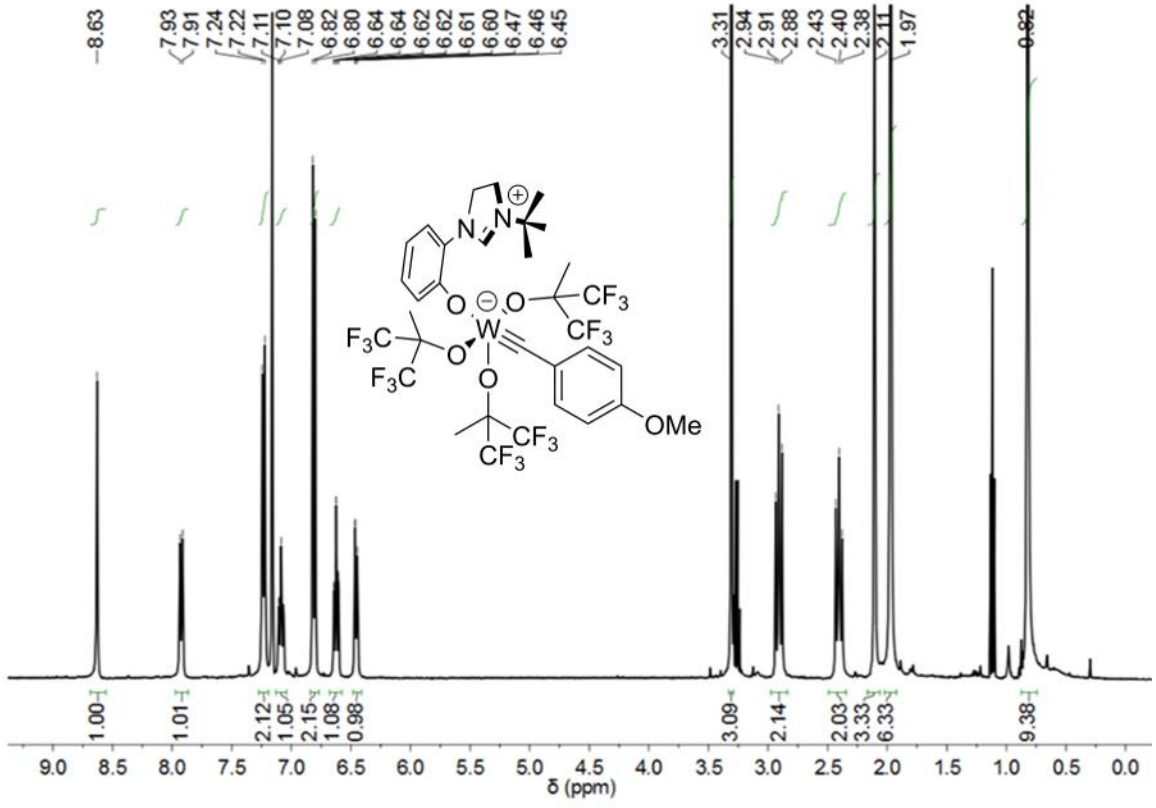

Figure S63: ^{1}H NMR (400 MHz, C_6D_6) spectrum of **W-5**.

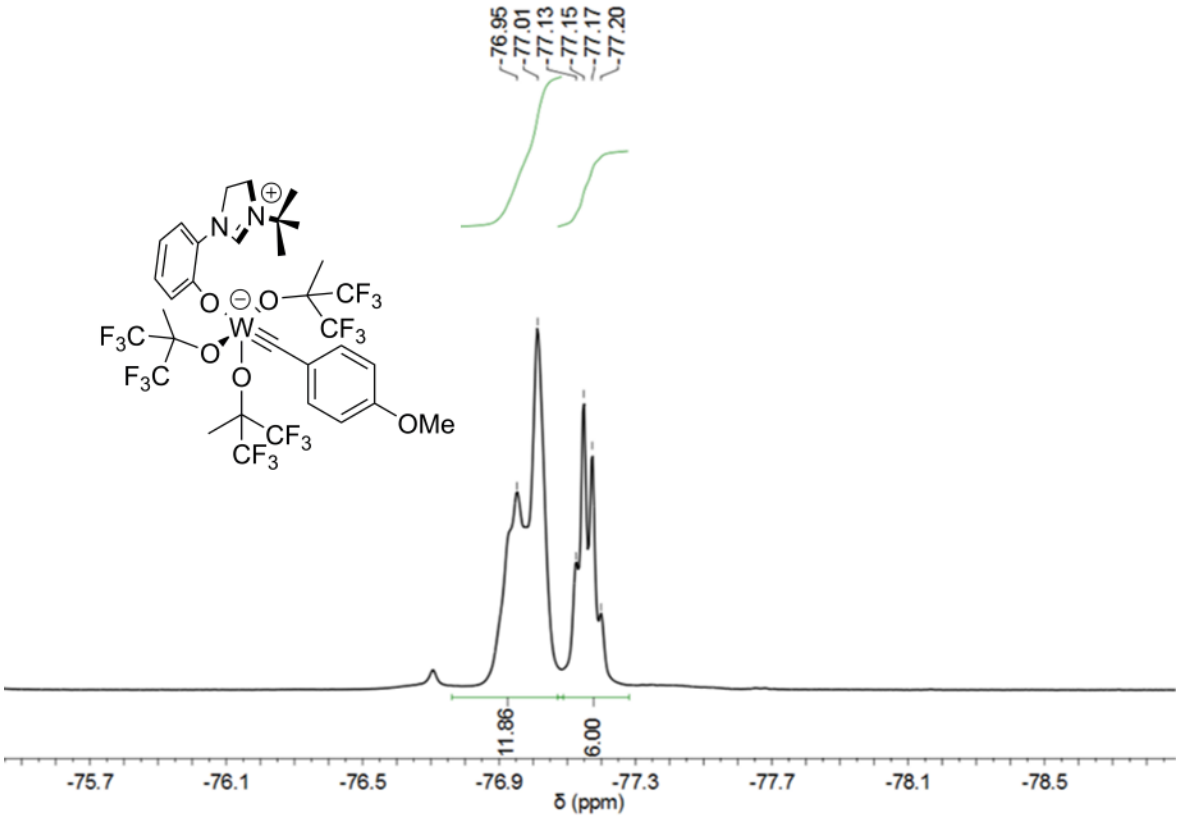

Figure S64: ^{19}F NMR (375 MHz, C_6D_6) spectrum of **W-5**.

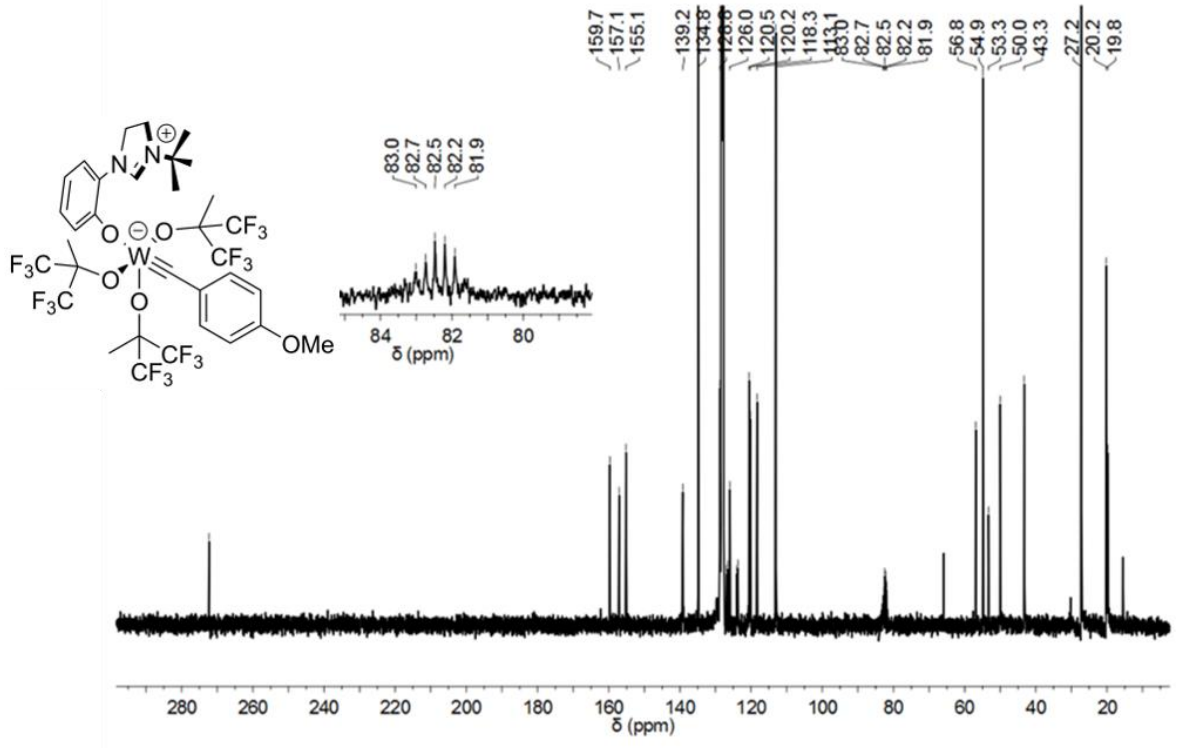

Figure S65: ^{13}C NMR (100 MHz, C_6D_6) spectrum of **W-5**.

7. *NMR spectra of mechanistic investigations*

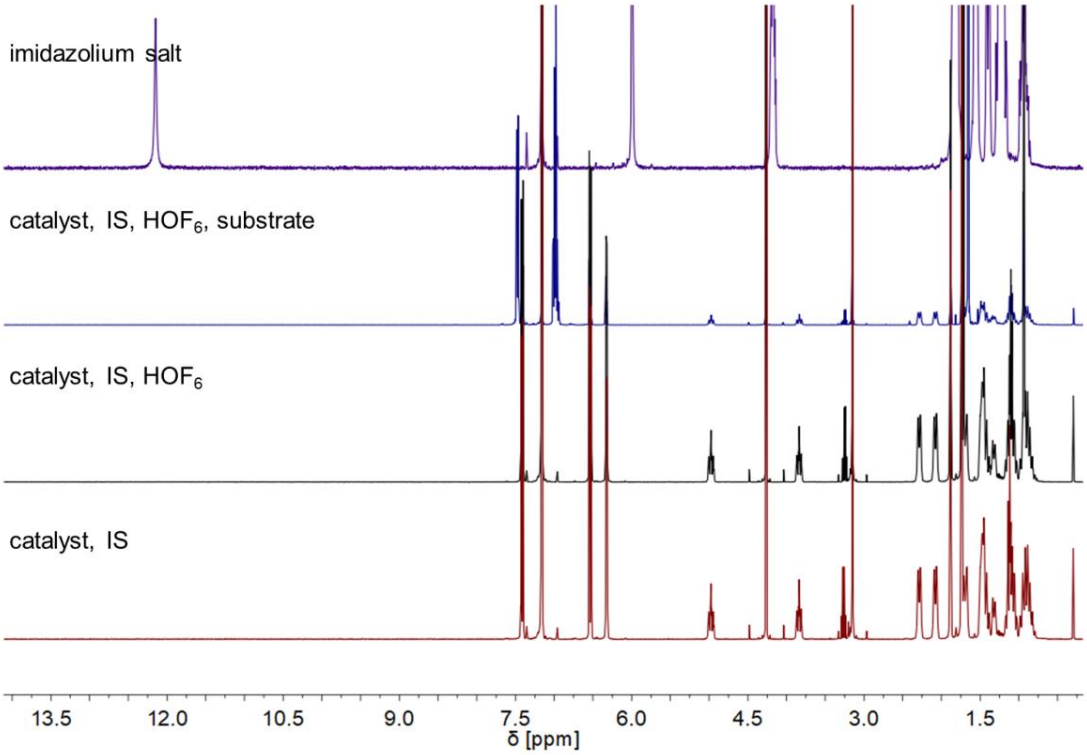

Figure S66: Stacked ^{1}H NMR spectra in C_6D_6. Catalyst: **Mo-3**. Bottom (red): catalyst and internal standard (IS). Black: catalyst, IS and hexafluoro-*tert*-butanol (HOF_6). Blue: catalyst, internal standard, HOF_6 and substrate (S1). Top (violet): corresponding imidazolium salt.

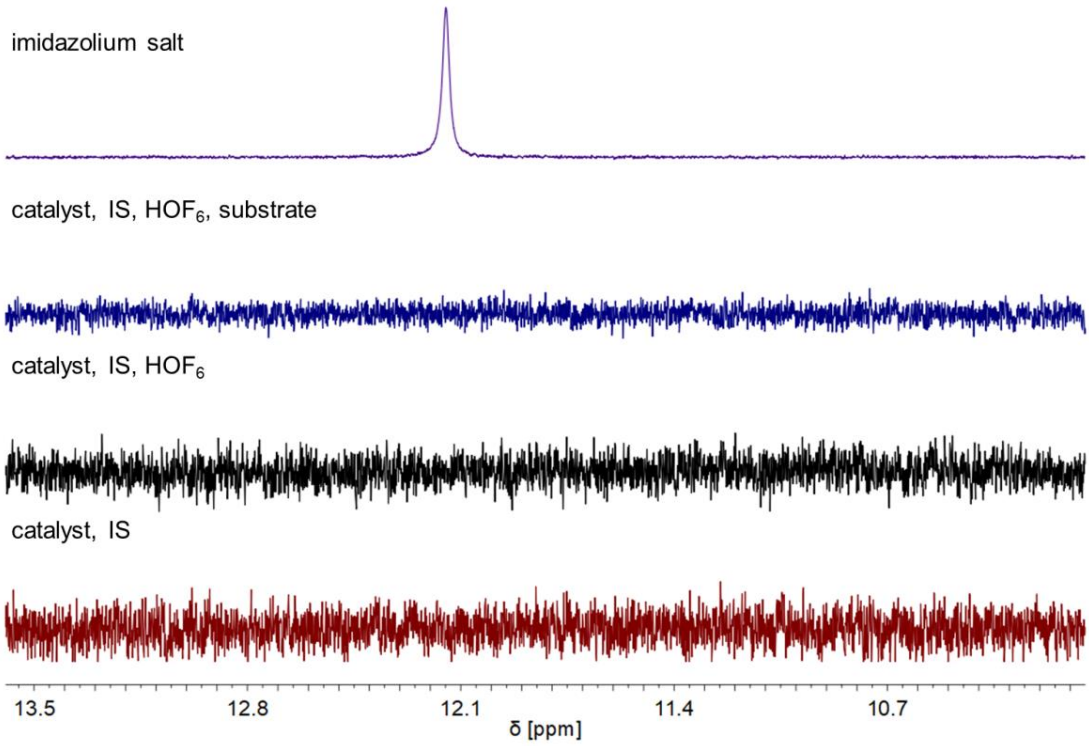

Figure S67: Zoom into the imidazolium proton region of stacked ^{1}H NMR spectra in C_6D_6. Catalyst: **Mo-3**. Bottom (red): catalyst and internal standard (IS). Black: catalyst, IS and hexafluoro-*tert*-butanol (HOF_6). Blue: catalyst, internal standard, HOF_6 and substrate (S1). Top (violet): corresponding imidazolium salt.

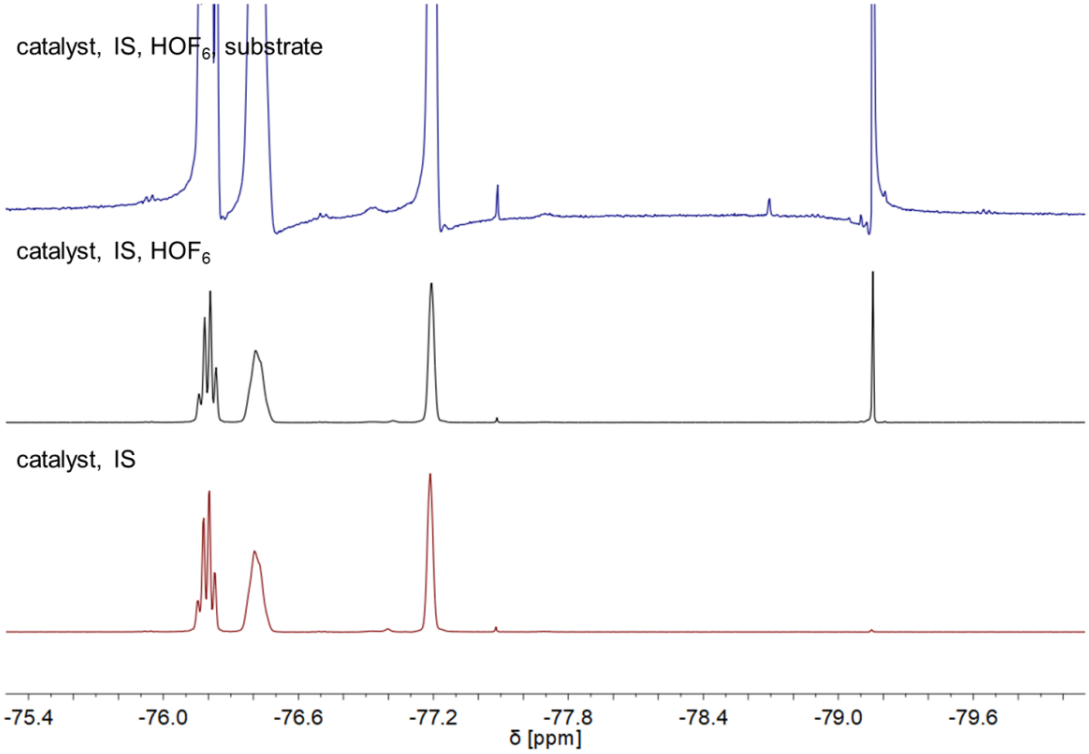

Figure S68: ^{19}F NMR spectra in C_6D_6. Catalyst: **Mo-3**. Bottom (red): catalyst and internal standard (IS). Black: catalyst, IS and hexafluoro-*tert*-butoxide (HOF_6). Top (Blue): catalyst, internal standard, HOF_6 and substrate (S1).

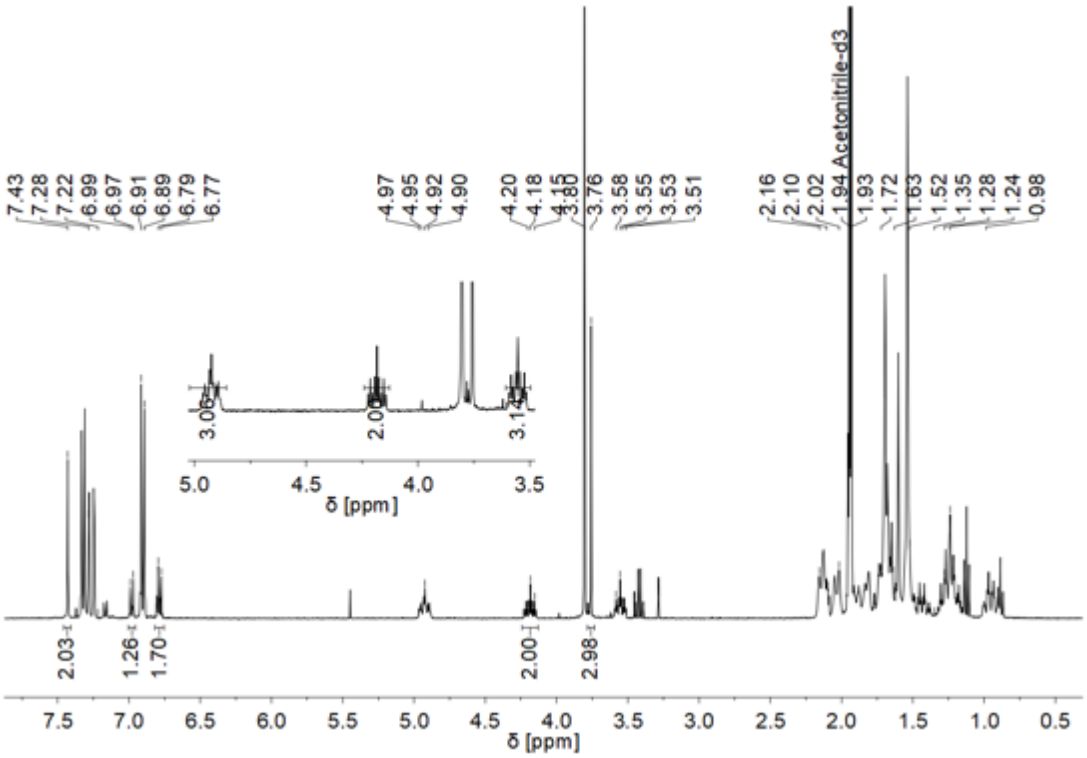

Figure S69: [1]H NMR spectrum of **Mo-3** in MeCN-d3. Integrated signals are assigned to the TBP (trigonal bipyramidal) structure.

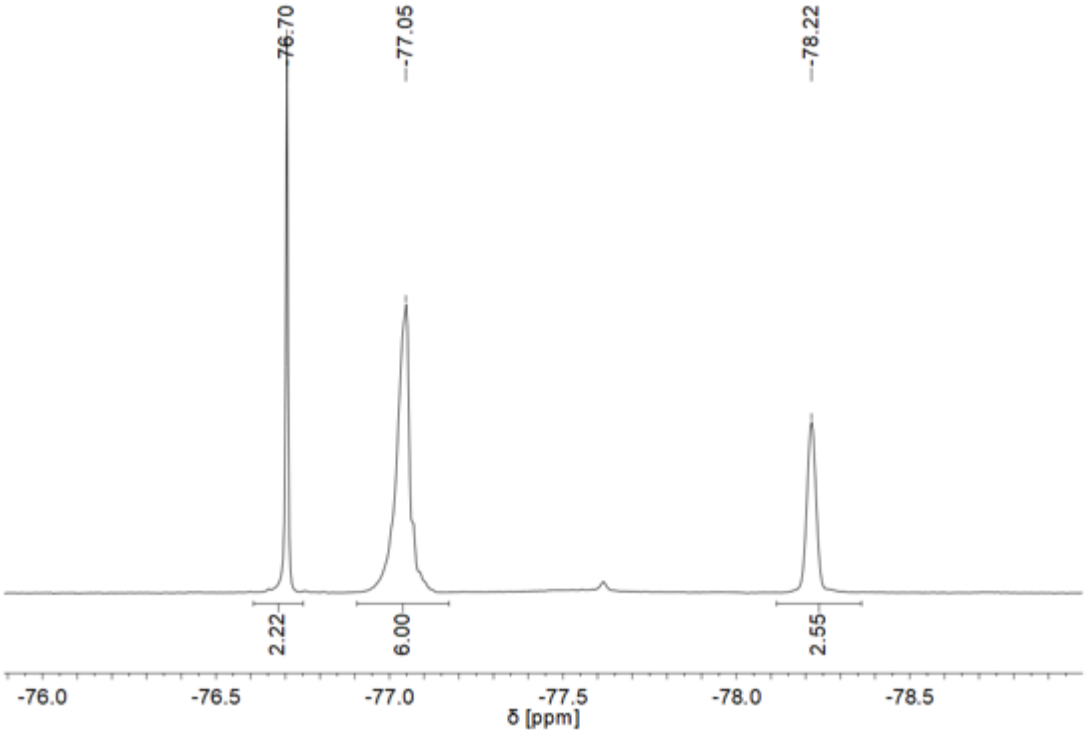

Figure S70: [19]F NMR spectrum of **Mo-3** in MeCN-d3. Resonance at δ = -76.7 ppm is assigned to the TBP (trigonal bipyramidal) structure.

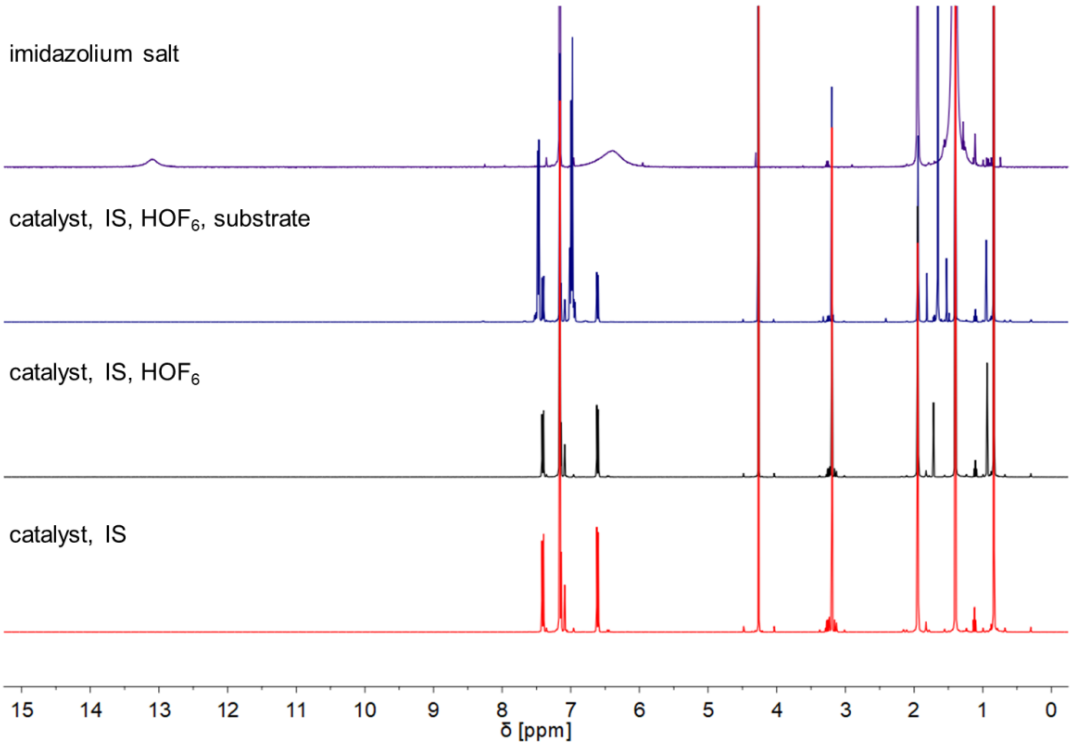

Figure S71: ^{1}H NMR spectra in C_6D_6. Catalyst: **Mo-4**. Bottom (red): catalyst and internal standard (IS). Black: catalyst, IS and hexafluoro-*tert*-butanol (HOF_6). Blue: catalyst, internal standard, HOF_6 and substrate. Top (violet): corresponding imidazolium salt.

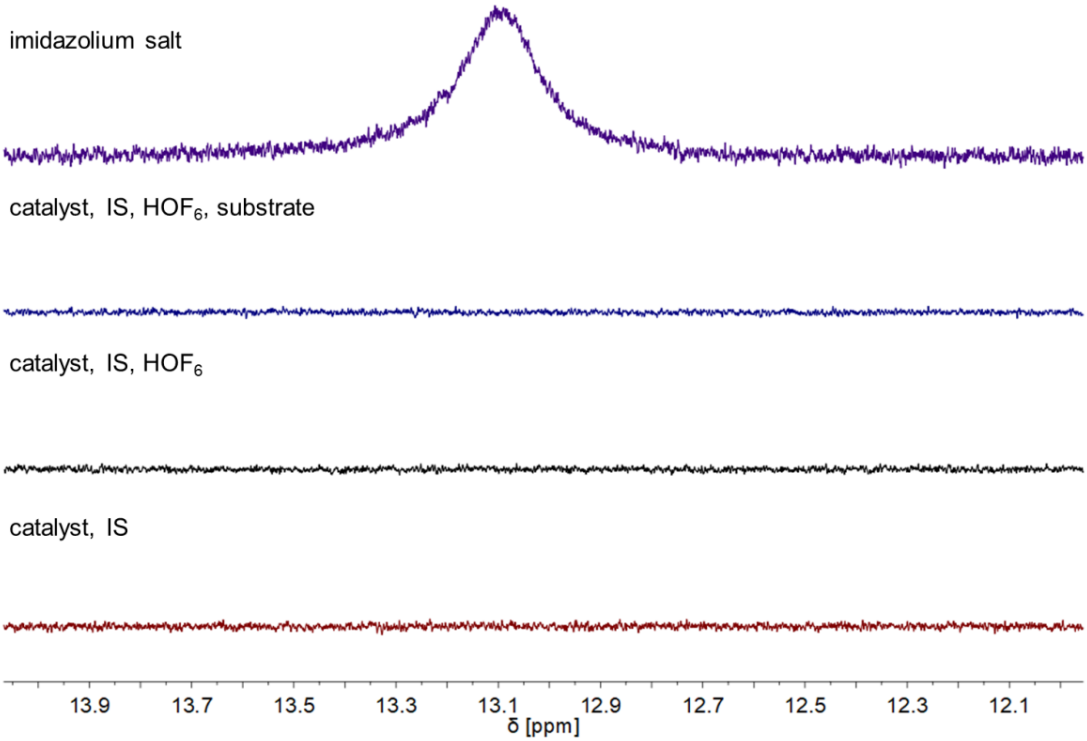

Figure S72: Zoom into the imidazolium proton region of stacked ^{1}H NMR spectra in C_6D_6. Catalyst: **Mo-4**. Bottom (red): catalyst and internal standard (IS). Black: catalyst, IS and hexafluoro-*tert*-butanol (HOF_6). Blue: catalyst, internal standard, HOF_6 and substrate. Top (violet): corresponding imidazolium salt.

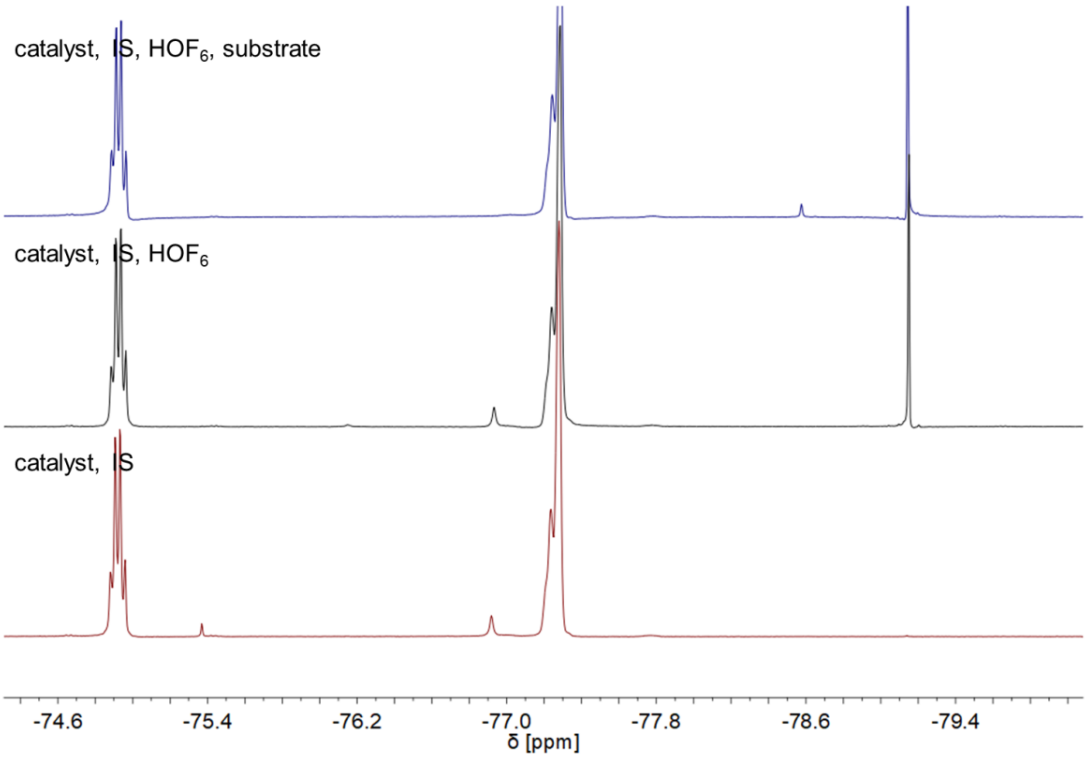

Figure S73: ^{19}F NMR spectra in C_6D_6. Catalyst: **Mo-4**. Bottom (red): catalyst and internal standard (IS). Black: catalyst, IS and hexafluoro-*tert*-butoxide (HOF_6). Top (blue): catalyst, internal standard, HOF_6 and substrate.

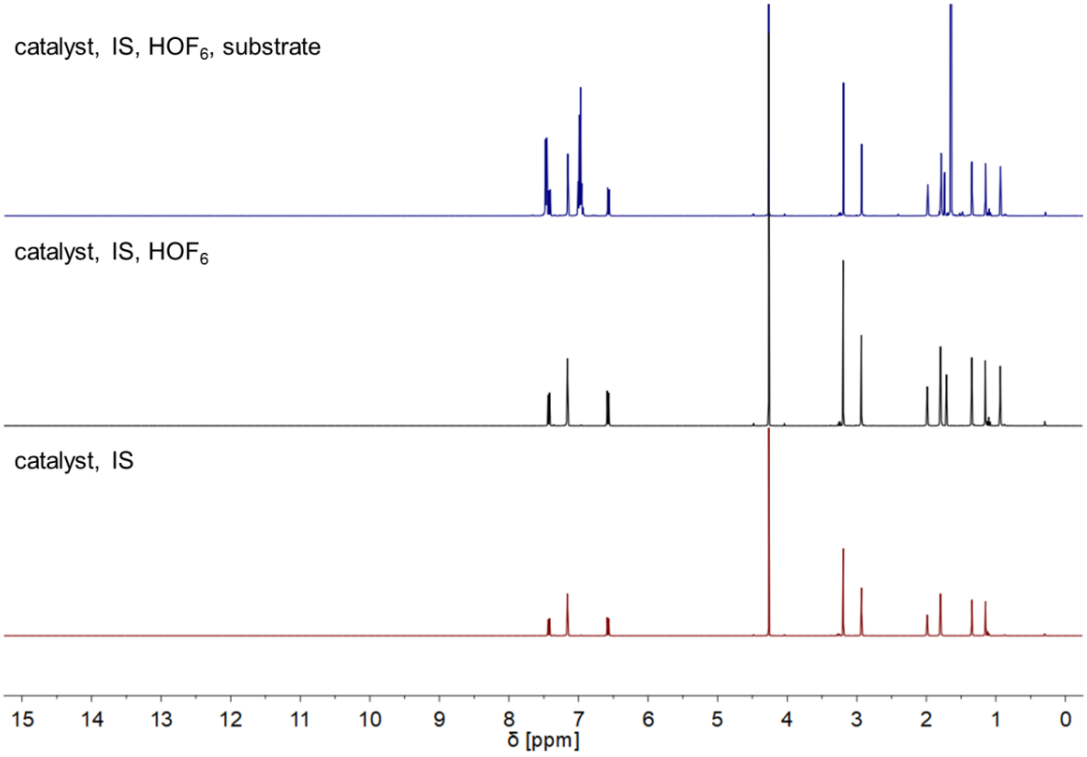

Figure S74: ^{1}H NMR spectra in C_6D_6. Catalyst: **Mo-5**. Bottom (red): catalyst and internal standard (IS). Black: catalyst, IS and hexafluoro-*tert*-butanol (HOF_6). Top (blue): catalyst, internal standard, HOF_6 and substrate.

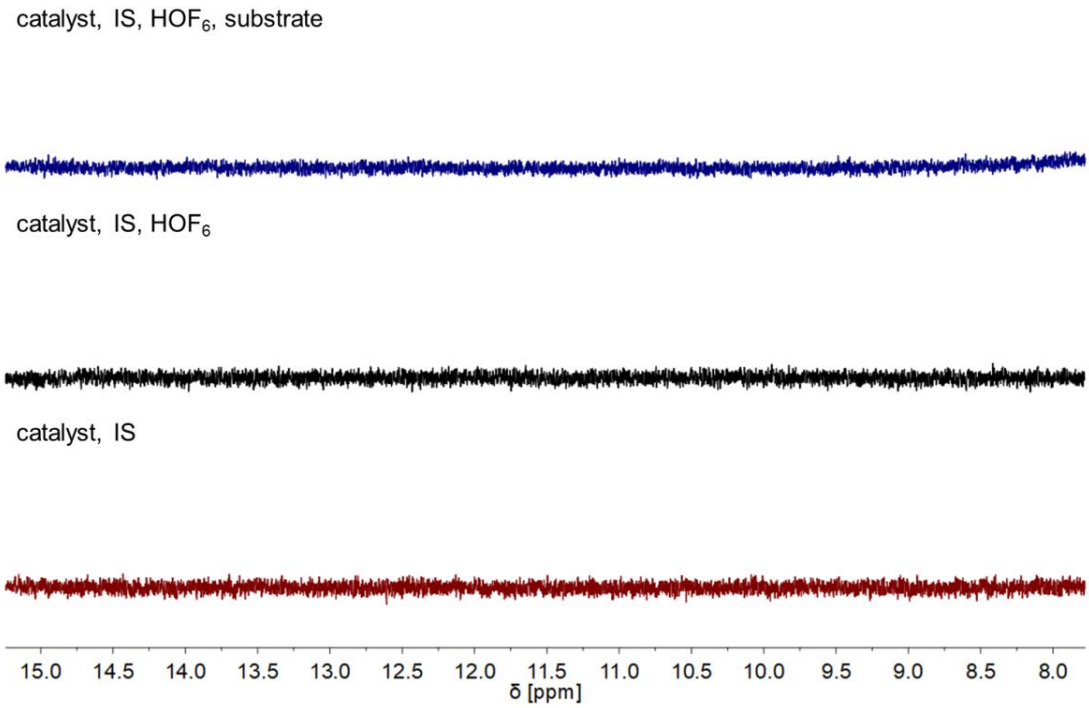

Figure S75: Zoom into the imidazolium proton region of stacked ^{1}H NMR spectra in C_6D_6. Catalyst: **Mo-5**. Bottom (red): catalyst and internal standard (IS). Black: catalyst, IS and hexafluoro-*tert*-butanol (HOF_6). Top (blue): catalyst, internal standard, HOF_6 and substrate.

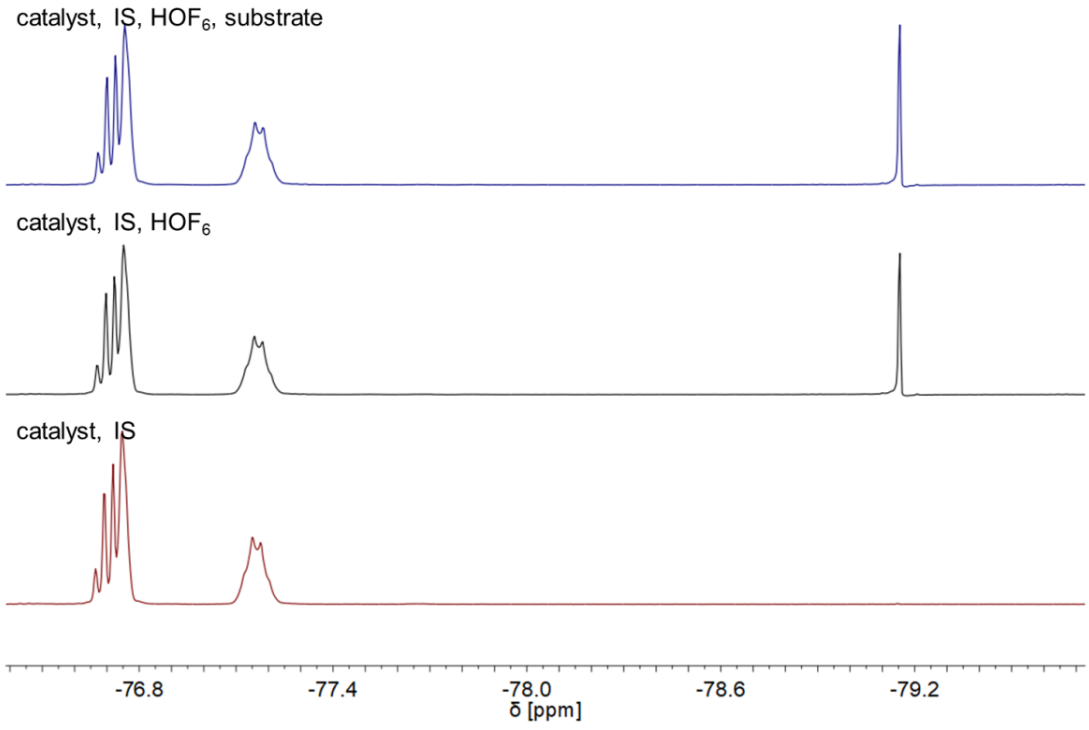

Figure S76: ^{19}F NMR spectra in C_6D_6. Catalyst: **Mo-5**. Bottom (red): catalyst and internal standard (IS). Black: catalyst, IS and hexafluoro-*tert*-butoxide (HOF_6). Top (blue): catalyst, internal standard, HOF_6 and substrate.

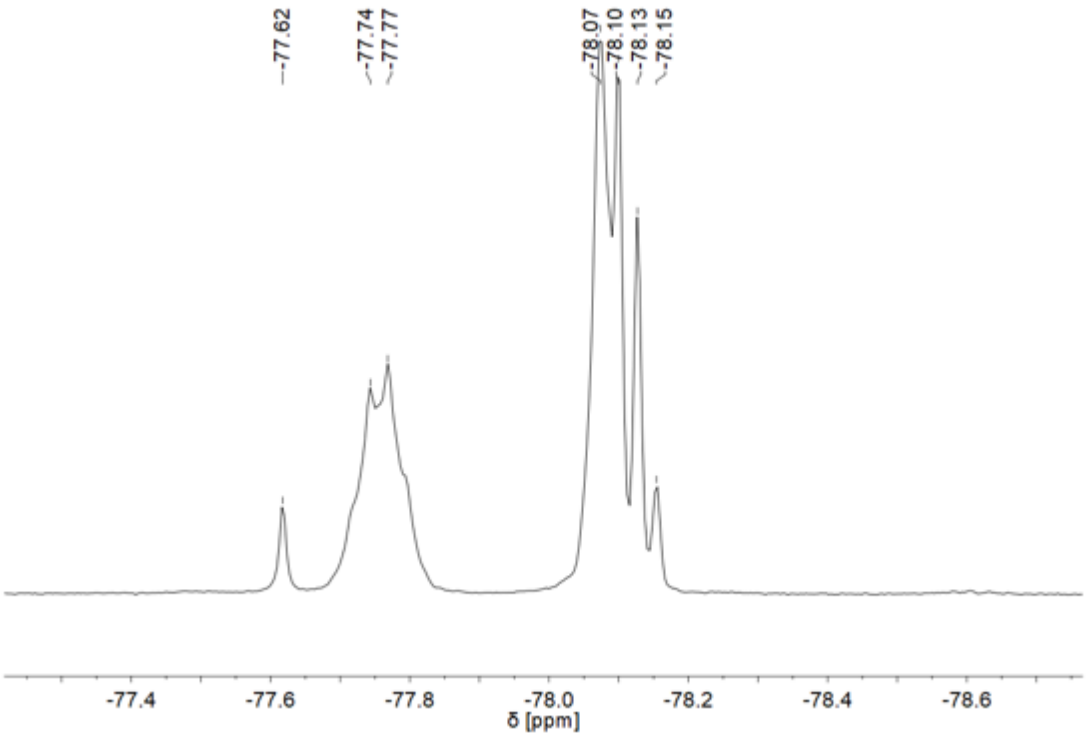

Figure S77: ^{19}F NMR spectrum of **Mo-5** in MeCN-d3.

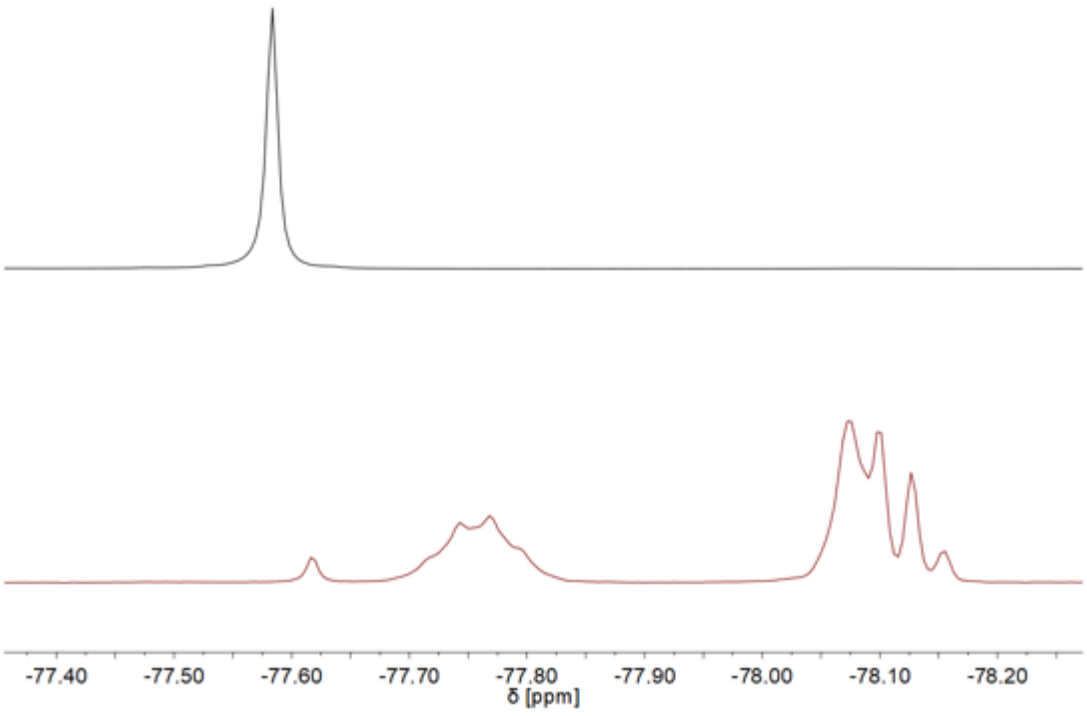

Figure S78: Stacking of ^{19}F NMR spectra in MeCN-d3. Bottom (red): **Mo-5**. Top (black): **Mo-1**.

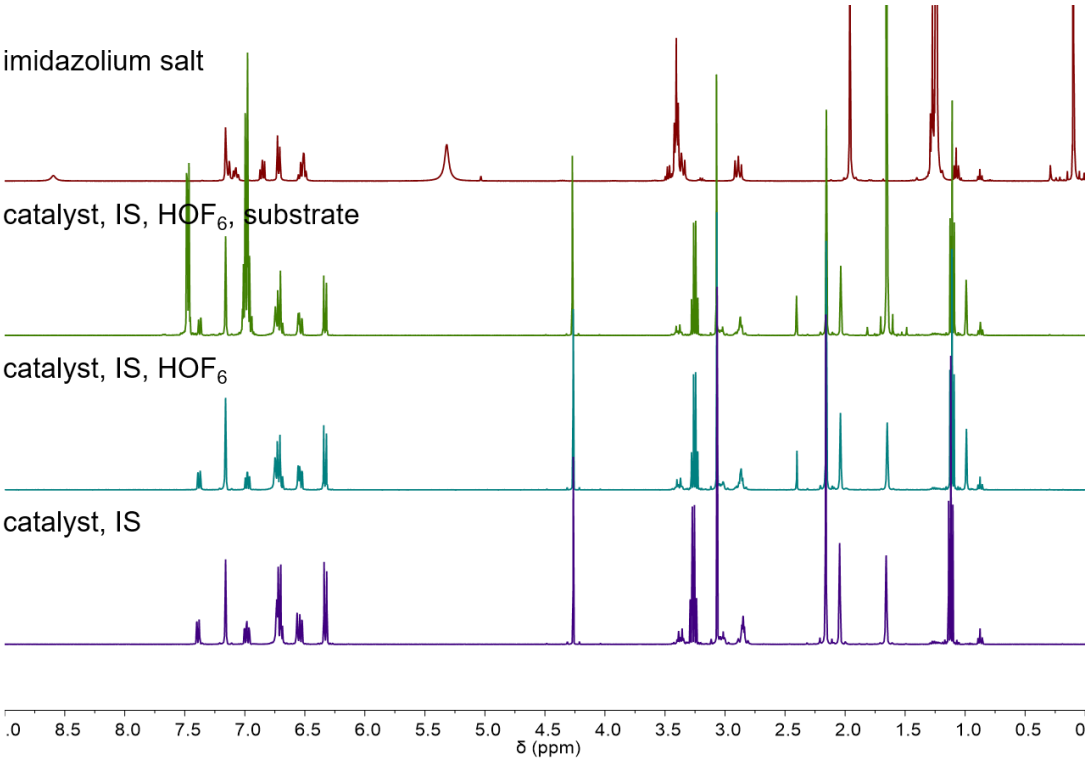

Figure S79: Stacked ^{1}H NMR spectra in C_6D_6. Catalyst: **Mo-8**. Bottom (violet): catalyst and internal standard (IS). Blue: catalyst, IS and hexafluoro-*tert*-butanol (HOF_6). Green: catalyst, IS, HOF_6 and substrate. Top (red): corresponding imidazolium salt.

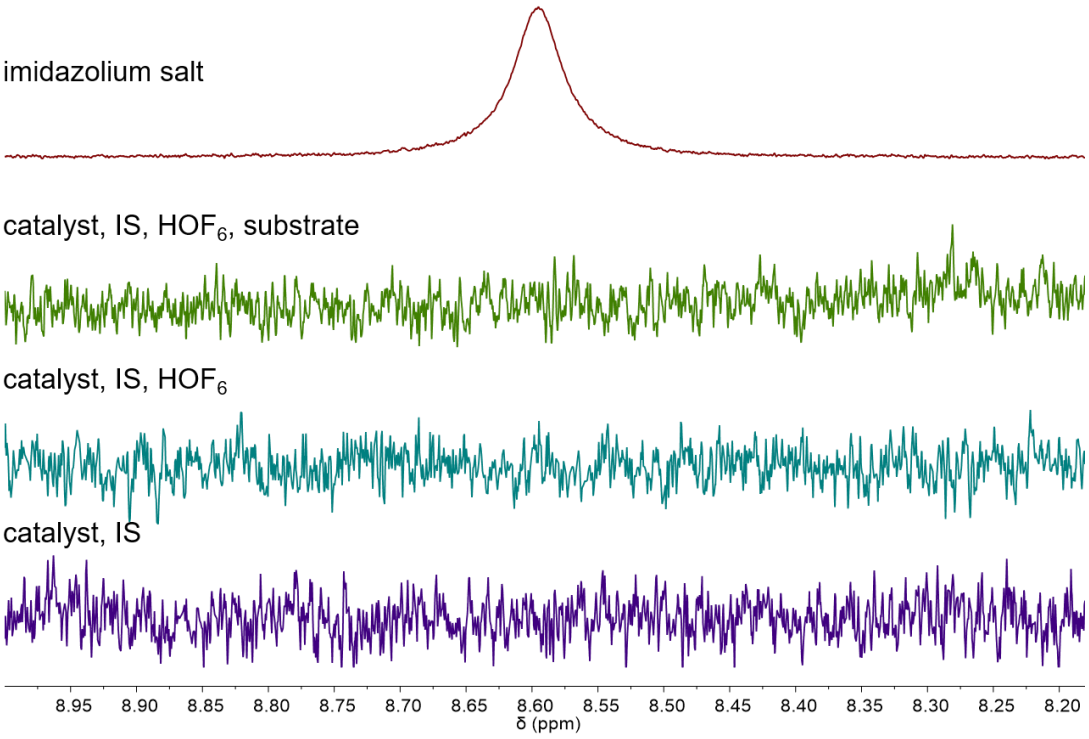

Figure S80: Zoom into the imidazolium proton region of stacked ^{1}H NMR spectra in C_6D_6. Catalyst: **Mo-8**. Bottom (violet): catalyst and internal standard (IS). Blue: catalyst, IS and hexafluoro-*tert*-butanol (HOF_6). Green: catalyst, IS, HOF_6 and substrate. Top (red): corresponding imidazolium salt.

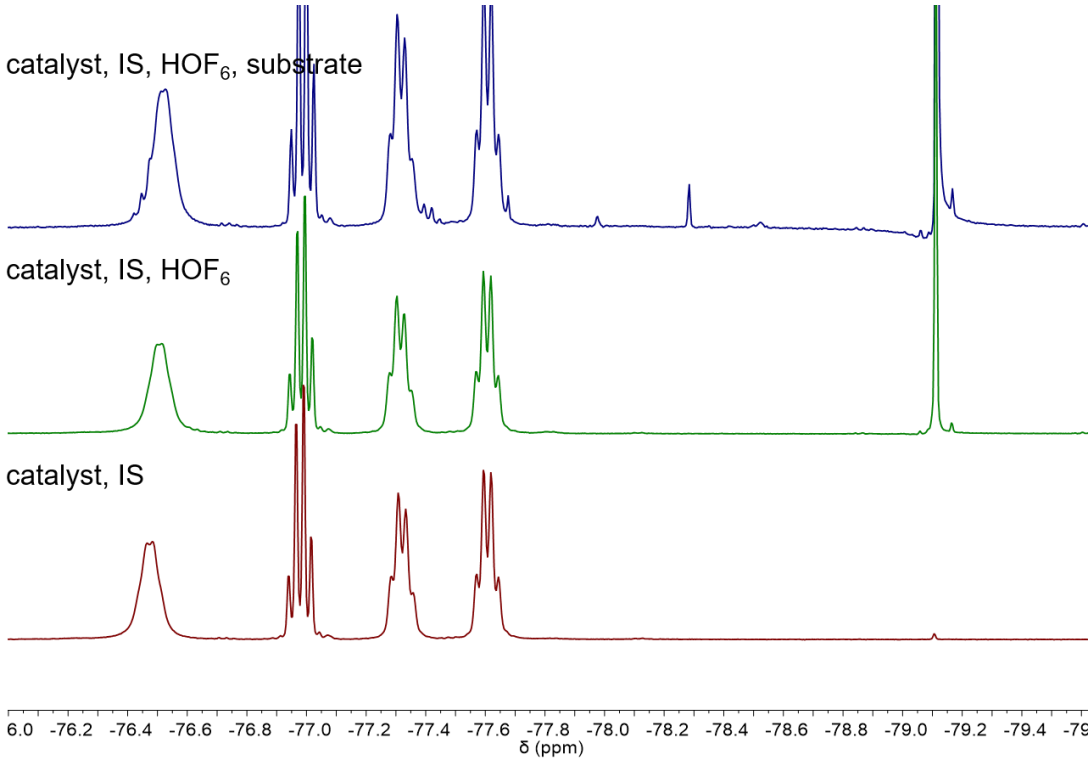

Figure S81: ^{19}F NMR spectra in C_6D_6. Catalyst: **Mo-8**. Bottom (red): catalyst and internal standard (IS). Green: catalyst, IS and hexafluoro-*tert*-butoxide (HOF_6). Top (blue): catalyst, IS, HOF_6 and substrate.

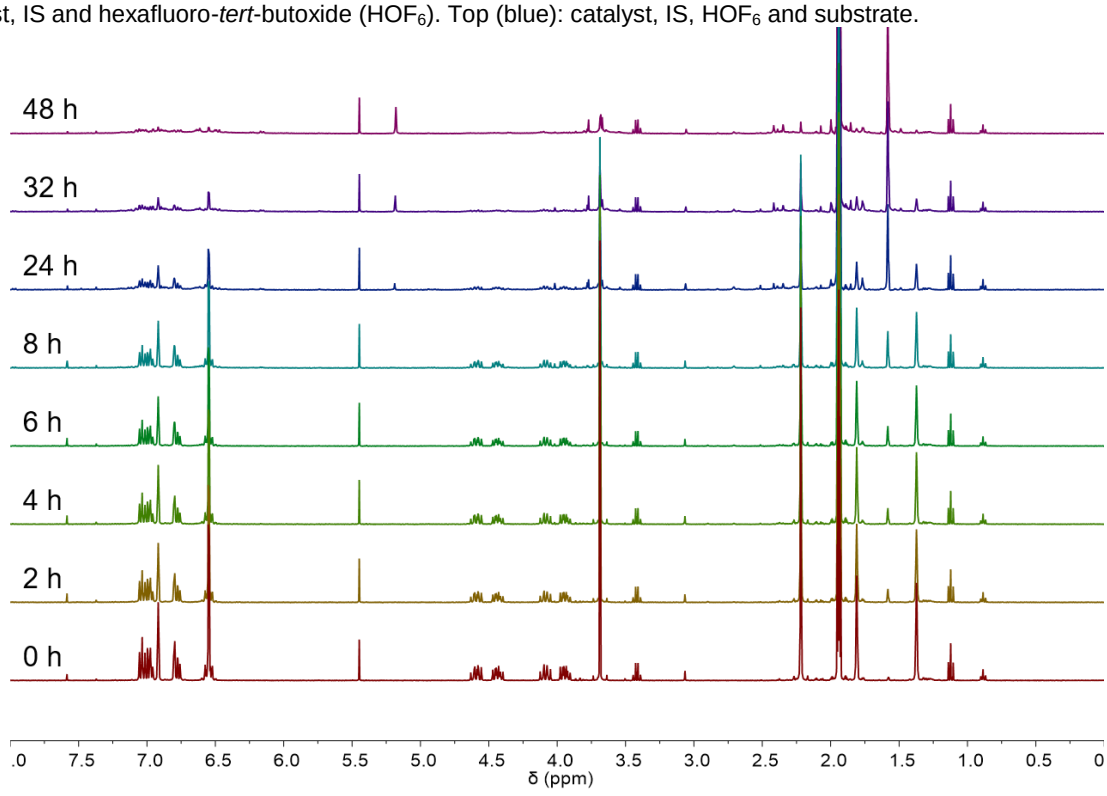

Figure S82: ^{1}H NMR spectra of **Mo-8** in acetonitrile-d3.

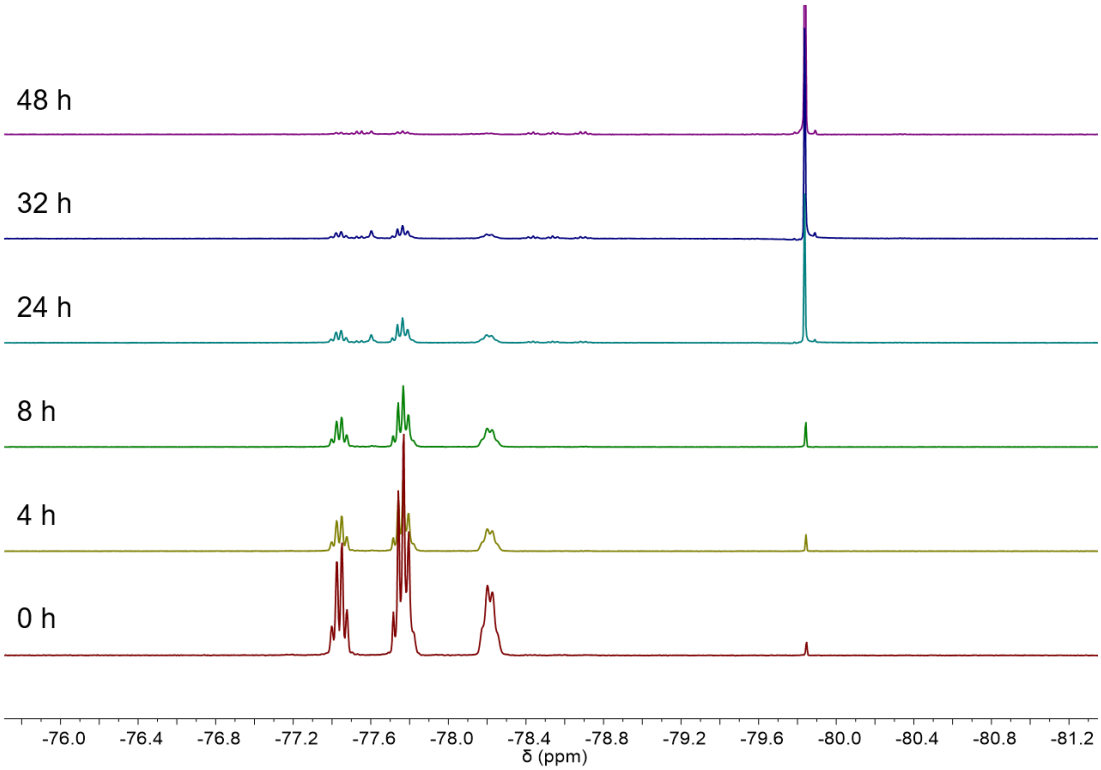

Figure S83: ^{19}F NMR spectra of **Mo-8** in acetonitrile-d3.

8. Crystal data

The supplemental file [om9b00481_si_002.xyz] contains the computed Cartesian coordinates of all of the molecules reported in this study. The file may be opened as a text file to read the coordinates, or opened directly by a molecular moedeling program such as Mercury (version 3.3 or later, http://www.ccdc.cam.ac.uk/pages/Home.aspx) for visualization and analysis.

8.1. Crystal data of Mo-3

Remark: Two inequivalent conformers (A and B) were found in the unit cell. In the article, only conformer A is shown. Here, data and plots of both conformers are presented.

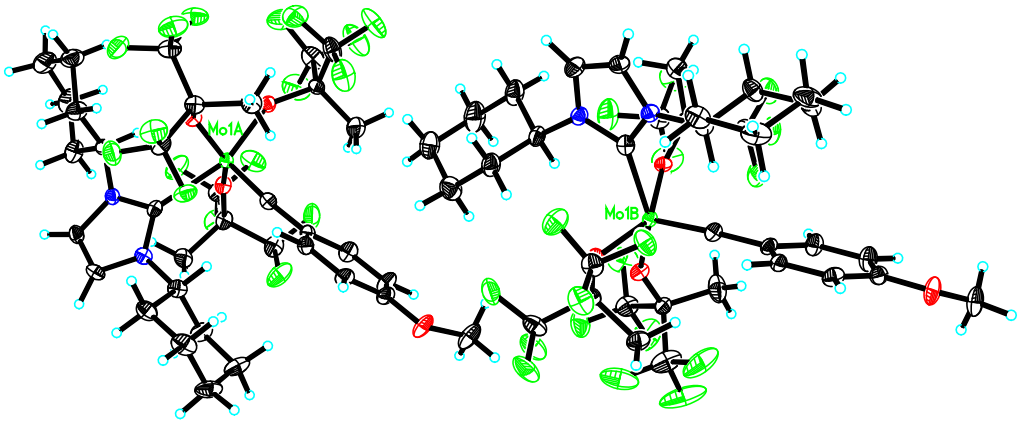

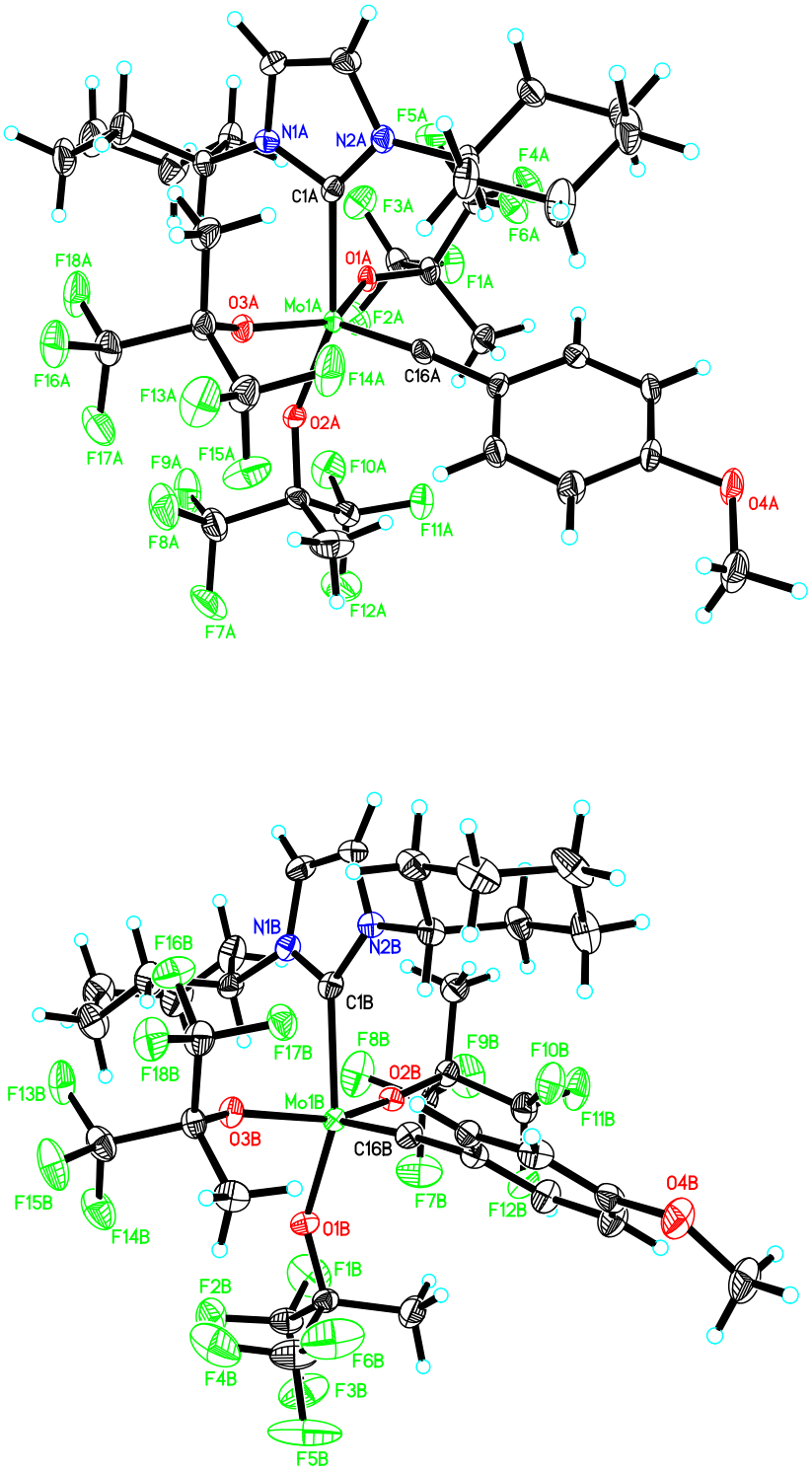

Figure S84: Single crystal X-ray structure of **Mo-3**. Both conformers together (A and B), conformer A and conformer B are shown.

*Crystal data and structure refinement for **Mo-3**.*

Empirical formula	$C_{35}H_{40}F_{18}MoN_2O_4$	
Formula weight	990.63	
Temperature	130(2) K	
Wavelength	0.71073 A	
Crystal system	Monoclinic	
Space group	$P2_1/n$	
Unit cell dimensions	a=22.740(2) Å	α = 90°
	b=10.6642(9) Å	β = 95.299(4)°
	c=33.166(3) Å	γ = 90°
Volume	8008.6(12) $Å^3$	
Z	8	
Calculated density	1.643 mg/m^3	
Absorption coefficient	0.452 mm^{-1}	
F(000)	4000	
Crystal size	0.14 x 0.13 x 0.12 mm	
Theta range for data collection	1.80 to 26.35°.	
Limiting indices	-21<=h<=28, -13<=k<=12, -26<=l<=41	
Reflections collected / unique	59529 / 16201 [R(int) = 0.0544]	
Completeness to θ = 26.35	99.1 %	
Absorption correction	Numerical	
Max. and min. transmission	0.8726 and 0.7686	
Refinement method	Full-matrix least-squares on F^2	
Data / restraints / parameters	16201 / 0 / 1089	
Goodness-of-fit on F^2	1.039	
Final R indices [I>2σ(I)]	R1 = 0.0512, wR2 = 0.1024	
R indices (all data)	R1 = 0.0969, wR2 = 0.1124	
Largest diff. peak and hole	1.322 and -1.254 $eÅ^{-3}$	

8.2. Crystal data of Mo-4

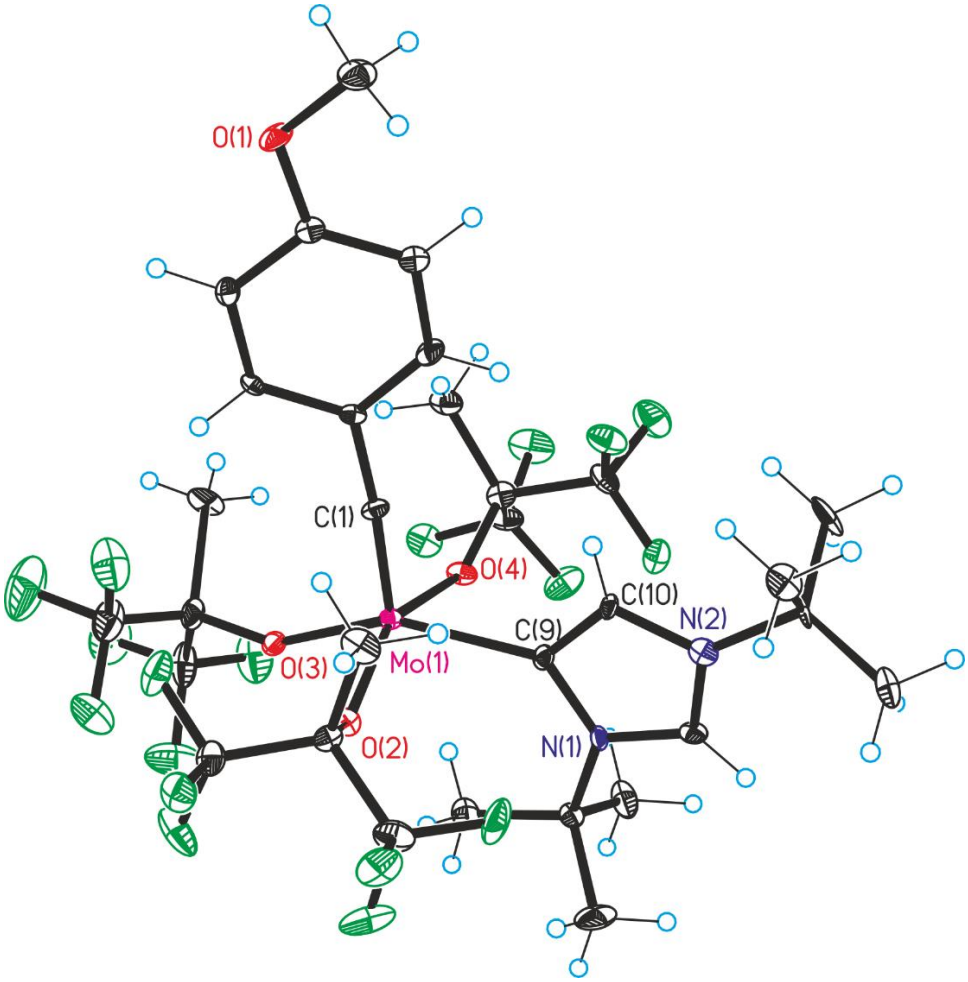

Figure S85: Crystal structure of **Mo-4**.

Crystal data and structure refinement for **Mo-4.**

Empirical formula	$C_{31}H_{36}F_{18}MoN_2O_4$	
Formula weight	938.56	
Temperature	193(2) K	
Wavelength	0.71073 Å	
Crystal system	Monoclinic	
Space group	$P2_1/c$	
Unit cell dimensions	a = 20.7436(19) Å	α = 90°
	b = 34.543(3) Å	β = 90.876(3)°
	c = 10.5388(9) Å	γ = 90°
Volume	7550.7(12) Å	
Z	8	

Density (calculated)	1.651 Mg/m^3
Absorption coefficient	0.474 mm^{-1}
F(000)	3776
Crystal size	0.130 x 0.060 x 0.020 mm^3
Theta range for data collection	2.154 to 22.500°.
Index ranges	-22<=h<=22, -37<=k<=37, -11<=l<=11
Reflections collected	87912
Independent reflections	9834 [R(int) = 0.1420]
Completeness to θ = 22.500°	99.9 %
Absorption correction	Semi-empirical from equivalents
Max. and min. transmission	0.942 and 0.818
Refinement method	Full-matrix least-squares on F^2
Data / restraints / parameters	9834 / 0 / 1012
Goodness-of-fit on F^2	1.033
Final R indices [$I>2\sigma(I)$]	R1 = 0.0811, wR2 = 0.1947
R indices (all data)	R1 = 0.1135, wR2 = 0.2147
Extinction coefficient	n/a
Largest diff. peak and hole	3.466 and -1.214 $eÅ^{-3}$

8.3. Crystal data of Mo-5

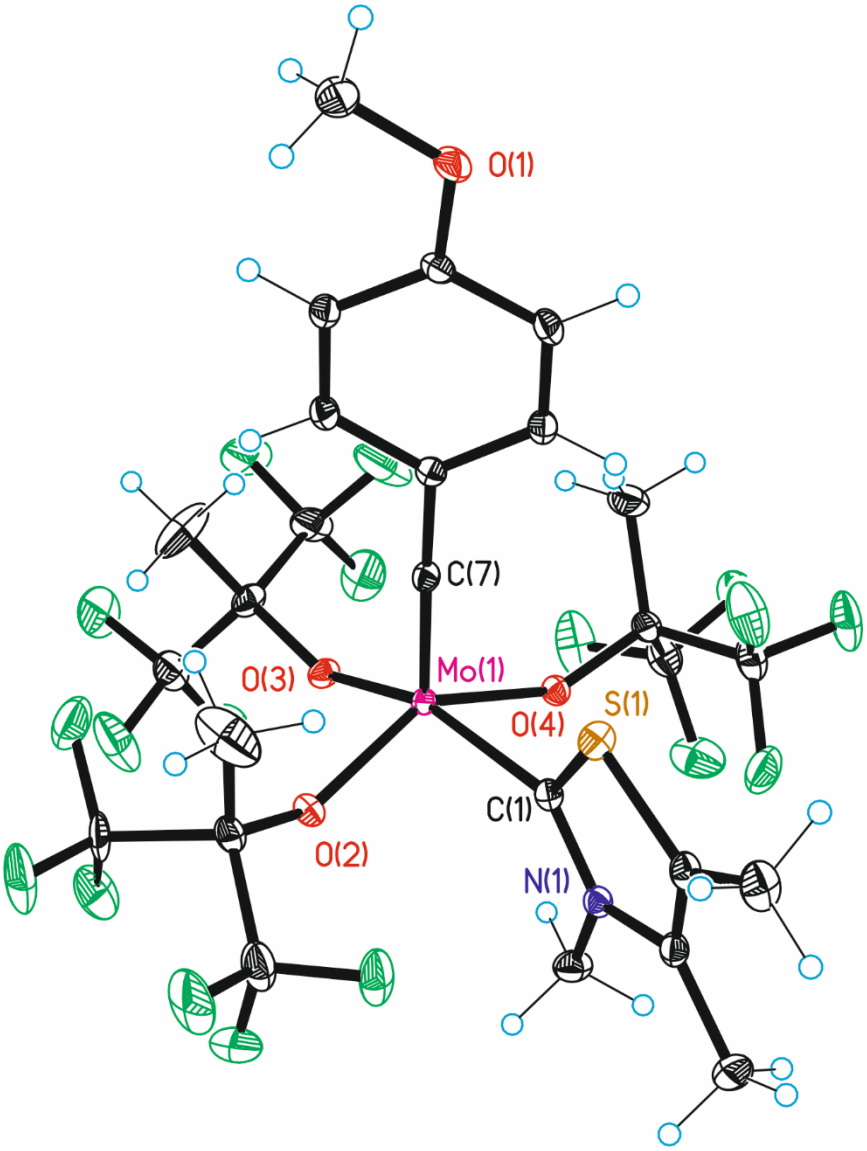

Figure S86: Single crystal X-ray structure of **Mo-5**.

*Crystal data and structure refinement for **Mo-5**.*

Empirical formula	$C_{26}H_{25}F_{18}MoNO_4S$	
Formula weight	885.47	
Temperature	193(2) K	
Wavelength	0.71073 Å	
Crystal system	Orthorhombic	
Space group	Pbca	
Unit cell dimensions	a = 10.3486(5) Å	α = 90°.
	b = 19.3302(11) Å	β = 90°.

	c = 32.5838(19) Å γ = 90°.
Volume	6518.1(6) $Å^3$
Z	8
Density (calculated)	1.805 mg/m^3
Absorption coefficient	0.604 mm^{-1}
F(000)	3520
Crystal size	0.200 x 0.180 x 0.160 mm^3
Theta range for data collection	2.107 to 25.195°.
Index ranges	-12<=h<=12, -23<=k<=23, -39<=l<=39
Reflections collected	136116
Independent reflections	5864 [R(int) = 0.0329]
Completeness to θ = 25.195°	100.0 %
Absorption correction	Semi-empirical from equivalents
Max. and min. transmission	0.746 and 0.705
Refinement method	Full-matrix least-squares on F^2
Data / restraints / parameters	5864 / 0 / 536
Goodness-of-fit on F^2	1.049
Final R indices [I>2σ(I)]	R1 = 0.0276, wR2 = 0.0665
R indices (all data)	R1 = 0.0319, wR2 = 0.0691
Extinction coefficient	n/a
Largest diff. peak and hole	0.435 and -0.501 $eÅ^{-3}$

8.4. Crystal data of Mo-7

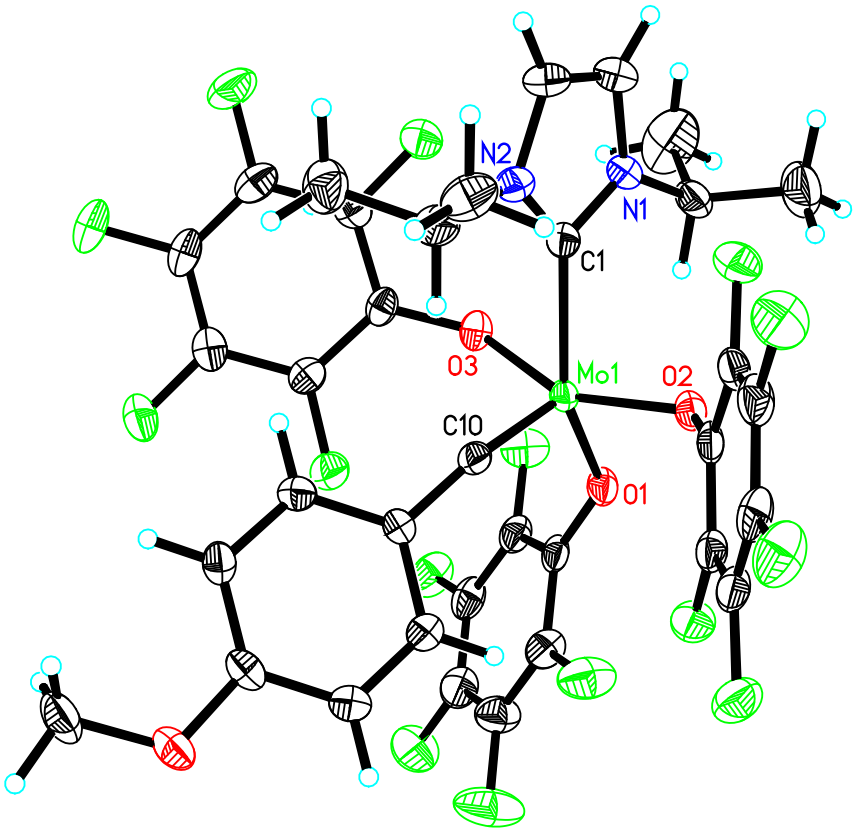

Figure S87: Single crystal X-ray structure of **Mo-7**.

Comment on checkcif:

A bit stronger vibration of the substituted isopropyl moiety – non-critical

F8…O2 intermolecular contact (2.82 A) – non-critical, maybe a checkcif problem.

*Crystal data and structure refinement for **Mo-7**.*

Empirical formula	$C_{35}H_{23}F_{15}MoN_2O_4$
Formula weight	916.49
Temperature	130(2) K
Wavelength	0.71073 Å
Crystal system	Monoclinic

Space group	$P2_1$	
Unit cell dimensions	a = 10.6604(6) Å	α = 90°
	b = 12.8387(9) Å	β = 98.076(2)°
	c = 12.9641(8) Å	γ = 90°
Volume	1756.74(19) $Å^3$	
Z	2	
Calculated density	1.733 mg/m^3	
Absorption coefficient	0.496 mm^{-1}	
F(000)	912	
Crystal size	0.42 x 0.19 x 0.07 mm	
Theta range for data collection	1.59 to 28.33 °	
Limiting indices	-14<=h<=8, -17<=k<=17, -17<=l<=17	
Reflections collected / unique	31743 / 8689 [R(int) = 0.0390]	
Completeness to θ = 28.33	99.4 %	
Absorption correction	Semi-empirical from equivalents	
Max. and min. transmission	0.7457 and 0.7036	
Refinement method	Full-matrix least-squares on F^2	
Data / restraints / parameters	8689 / 1 / 519	
Goodness-of-fit on F^2	1.008	
Final R indices [I>2σ(I)]	R1 = 0.0305, wR2 = 0.0577	
R indices (all data)	R1 = 0.0430, wR2 = 0.0613	
Largest diff. peak and hole	0.369 and -0.504 $eÅ^{-3}$	

8.5. Crystal data of Mo-8

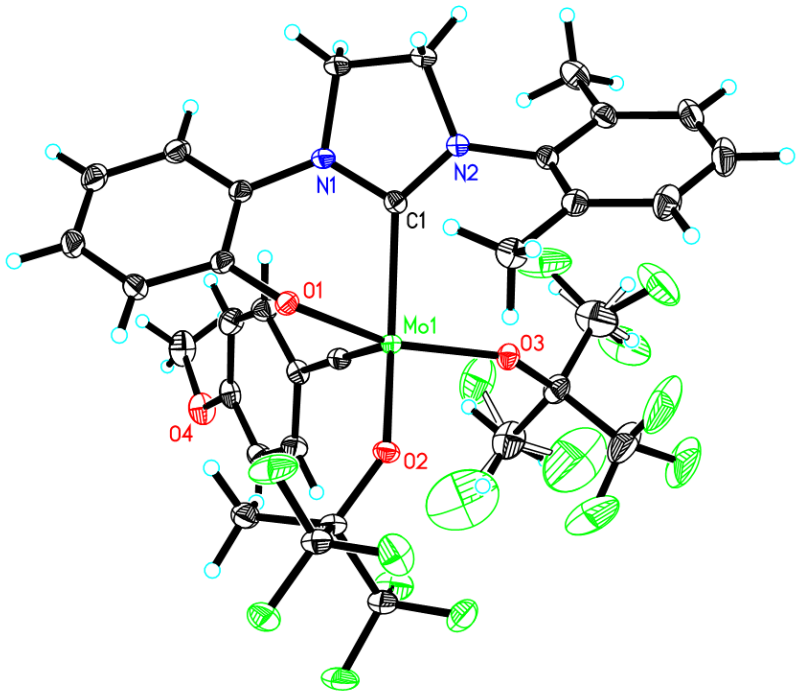

Figure S88: Single crystal X-ray structure of **Mo-8**.

Comment on checkcif:

Disordered situation of $–CF_3$ moieties, smeared electron density – non-critical; displacement parameters converged.

*Crystal data and structure refinement for **Mo-8**.*

Empirical formula	$C_{33}H_{30}F_{12}MoN_2O_4$	
Formula weight	842.53	
Temperature	130(2) K	
Wavelength	0.71073 A	
Crystal system	Triclinic	
Space group	P-1	
Unit cell dimensions	a = 11.5190(6) Å	α = 98.704(4)°
	b = 12.5145(7) Å	β = 109.748(3)°
	c = 14.1759(1) Å	γ = 113.041(2)°
Volume	1672.35(19) A^3	
Z	2	
Calculated density	1.673 Mg/m^3	

Absorption coefficient	0.501 mm^{-1}
F(000)	848
Crystal size	0.36 x 0.25 x 0.20 mm
Theta range for data collection	1.62 to 30.59°
Limiting indices	-16<=h<=16, -17<=k<=17, -20<=l<=20
Reflections collected / unique	38040 / 10208 [R(int) = 0.0320]
Completeness to θ = 30.59	99.2 %
Absorption correction	Semi-empirical from equivalents
Max. and min. transmission	0.7461 and 0.7153
Refinement method	Full-matrix least-squares on F^2
Data / restraints / parameters	10208 / 44 / 501
Goodness-of-fit on F^2	1.051
Final R indices [I>2σ(I)]	R1 = 0.0292, wR2 = 0.0707
R indices (all data)	R1 = 0.0383, wR2 = 0.0741
Largest diff. peak and hole	0.964 and -0.598 $e.A^{-3}$

8.6. Crystal data of Mo-10

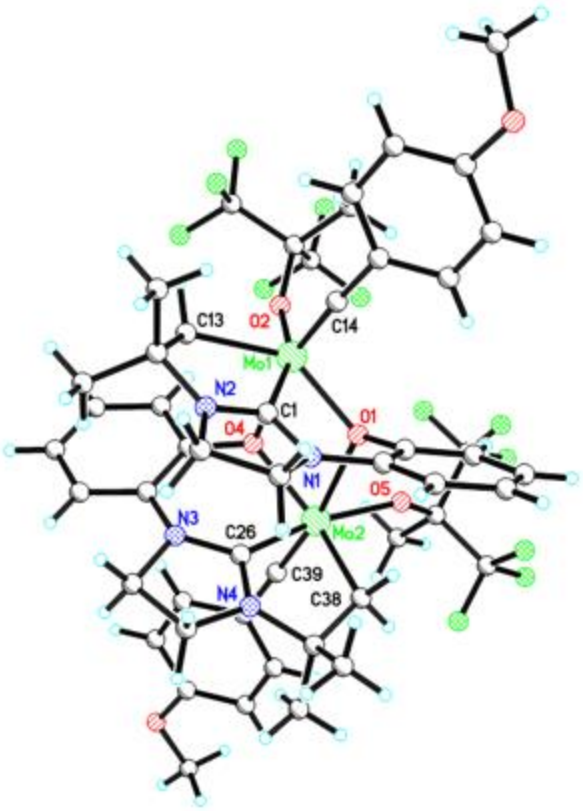

Figure S89: Single crystal X-ray structure of **Mo-10**.

Comment on checkcif:

Slightly enlarged displacement parameters of terminal carbon – non-critical.

*Crystal data and structure refinement for **Mo-10**.*

Empirical formula	$C_{50}H_{52}F_{12}Mo_2N_4O_6$	
Formula weight	1224.83	
Temperature	130(2) K	
Wavelength	0.71073 A	
Crystal system	monoclinic	
Space group	$P2_1/n$	
Unit cell dimensions	a = 12.4862(6) Å	α = 90°
	b = 21.3116(9) Å	β = 103.530(2)°
	c = 21.1102(9) Å	γ = 90°
Volume	5461.5(4) A^3	
Z	4	

Calculated density	1.490 Mg/m^3
Absorption coefficient	0.549 mm^{-1}
F(000)	2480
Crystal size	0.141 x 0.115 x 0.095 mm
Theta range for data collection	1.377 to 26.408°
Limiting indices	-14<=h<=15, -26<=k<=21, -26<=l<=21
Reflections collected / unique	51532 / 11206 [R(int) = 0.0496]
Completeness to θ = 25.242	99.9 %
Absorption correction	Semi-empirical from equivalents
Max. and min. transmission	0.7454 and 0.6757
Refinement method	Full-matrix least-squares on F^2
Data / restraints / parameters	11206 / 0 / 675
Goodness-of-fit on F^2	1.018
Final R indices [I>2σ(I)]	R1 = 0.0359, wR2 = 0.0779
R indices (all data)	R1 = 0.0597, wR2 = 0.0828
Largest diff. peak and hole	0.659 and -0.372 $e.A^{-3}$

****

Notice: Heavily disordered solvent (DCM overlapped with THF) was excluded with squeeze (PLATON), resulting in a clear improvement in the standard deviations of the geometry parameters.

****

8.7. Crystal data of W-4

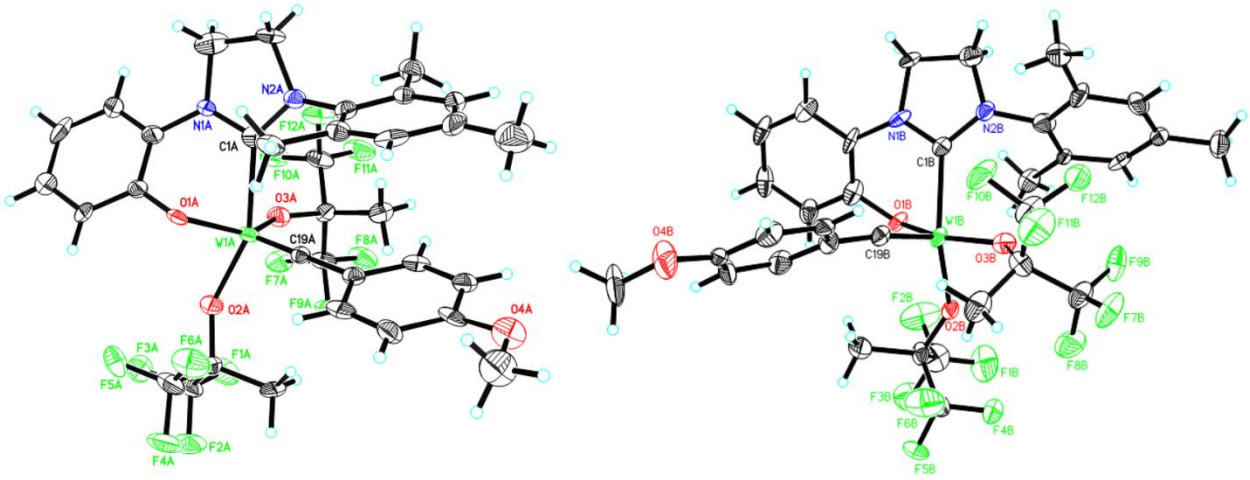

Figure S90: Single crystal X-ray structure of **W-4**. Conformer A and conformer B are shown.

Comment on checkcif:

A R(int) value of ~0.15 indicates a non-optimal crystal quality. Co-crystallized solvent molecules could be one reason for this property. Consequently, the overall estimated standard deviation of the C-C bonds is not below 1pm (1.797 pm). These properties also have synergetic effects on the other detected (weak) C-Alerts. (e.g. strong elongation of the displacement parameters of the solvent molecules).

A small amount of solvent density volume (51 A^3) could not be localized.

In-plane vibrations of substituted phenyl-moieties often result in strong elongation of the displacement parameters of the terminal substituents (e.g. methoxy groups).

This behaviour also has an influence on the orientation of the thermal ellipsoids (Hirshfield-difference).

*Crystal data and structure refinement for **W-4**.*

Empirical formula	$C_{38}H_{42}F_{12}N_2O_5W$
Formula weight	1018.59
Temperature	130(2) K
Wavelength	0.71073 Å
Crystal system, space group	Triclinic, P-1
Unit cell dimensions	a = 15.2431(18) Å α = 106.139(6)° b = 17.0161(16) Å β = 109.867(6)° c = 17.955(2) Å γ = 94.334(5)°
Volume	4132.3(8) $Å^3$
Z, Calculated density	4, 1.637 Mg/m^3

Absorption coefficient	2.893 mm^{-1}
F(000)	2024
Crystal size	0.08 x 0.08 x 0.05 mm
Theta range for data collection	1.27 to 25.00 deg.
Limiting indices	-18<=h<=18, -19<=k<=20, -21<=l<=21
Reflections collected / unique	60291 / 14447 [R(int) = 0.1492]
Completeness to theta = 25.00	99.30%
Absorption correction	Numerical
Max. and min. transmission	0.9285 and 0.7380
Refinement method	Full-matrix least-squares on F^2
Data / restraints / parameters	14447 / 148 / 1061
Goodness-of-fit on F^2	1.034
Final R indices [I>2sigma(I)]	R1 = 0.0651, wR2 = 0.1156
R indices (all data)	R1 = 0.1669, wR2 = 0.1340
Largest diff. peak and hole	3.324 and -2.390 e. $Å^{-3}$

8.8. Crystal data of W-8

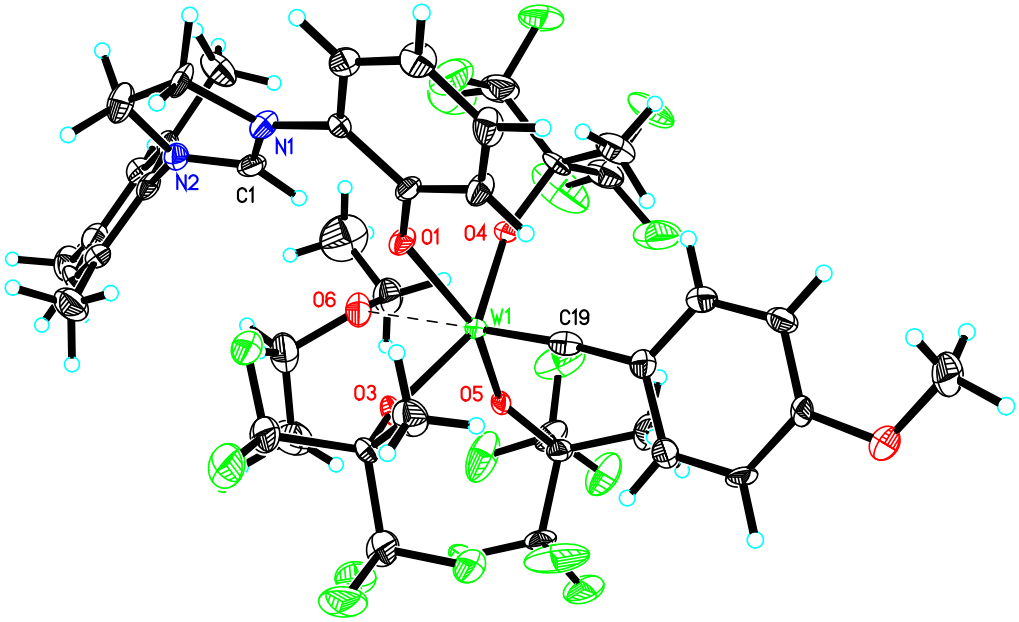

Figure S91: Crystal structure of W-8.

Comment on checkcif:

Sometimes in disordered structures, atoms (e.g. F) show an asymmetric behaviour of their displacement parameters, because of smeared electron density. A value of 3.3 prolat is non-critical.

An overall estimated standard deviation of 1.271 pm (C-C bonds) is not unusual, if the influence of delocalized electron density (disorder) is evident.

*Crystal data and structure refinement for **W-8**.*

Empirical formula	$C_{42}H_{46}F_{18}N_2O_6W$
Formula weight	1200.66
Temperature	130(2) K
Wavelength	0.71073 Å
Crystal system, space group	Monoclinic, P_21/c
Unit cell dimensions	a = 12.8693(12) Å α = 90° b = 16.9392(13) Å β = 102.129(4)° c = 21.5128(18) Å γ = 90°
Volume	4585.0(7) $Å^3$
Z, Calculated density	4, 1.739 Mg/m^3
Absorption coefficient	2.641 mm^{-1}

F(000)	2384
Crystal size	0.22 x 0.21 x 0.06 mm
Theta range for data collection	1.54 to 26.45 deg.
Limiting indices	-16<=h<=8, -18<=k<=21, -25<=l<=26
Reflections collected / unique	30912 / 9308 [R(int) = 0.0696]
Completeness to theta = 26.45	98.40%
Absorption correction	Numerical
Max. and min. transmission	0.9096 and 0.5926
Refinement method	Full-matrix least-squares on F^2
Data / restraints / parameters	9308/12/634
Goodness-of-fit on F^2	1.049
Final R indices [I>2sigma(I)]	R1 = 0.0620, wR2 = 0.1214
R indices (all data)	R1 = 0.1047, wR2 = 0.1311

Concerning the level X alert in the checkcif:

The coordination of diethyl ether to the tungsten complex changes the electronic situation compared to free diethyl ether in the unit cell. The short distances of O6 to O5 and O4 are a result of this coordination.

- [1] W. A. Herrmann, V. P. W. Böhm, C. W. K. Gstöttmayr, M. Grosche, C.-P. Reisinger, T. Weskamp Synthesis, structure and catalytic application of palladium(II) complexes bearing N-heterocyclic carbenes and phosphines. *J. Organomet. Chem.* **2001**, *617-618*, 616-628.
- [2] M. Hans, J. Lorkowski, A. Demonceau, L. Delaude Efficient synthetic protocols for the preparation of common *N*-heterocyclic carbene precursors. *Beilstein J. Org. Chem.* **2015**, *11*, 2318-2325.
- [3] K. D. Anastasie, N. Claudia, R. Michael, G. M. Timo, K. Markus Intramolecular stereoselective protonation of aldehyde-derived enolates. *Angew. Chem.* **2010**, *122*, 8545-8547; *Angew. Chem. Int. Ed.* **2010**, *49*, 8367-8369.
- [4] T. Schaub, U. Radius Efficient C-F and C-C activation by a novel *N*-heterocyclic carbene-nickel(0) complex. *Chem. Eur. J.* **2005**, *11*, 5024-5030.
- [5] M. v. d. Ende, P. M. Hauser, C. Lienert, D. Wang, W. Frey, M. R. Buchmeiser Ti(IV) complexes with bidentate *O*-chelating *N*-heterocyclic carbenes for use in the homopolymerization of ethylene and its copolymerization with cyclic olefins. *ChemCatChem* **2018**, *11*, 744-752.
- [6] A. W. Waltman, R. H. Grubbs A new class of chelating *N*-heterocyclic carbene ligands and their complexes with palladium. *Organometallics* **2004**, *23*, 3105-3107.
- [7] A. J. Arduengo III, J. S. Dolphin, G. Gurău, W. J. Marshall, J. C. Nelson, V. A. Petrov, J. W. Runyon Synthesis and complexes of fluoroalkoxy carbenes. *Angew. Chem. Int. Ed.* **2013**, *52*, 5110-5114.
- [8] J. J. Song, J. T. Reeves, D. R. Fandrick, Z. Tan, N. K. Yee, C. H. Senanayake, in *Encyclopedia of Reagents for Organic Synthesis*, Wiley VCH, **2008**.
- [9] A. J. Arduengo, R. Krafczyk, R. Schmutzler, H. A. Craig, J. R. Goerlich, W. J. Marshall, M. Unverzagt Imidazolylidenes, imidazolinylidenes and imidazolidines. *Tetrahedron* **1999**, *55*, 14523-14534.
- [10] A. J. Arduengo, J. R. Goerlich, W. J. Marshall A stable diaminocarbene. *J. Am. Chem. Soc.* **1995**, *117*, 11027-11028.
- [11] J. Heppekausen, R. Stade, A. Kondoh, G. Seidel, R. Goddard, A. Fürstner Optimized synthesis, structural investigations, ligand tuning and synthetic evaluation of silyloxy-based alkyne metathesis catalysts. *Chem. Eur. J.* **2012**, *18*, 10281-10299.
- [12] M. Koy, I. Elser, J. Meisner, W. Frey, K. Wurst, J. Kästner, M. R. Buchmeiser High oxidation state molybdenum *N*-heterocyclic carbene alkylidyne complexes: Synthesis, mechanistic studies, and reactivity. *Chem. Eur. J.* **2017**, *23*, 15484-15490.
- [13] A. D. Lackner, A. Fürstner The triple-bond metathesis of aryldiazonium salts: A prospect for dinitrogen cleavage. *Angew. Chem.* **2015**, *127*, 13005-13009; *Angew. Chem. Int. Ed.* **2015**, *54*, 12814-12818.
- [14] A. M. Geyer, E. S. Wiedner, J. B. Gary, R. L. Gdula, N. C. Kuhlmann, M. J. A. Johnson, B. D. Dunietz, J. W. Kampf Synthetic, mechanistic, and computational investigations of nitrile-alkyne cross-metathesis. *J. Am. Chem. Soc.* **2008**, *130*, 8984–8999.
- [15] D. G. Gusev Electronic and steric parameters of 76 *N*-heterocyclic carbenes in $Ni(CO)_3(NHC)$. *Organometallics* **2009**, *28*, 6458-6461.
- [16] Y. Zhao, D. G. Truhlar The M06 suite of density functionals for main group thermochemistry, thermochemical kinetics, noncovalent interactions, excited states, and transition elements: two new functionals and systematic testing of four M06-class functionals and 12 other functionals. *Theor. Chem. Acc.* **2008**, *120*, 215-241.
- [17] F. Weigend, R. Ahlrichs Balanced basis sets of split valence, triple zeta valence and quadruple zeta valence quality for H to Rn: Design and assessment of accuracy. *Phys. Chem. Chem. Phys.* **2005**, *7*, 3297-3305.

- [18] a) R. Ahlrichs, M. Bär, M. Häser, H. Horn, C. Kölmel Electronic structure calculations on workstation computers: The program system turbomole. *Chem. Phys. Lett.* **1989**, *162*, 165-169; b) TURBOMOLE V7.0.1 2015, a development of University of Karlsruhe and Forschungszentrum Karlsruhe GmbH, 1989-2007, TURBOMOLE GmBH, since 2007, available from http://www.turbomole.com.
- [19] J. Kästner, J. M. Carr, T. W. Keal, W. Thiel, A. Wander, P. Sherwood DL-FIND: an open-source geometry optimizer for atomistic simulations. *J. Phys. Chem. A* **2009**, *113*, 11856-11865.
- [20] S. Metz, J. Kästner, A. A. Sokol, T. W. Keal, P. Sherwood ChemShell-a modular software package for QM/MM simulations. *Wiley Interdisciplinary Reviews: Computational Molecular Science* **2014**, *4*, 101-110.
- [21] I. M. Alecu, J. Zheng, Y. Zhao, D. G. Truhlar Computational thermochemistry: Scale factor databases and scale factors for vibrational frequencies obtained from electronic model chemistries. *J. Chem. Theory Comput.* **2010**, *6*, 2872.